

**Versatile and Potentially Scalable Method for Synthesis of Janus Nanoparticles**

by

Alan Michael Hanley

A thesis submitted to the Graduate Faculty of  
Auburn University  
in partial fulfillment of the  
requirements for the Degree of  
Master of Science

Auburn, Alabama  
May 7, 2016

Keywords: Janus Nanoparticles, Nanoparticle Synthesis, TEM Imaging, Dark-field Microscopy

Copyright 2016 by Alan Michael Hanley

Approved by

Allan E. David, Chair, John W. Brown Assistant Professor of Chemical Engineering  
W. Robert Ashurst, Uthlaut Family Endowed Associate Professor of Chemical Engineering  
James Radich, Assistant Professor of Chemical Engineering

## **Abstract**

Researchers are constantly working toward developing “smarter” materials that can be designed or programmed to do a certain task. Examples of such tasks would be self-assembling into an organized structure or targeting a certain protein in the human body. Janus nanoparticles, nanoparticles with two distinct and different hemispheres, have been researched over the past few decades in the pursuit of developing smarter materials. While Janus nanoparticles can be designed to accomplish a number of tasks, they have no use to society as a whole if they cannot be produced at an industrial quantity. Another large problem that keeps research on Janus nanoparticles from moving forward is the rigid regulations regarding nanoparticle configurations inherent in all of the existing methods; the methods described in current publications are usually limited to producing one type of Janus nanoparticle. Due to this roadblock, we have developed a new method for producing Janus nanoparticles that has the potential for scalability as well as a high level of flexibility when designing the hemispheres. Essentially, this method has the potential to produce numerous different Janus nanoparticle configurations at quantities that can support an industrial demand. The purpose of this research is to develop a complete understanding of this method, then utilize it to examine different Janus nanoparticle configurations. With the development of this new synthesis method, Janus nanoparticles will finally have the opportunity to be elevated from laboratory experiments and utilized in real-world applications. Janus nanoparticles have applications in drug delivery, enhanced protective coatings, and ultra-thin-display screens, just to name a few.

## **Acknowledgements**

First and foremost, I need to thank all of the members of my family for their love and support both before and during the course of this work. To my parents, Tom and Norma, and to my siblings, Jeff, Andrew, and Caitlin, you have all been integral to the success of this project. For all the difficult times I questioned my abilities and began to lose hope in what I was doing, you all shared in the effort to help me continue on and reach my goals.

This work would not have been possible without the guidance of my advisor, Dr. Allan David. Thank you for taking a chance on me and giving me control of a project that is clearly important to you, as well as helping me every step of the way. Special thanks to all past and previous members of the David lab group, including Dr. Young Suk Choi who constantly exceeds the limitations of what a post doc does to help the graduate students, Tareq Anani, Xin Fan, and Hunter Rogers, for welcoming me in and showing me the ropes when I joined this lab group, Alex Kelly, who through his own nanoparticle research was able to give invaluable insight into mine, as well as the remaining members of team, Richard Cullum, Prachi Sangle, Barry Yeh, Ricky Whitener, Chelsea Harris, and a number of undergraduate researcher assistants, whose inputs ranged from an extra set of eyes when analyzing results to a few calming words to remind me that even in the tougher moments, my research still inspires me.

Special recognition needs to be given to Dr. Michael E. Miller, who educated me on the operation of the Transmission Electron Microscope, as well as Dr. Vitaly Vodyanoy and Oleg Pustovyy, who examined my samples using there advanced optical microscope. The images yielded from these techniques were invaluable in my continued research.

I would like to thank the Chemical Engineering Department at the University of Louisville where I got my start, specifically Dr. Gerold Willing, who advised my research during my time at Louisville. Without the foundation that you helped me build, I would not be where I am today.

Finally, I would like to thank the Chemical Engineering Department here at Auburn University. You have cultivated a much stronger and more capable engineer than I ever thought I could become, and any success I achieve in the future can undoubtedly be linked to the effort you put into me.



## Table of Contents

|  |      |
|--|------|
| Abstract.....  | ii   |
| Acknowledgements.....  | iii  |
| List of Tables.....  | viii |
| List of Figures.....   | ix   |
| Chapter 1: Introduction.....   | 1    |
| 1.1: History and Properties of Janus Nanoparticles.....                      | 1    |
| 1.2: Application of Janus Nanoparticles.....                                 | 2    |
| 1.2.1: Janus Nanoparticles for Improved Protective Coatings.....             | 3    |
| 1.2.2: Janus Nanoparticles for Drug Delivery.....                            | 4    |
| 1.2.3: Janus Nanoparticles for Improved Emulsion Stabilizers.....            | 6    |
| 1.2.4: Other Application for Janus Nanoparticles.....                        | 8    |
| 1.3: Synthesis Methods for Janus Nanoparticles.....                          | 10   |
| 1.3.1: Synthesizing Janus Nanoparticles via the Masking Method.....          | 10   |
| 1.3.2: Synthesizing Janus Nanoparticles via block-copolymers .....           | 16   |
| 1.3.3: Synthesizing Janus Nanoparticles via Phase Separation.....            | 18   |
| 1.4: Challenges with Janus Nanoparticles.....                                | 23   |
| Chapter 2: Synthesizing Janus Nanoparticles using an Iron Oxide Core.....    | 25   |
| 2.1: Introduction.....   | 25   |
| 2.2: Experimental.....   | 26   |
| 2.2.1: Materials.....  | 26   |
| 2.2.2: Synthesizing Oleic Acid Coated Iron Oxide Magnetic Nanoparticles..... | 26   |

|  |    |
|--|----|
| 2.2.3: Synthesizing Citric Acid Coated Iron Oxide Magnetic Nanoparticles.....                            | 28 |
| 2.2.4: Synthesizing JNPs with a CA-MNP core.....   | 28 |
| 2.2.5: Complete Coating of either Oleylamine or mPEG-NH <sub>2</sub> on CA-MNPs.....                     | 30 |
| 2.3: Results and Discussion  |    |
| 2.3.1: Analyzing Nanoparticles using Dynamic Light Scattering.....                                       | 30 |
| 2.3.2: Analyzing Nanoparticles using Fourier-Transform Infrared Spectroscopy.                            | 32 |
| 2.3.3: Analysis of Nanoparticles at Hexane/Water Interface.....  | 36 |
| 2.3.4 Analysis of JNPs in Different Solvents.....  | 39 |
| 2.4: Conclusions.....  | 41 |
| Chapter 3: Synthesizing Janus Nanoparticles using a Silica Core with an CA-MNP Hemisphere.....           | 42 |
| 3.1: Introduction.....   | 42 |
| 3.2: Experimental.....   | 42 |
| 3.2.1: Materials.....  | 42 |
| 3.2.2: Synthesizing JNPs with a Silica Core and a CA-MNP Functionalized Hemisphere.....                  | 43 |
| 3.2.3: Synthesizing Silica Nanoparticles Completely Coated with Oleylamine...44                          |    |
| 3.2.4: Synthesizing Silica Nanoparticles Completely Coated with PEG.....                                 | 45 |
| 3.2.5: Synthesizing Silica Nanoparticles Completely Coated with CA-MNPs and mPEG-NH <sub>2</sub> .....   | 45 |
| 3.2.6: Synthesizing Silica Nanoparticles Freely Mixed with both mPEG-NH <sub>2</sub> and oleylamine..... | 45 |
| 3.3: Results and Discussion.....   | 46 |
| 3.3.1: Analysis of JNPs and Control Nanoparticles.....   | 46 |
| 3.4: Conclusions.....  | 52 |
| Chapter 4: Synthesizing Janus Nanoparticles using a Silica Core with a Hemisphere Coated with FITC.....  | 53 |
| 4.1: Introduction.....   | 53 |

|   |    |
|---|----|
| 4.2: Experimental.....  | 53 |
| 4.2.1: Materials.....   | 53 |
| 4.2.2: Synthesizing Janus Nanoparticles with a Silica Core and a Hemisphere Functionalized with PEG.....        | 54 |
| 4.2.3: Synthesizing JNPs with a Silica Core and a Hemisphere Functionalized with FITC.....                      | 55 |
| 4.3: Results and Discussion.....  | 56 |
| 4.3.1: Analysis of JNPs Coated with FITC or PEG using an Optical Microscope.....                                | 56 |
| 4.3.2: Analysis of JNPs Coated with FITC using an Optical Microscope Outfitted with a Dark-Field Condenser..... | 59 |
| 4.4: Conclusions.....   | 62 |
| Chapter 5: Overall Conclusions and Continued Investigation JNP Synthesis Method.....                            | 64 |
| References.....   | 66 |

## List of Tables

|     |   |    |
|-----|---|----|
| 2.1 | Heating Cycle for Synthesizing O-MNPs.....  | 27 |
| 2.2 | Heating Cycle for Synthesizing CA-MNPs..... | 28 |

## List of Figures

- 1.1: Illustration of a JNP and the self-assembled structures that they can form. The core nanoparticle is represented in black, while the blue and orange lines represent compounds grafted to opposing sides of the nanoparticle, each with their own set of properties. Compounds of varying sizes as well as other nanoparticles can all act as modifiers for hemispheres. JNPs can form self-assembled monolayers (top right), micelles (middle right), and liposomal structures (bottom right).....2
- 1.2: Strategy developed by Synytska et al for coating textile with JNPs to produce a hydrophobic coating. JNPs will bond to the textile fibers do to the functionalization of one of their hemispheres, while the octyltrichlorosilane bonded to the opposing hemisphere will repel water from the fibers. Reprinted with permission from Synytska et al. Copyright 2011, American Chemical Society. ....3
- 1.3: TEM images of antimicrobial Janus nanorods. The darker head groups are composed of silver nanoparticles bonded to iron oxide nanoparticles, and the tail group is composed of silica nanoparticles. Reproduced from Zhang et al. with permission from the Royal Society of Chemistry.....4
- 1.4: Images showing the different uptake timelines of a JNP with anti-CD3/metallic hemispheres (a) and a nanoparticle completely coated in anti-CD3 antibodies (b). As predicted, the nanoparticle in (b) is easily absorbed into the cell. In (a), the anti-CD3 hemisphere (shown in red) is absorbed first, then the cell develops around the opposing hemisphere of the particle until the nanoparticle is completely absorbed. Reprinted with permission from Gao & Yu. Copyright 2013, American Chemical Society. ....5
- 1.5: Janus nanostructures composed of a silica coated upconversion nanoparticle and mesoporous organosilica nanostructure. Reprinted with permission from X. Li et al. Copyright 2014, American Chemical Society. ....7
- 1.6: Sample of emulsions stabilized with JNPs. Sample a-d contain a fixed internal phase volume fraction with varied amounts of JNPs versus the total weight of the oil phase (a - 0.055%, b – 0.11%, c – 0.16%, d – 0.22%). Looking at a-d, the line between the emulsion and the oil phase becomes less clear, signifying a more stable emulsion. It is also important to notice that large droplets (black dots in emulsion) that appear in (a) and slowly diminish in (b), (c), and (d). This phenomenon identifies a more stable and uniform emulsion, again strengthening the assertion that JNPs help stabilize emulsions. Vial e-g have a fixed % of JNPs (0.16%) and vary in internal phase volume fraction (83.3%, 87.5%, and 90% respectively). All vials show no noticeable oil phase, further asserting this theory. (Photographs of these emulsions were taken 24 hours after mixing). Adapted from Yi et al. with permission of The Royal Society of Chemistry.....8

|  |    |
|--|----|
| 1.7: Strategy to develop nanostructures that can act as electrochemical biorecognition-signaling systems for biotin. First, the gold and silica nanoparticles are bound together, then horseradish peroxidase is used to coat the silica face of the structure. Streptavidin is then added to the gold nanoparticle surface, followed by PEG-SH, which will bond to the remaining open sites on the gold nanoparticle surface. Reproduced from Sánchez et al. with permission Elsevier. ....                           | 9  |
| 1.8: Illustration of how Sardar et al. used solid-liquid masking to produce JNPs. Gold nanoparticle are bonded to a silanized flat plate, then modified with a polymer suspended in a liquid. The particles are then released via sonication and modified with one of two new polymers on their unmodified hemisphere. Reprinted with permission from Sardar et al. Copyright 2007, American Chemical Society. ....  | 11 |
| 1.9: Illustration of JNPs synthesized by a particle-on-particle solid-liquid interface masking method. Smaller nanoparticles are grafter to the surface of larger nanoparticles, modified on one hemisphere, then released as multimodal nanoparticles. Reprinted with permission from J. Li et al. Copyright 2013, American Chemical Society.....   | 12 |
| 1.10: Illustration of how JNPs can be formed using wax-in-water emulsion. While the pink polygons in this illustration represent APTES, this method will allow the use of many different modifying compounds; the compound will depend on what can bond to the nanoparticle surface. Reprinted with permission from Perro et al., 2009, with permission from Elsevier. ....  | 13 |
| 1.11: Illustration of how Janus nanostructures can be formed using liquid-liquid interface masking. Once the organic solvent and aqueous liquid are emulsified, the iron oxide nanoparticles (shown in pink) will form a protective barrier around the microdroplets of organic solvent, and thus exposing one of their hemispheres. The silver nanoparticles in the aqueous solution are then free to bond to that hemisphere. Adapted with permission from Gu .et al. Copyright 2005, American Chemical Society..... | 14 |
| 1.12: Illustration of how JNPs can be formed at the gas-liquid interface. Once the nanoparticle layer is formed at the surface barrier, scientists are able to modify one hemisphere of the nanoparticles as long as the modifying compound is contained in the aqueous layer. Reprinted with the permission of Pradhan et al., 2007, with the permission of John Wiley and Sons, Inc. ....  | 15 |
| 1.13: Illustration showing the process of synthesizing JNPs using block copolymers. Reprinted with permission from Erhardt et al. Copyright 2001, American Chemical Society.....   | 16 |
| 1.14: Illustration of synthesis method for JNP using a thin film comprised of diblock copolymers and a secondary PEG compound to form a second hemisphere. Reproduced from Poggi et al. with permission from The Royal Society of Chemistry. ....  | 17 |
| 1.15: Illustration of how gold/titania Janus nanostructures were formed using diblock copolymers as a stabilizing structure. Reprinted with permission from Fe et al., 2011, with permission from Elsevier. ....   | 18 |

|   |    |
|---|----|
| 1.16: Illustration of the JNPs synthesized via electrohydrodynamic co-jetting. The wavy blue lines represent the PEG compound that was attached to improve bioavailability; the grey circles indicated biotin both bound to the nanoparticle surface and the PECAM antibody; the grey rectangular polygons represent streptavidin that will bind to biotin. The green side of the nanoparticle represents the hemisphere coated with acetylene, while the red side represents the hemisphere coated with biotin. Adapted with the permission of Yoshida et al., 2009, with the permission of John Wiley & Sons, Inc. .... | 19 |
| 1.17: Illustration of the co-jetting process that was used by Xie et al. to form JNPs. Reprinted with permission from Xie et al. Copyright 2012, American Chemical Society.....   | 20 |
| 1.18: Confocal laser scanning microscope images taken of the JNPs created via co-jetting by Xie et al. Image (a) shows the JNPs that were synthesized using the dyes Nile red and Rh-6G; image (b) shows the JNPs that were synthesized using Nile red and FITC-dextran. Reprinted with permission from Xie et al. Copyright 2012, American Chemical Society.....   | 21 |
| 1.19: Illustration of how Janus nanostructures can be synthesized using phase separation. By understanding how compounds will react to heat or other compounds, more complex structures can be created. Reprinted with permission from Gu et al. Copyright 2004, American Chemical Society.....   | 22 |
| 1.20: Illustration of a flame synthesis apparatus used to create JNPs. Adapted with the permission of Zhao & Gao, 2009, with the permission of John Wiley & Sons, Inc.....  | 23 |
| 2.1: Setup for reaction vessel for synthesizing O-MNPs.....   | 27 |
| 2.2: Column with Silica particle pack where formation of JNPs will occur. Pack is supported by a small filter at the end of the column.....   | 29 |
| 2.3: Illustration of the strategy used to assemble a JNP with a CA-MNP core. Oleylamine molecules will bond with the activated carboxylic acid groups, anchoring the CA-MNP to the silica pack particle. mPEH-NH <sub>2</sub> will form the second hemisphere of the JNP .....  | 30 |
| 2.4: Graph showing the average hydrodynamic diameter of the O-MNPs in hexane (blue line), CA-MNPs in water (red line), and JNPs in chloroform (green line). O-MNP samples show an average hydrodynamic diameter range from 9-20 nm with a 12 nm diameter occurring most frequently. CA-MNP samples show an average diameter range from 11-20 nm with a 14 nm diameter occurring most frequently. JNP samples show an average diameter range from 11-19 nm with a 14 nm diameter occurring most frequently.....  | 31 |
| 2.5: FTIR graph of CA-MNPs.....   | 33 |
| 2.6: FTIR graph for CA-MNP coated with PEG.....   | 34 |
| 2.7: FTIR graph for CA-MNP coated with Oleylamine.....  | 35 |
| 2.8: FTIR graph of JNPs.....  | 36 |

|   |    |
|---|----|
| 2.9: Sample of nanoparticles suspended in a 1:1 hexane water mixture. The first vial (far left) has no nanoparticles. The second vial has 10 $\mu$ L of O-MNPs in hexane added to the mixture. The third vial has 10 $\mu$ L of CA-MNPs in DI water added to the mixture. The fourth vial (far right) has 10 $\mu$ L of JNPs in chloroform added to the mixture.....  | 37 |
| 2.10: Vials from the second hexane/water interface experiment. Vials 1-4 (starting on the left) are the same vials from Figure 2.11, but 4 has been agitated. The chloroform is allowed to mix with the hexane, dispersing the JNPs into the upper layer. Vial 5 is the same hexane/water mixture with 10 $\mu$ L of JNPs in hexane added to the mixture.....   | 38 |
| 2.11: Graph showing the average size of the JNPs suspended in chloroform (blue line) and the average hydrodynamic diameter of JNPs suspended in hexane (red line) JNPs suspended in chloroform show an average diameter range from 8-15 nms; JNPs suspended in hexane show an average diameter range from 100-240 nm.....   | 39 |
| 2.12: Optical Microscope Images of JNPs suspended in water with free oleylamine.....  | 40 |
| 3.1: Illustration of the strategy used to assemble a JNP with a silica core. Hydrophobic tail groups of the oleylamine molecules will attract to the C <sub>18</sub> groups, then bond with one aldehyde group of the glutaraldehyde molecules. The other side of glutaraldehyde will be free to bond with the silica nanoparticle. Activated CA-MNPs will then be added to bond with the remaining amine groups on the silica nanoparticles. Finally, the exposed side of the CA-MNPs will be coated of mPEG-NH <sub>2</sub> ..... | 44 |
| 3.2: FTIR data (wavelength vs. % transmittance) collected from all of the control groups formed using 300 nm silica nanoparticles (top to bottom): unmodified aminated silica nanoparticles, oleylamine coated silica nanoparticles, PEG coated silica nanoparticles, CA-MNP/PEG coated silica nanoparticles, and silica nanoparticles that were freely mixed with both PEG and oleylamine. ...   | 46 |
| 3.3: TEM images taken of all the control group nanoparticles. A) 300 nm silica nanoparticles totally coated with PEG. B) 300 nm silica nanoparticles totally coated with oleylamine. C) 300 nm silica nanoparticles totally coated first with CA-MNPs, then totally coated with PEG. D) 300 nm silica nanoparticles freely mixed with oleylamine and PEG simultaneously.....  | 48 |
| 3.4: TEM image of JNPs composed of a silica core with hemispheres of oleylamine and CA-MNPs/PEG.  | 49 |
| 3.5: TEM image of a JNP composed of a silica core with hemispheres of oleylamine and CA-MNPs/PEG.   | 50 |
| 3.6: Percent coverage of 120 nm JNPs determined from examination of TEM images. “Percentage coverage” indicates the amount of the nanoparticle that was covered with smaller iron oxide nanoparticles. The mean coverage for this data is 53.9% with a standard deviation of 23.00.....   | 51 |
| 4.1: Illustration of the strategy used to assemble a JNP with a silica core and a mPEG-NHS hemisphere. Fatty amine molecules will coat one hemisphere of the silica nanoparticle core; the other side of the silica nanoparticles will be coated with mPEG-NHS.....   | 55 |
| 4.2: Illustration of the strategy used to assemble a JNP with a silica core and a FITC hemisphere. Fatty amine molecules will coat one hemisphere of the silica nanoparticle core; the other side of the silica nanoparticles will be coated with FITC.....   | 56 |
| 4.3: Optical microscope images of JNPs with oleylamine and PEG hemispheres suspended in water with additional free oleylamine. The resulting structures range in size from 4-5 microns.....   | 57 |



|  |    |
|--|----|
| 4.4: 100X images of JNPs composed of a oleylamine hemisphere and a PEG hemisphere without a filter (left) and with a fluorescent filter (right).....   | 58 |
| 4.5: 100X images of JNPs composed of a oleylamine hemisphere and a FITC hemisphere without a filter (left) and with a fluorescent filter (right).....  | 58 |
| 4.6: Images from an optical microscope equipped with a dark field condenser of JNPs with a PEG functionalized hemisphere (image enlargement using digital zoom has been applied). In the left side image, no filter is being applied; on the right side image, a fluorescent filter is applied to limit the incoming light to between 470 nm and 525 nm..... | 60 |
| 4.7: Images from an optical microscope equipped with a dark field condenser of JNPs with a PEG functionalized hemisphere (image enlargement using digital zoom has been applied). In the left side image, no filter is being applied; on the right side image, a fluorescent filter is applied to limit the incoming light to between 470 nm and 525 nm..... | 61 |
| 4.8: Overlay of images seen in Figure 4.7 on JNP partially coated with FITC.....   | 62 |
| 5.1: Illustration of glass slide (represented by blue block) functionalized with long chain hydrocarbons creating a hydrophobic surface.....   | 65 |

## **Chapter 1**

### **Introduction**

#### **1.1 History and Properties of Janus Nanoparticles**

Researchers have investigated multimodal nanoparticles (nanoparticles with two distinct hemispheres) for the past 30 years. (Cho & Lee, 1985) Named after the two-faced Roman god Janus, Janus nanoparticles (JNPs) are of interest to engineering researchers due to their unique properties, most notably their ability to self-assemble. (de Gennes, 1992) Janus nanoparticles have the ability to self assemble into different structures, including monolayers, micelles, and liposomes. (Lattuada & Hatton, 2011) This self-assembly can occur in both the liquid and gas phase and will be dependent on the properties of each hemisphere. Specifically, intermolecular forces between the JNPs as well as attractive/repulsive forces between the JNPs and their surrounding environment (solvent, gas, or solid structure) will determine the final structure of these nanoparticles. Hemispheres of JNPs can also be designed to carry drugs, adhere to surfaces, and react with other compounds; this ability along with self-assembly gives JNPs many applicable areas. Figure 1 shows a graphical representation of a JNP and possible self-assembled configurations.

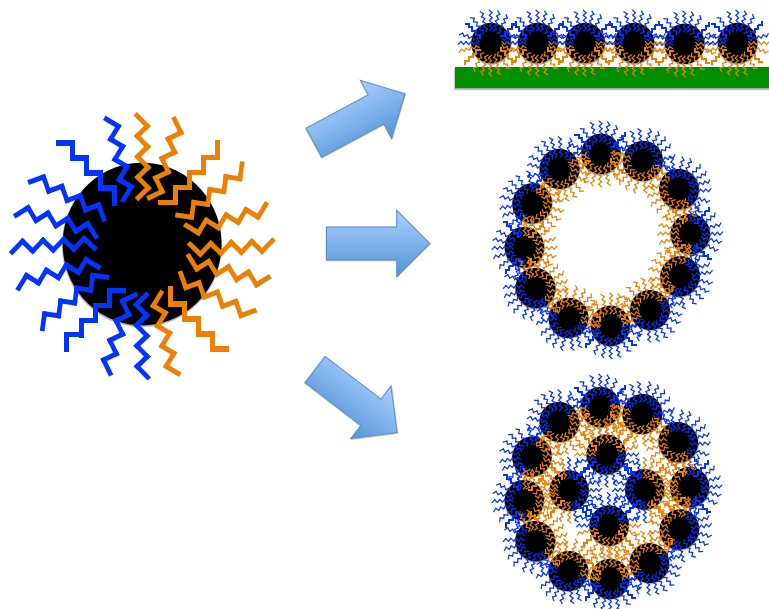


**Figure 1.1** Illustration of a JNP and the self-assembled structures that they can form. The core nanoparticle is represented in black, while the blue and orange lines represent compounds grafted to opposing sides of the nanoparticle, each with their own set of properties. Compounds of varying sizes as well as other nanoparticles can all act as modifiers for hemispheres. JNPs can form self-assembled monolayers (top right), micelles (middle right), and liposomal structures (bottom right)

## 1.2 Applications for Janus Nanoparticles

JNPs have applications in multiple fields of engineering, including but not limited to chemical, biological, materials engineering. In biological engineering, researchers have utilized JNPs to develop nanoparticles with a controlled affinity to human endothelial cells, which can lead to advances in the development of biomaterials (Yoshida et al., 2009). In 2010, JNPs coated partially with platinum were used to catalyze the decomposition of hydrogen peroxide, which in turn developed silica/platinum nanomotors (Valadares et al., 2010). These nanomotors are important in the development of microfluidic devices; JNPs offers an additional way to synthesize them. Popular applications for JNPs include improved coatings, drug delivery vehicles, and emulsion stabilizers.

### 1.2.1 Janus Nanoparticles for Improved Protective Coatings

A popular area of research for JNPs involves the development of self-assembled protective coatings. Coatings consisting of particles on the nanoscale have the ability to form a more tightly packed layer over a surface when compared to layers developed using larger particles. The differing hemispheres of JNPs allow the particle to bond to or have a high affinity to a specific surface as well as attract and/or repel a foreign substance. In 2011, a research team from the Leibniz Institute of Polymer Research in Dresden Germany developed a JNP with a hemisphere that can bond to textile and a hydrophobic hemisphere to repel water molecules. By modifying one side of the particles with octyltrichlorosilane, a long chain hydrocarbon and hydrophobic compound, researchers were able to repel water from the textile fibers with contact angles as great as  $120^\circ$  (Synytska, Khanum, Ionov, Cherif, & Bellmann, 2011). Figure 1.2 shows graphical representations and microscope images of these JNPs.

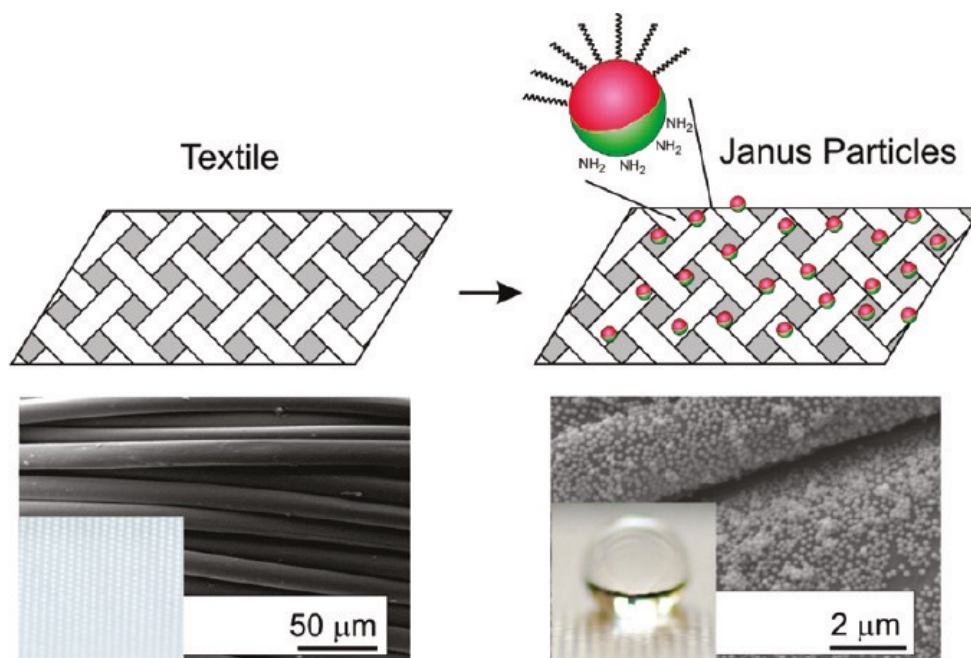


**Figure 1.2** Strategy developed by Synytska et al for coating textile with JNPs to produce a hydrophobic coating. JNPs will bond to the textile fibers due to the functionalization of one of their hemispheres, while the octyltrichlorosilane bonded to the opposing hemisphere will repel water from the fibers. Reprinted with permission from Synytska et al. Copyright 2011, American Chemical Society.

JNPs have also been designed to have antimicrobial properties in the pursuit of developing an improved antimicrobial coating. In 2012, a research group from Jilan University in China developed antimicrobial Janus nanorods (organized group of JNPs) using  $\text{Fe}_3\text{O}_4$  (iron oxide),  $\text{SiO}_2$  (silica), and Ag (silver) nanoparticles. (Zhang et al., 2012). Nanorods assembled with an iron oxide head group and a silica tail were exposed to silver nanoparticles, which bond to the iron oxide head group. Iron oxide nanoparticles give these nanorods magnetic properties, and the silica nanoparticles increases biocompatibility and hydrophobicity. Figure 1.3 shows microscope images of these nanorods. These nanorods were found to be effective at preventing bacterial growth.

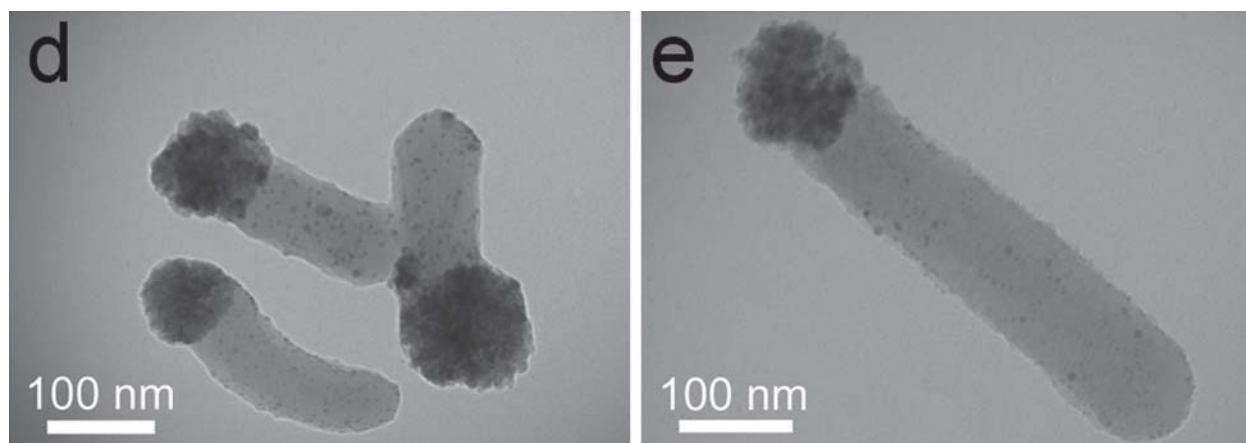


**Figure 1.3** TEM images of antimicrobial Janus nanorods. The darker head groups are composed of silver nanoparticles bonded to iron oxide nanoparticles, and the tail group is composed of silica nanoparticles. Reproduced from Zhang et al. with permission from the Royal Society of Chemistry.

### 1.2.2 Janus Nanoparticles for Drug Delivery

JNPs have also been investigated for use as targeted drug delivery vehicles. In 2013, Yuan Gao and Yan Yu from the department of Chemistry from Indiana University began experimenting with JNPs as possible drug delivery vehicles. Specifically, they set out to understand the particle-to-cell interactions between a functionalized JNP and a target cell. (Gao & Yu, 2013) By coating one side of their nanoparticles with anti-CD3 antibodies, which bind T cell receptor complexes leading to endocytosis, and the opposing side with aluminum coated with Bis(trimethylsilyl)acetamide (BSA), Gao and Yu were able to examine how these particles are absorbed into a target cell. They found that these nanoparticles will absorb into the target cell, but the speed of the absorption will depend on the nanoparticle orientation once

it encounters the cell. Figure 1.4 shows images of how these nanoparticles are absorbed into cells. Absorption was found to be faster if the antibody hemisphere contacted the cell wall first as opposed to the metallic hemisphere. The cell will appear to bond to the nanoparticle and pull the nanoparticle in via its antibody-coated side, but form around the metallic side until the nanoparticle is completely engulfed within the cell. This process is similar if the metallic hemispheres contact the cell first, but since the cell must first form around the nanoparticle in an attempt to reach the antibody-coated hemisphere, the process is slower.

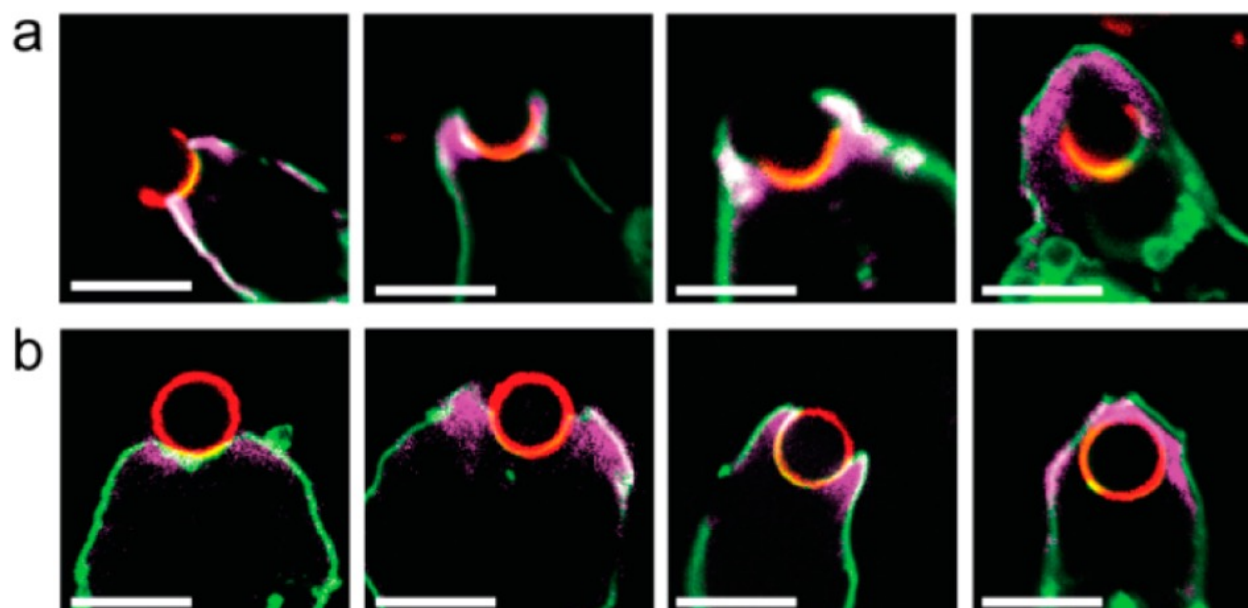


**Figure 1.4** Images showing the different uptake timelines of a JNP with anti-CD3/metallic hemispheres (a) and a nanoparticle completely coated in anti-CD3 antibodies (b). As predicted, the nanoparticle in (b) is easily absorbed into the cell. In (a), the anti-CD3 hemisphere (shown in red) is absorbed first, then the cell develops around the opposing hemisphere of the particle until the nanoparticle is completely absorbed. Reprinted with permission from Gao & Yu. Copyright 2013, American Chemical Society.

Researchers also investigated using one nanoparticle to carry multiple drugs to one location. A group from the Sanford-Burham Medical Research Institute in La Jolla, Ca were able to prepare JNPs with hemispheres consisting of paclitaxel and doxorubicin hydrochloride. (Xie, She, Wang, Sharma, & Smith, 2012) This method of coating the drug molecules on respective sides of one nanoparticle allows for delivery of both of these drugs to one site. Upon in-vitro testing, the drug release profiles of the Janus

nanoparticles were essentially the same as the profiles yielded from monophasic particle delivery vehicles.

In 2014, researchers from Fudan University in Shanghai were also able to develop a dual-hemisphere drug delivery vehicle. (X. Li et al., 2014) Researchers coated an upconversion nanoparticle (they used two different fluorophore cores in their experiments) with mesoporous silica, then grew a mesoporous organosilica nanocomposite on one side of the original nanoparticle, creating a nanostructure in the size range of 300 nm. The silica coated structure is hydrophilic, has a specific pore size, and near infrared (NIR) and UV-vis optical properties; this means that a specific drug can be loaded to this structure and released via a light triggered mechanism. The organosilica structure is hydrophobic, has a different pore size and is more susceptible to changes in temperature, meaning a different drug can be loaded to this structure and released via a heat change. Researchers found that their Janus nanostructures could achieve more than a 50% greater release of cancer killing drugs when compared to single-triggered drug delivery systems. Figure 1.5 shows an illustration of these Janus nanostructures.

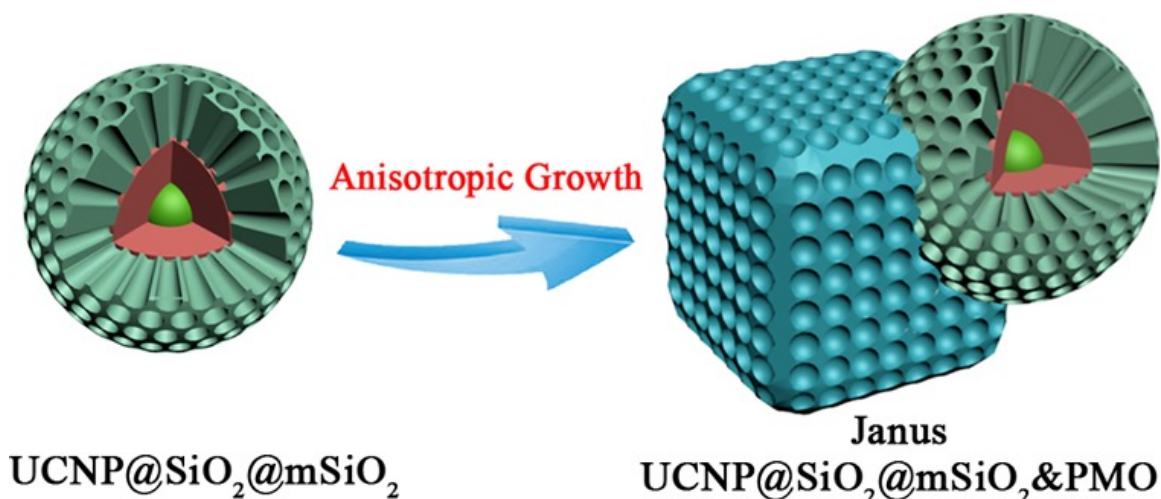


**Figure 1.5** Janus nanostructures composed of a silica coated upconversion nanoparticle and mesoporous organosilica nanostructure. Reprinted with permission from X. Li et al. Copyright 2014, American Chemical Society.

### 1.2.3 Janus Nanoparticles for Improved Emulsion Stabilizers

Researchers have identified that both surfactants and nanoparticles can be used to stabilize emulsions; nanoparticles can adsorb to the oil-water interface and the amphiphilic nature of surfactants

helps reduce interfacial tension between the emulsified liquids. (Katepalli, 2014) Amphiphilic JNPs can combine the advantages of nanoparticles and surfactants in form improved emulsion stabilizers. In 2014, Nina Zahn and Guido Kickelbel from Saarland University in Saarbrücken, Germany were able to create amphiphilic JNPs that produced emulsions that remained stable for longer durations than emulsion stabilized by monophasic nanoparticles. (Zahn & Kickelbick, 2014) Zahn and Kickelbel modified anatase (mineral form of titanium) and silica nanoparticles with hydrophobic and hydrophilic compounds to form dual-hemispheres, then used these nanoparticles to stabilize an oil-in-water Pickering emulsion. When comparing this emulsion to others done with unmodified nanoparticles, the JNP structures showed a significantly longer stabilized duration. More specifically, of the nanoparticle configurations that they tested, unmodified anatase nanoparticles stabilized the emulsion for 10 minutes, while the JNP configurations showed stability from 8 hours to over 2 days.

In 2015, knowing that JNPs can act as effective emulsion stabilizers, a research group at the Key Laboratory of Polymeric Materials and Application Technology in the Hunan Province of China used JNPs to form macrocellular polymer foams with imbedded palladium particles to act as a catalyst for the Suzuki-Miyaura carbon-carbon coupling reaction. (Yi, Xu, Gao, Li, & Chen, 2015) JNPs were created by crosslinking poly(4-vinylpyridine) and poly(methyl methacrylate)-b-poly(4-vinylpyridine)(PMMA-b-P4VP) polymers to create a nanoparticle with a P4VP head group and a PMMA tail group. Once these JNPs were adsorbed to the liquid-liquid interface, palladium particles could be loaded on the PMMA head group and used to catalyze the reaction. These nanoparticles were found to act as effective stabilizing agents for their emulsions. Figure 1.6 shows samples of their emulsions with different JNP concentrations, as well as samples with different internal phase volume fractions.



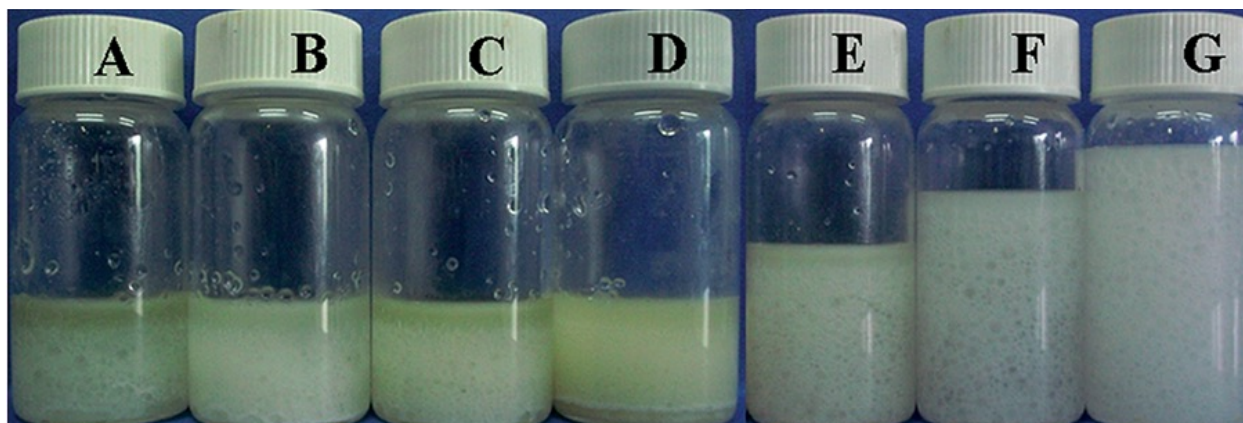


**Figure 1.6** Sample of emulsions stabilized with JNPs. Sample a-d contain a fixed internal phase volume fraction with varied amounts of JNPs versus the total weight of the oil phase (a - 0.055%, b – 0.11%, c – 0.16%, d – 0.22%). Looking at a-d, the line between the emulsion and the oil phase becomes less clear, signifying a more stable emulsion. It is also important to notice that large droplets (black dots in emulsion) that appear in (a) and slowly diminish in (b), (c), and (d). This phenomenon identifies a more stable and uniform emulsion, again strengthening the assertion that JNPs help stabilize emulsions. Vial e-g have a fixed % of JNPs (0.16%) and vary in internal phase volume fraction (83.3%, 87.5%, and 90% respectively). All vials show no noticeable oil phase, further asserting this theory. (Photographs of these emulsions were taken 24 hours after mixing). Adapted from Yi et al. with permission of The Royal Society of Chemistry.

#### 1.2.4 Other Application for Janus Nanoparticles

JNPs have other applications that have not been as heavily researched. In 2013, a research group from the Complutense University of Madrid in Spain used a Janus nanostructure to develop an electrochemical biorecognition signaling system. Using both silica and gold nanoparticles, researchers were able to develop a nanostructure that could recognize the presence of biotin on a gold surface. (Sánchez, Díez, Martínez-Ruíz, Villalonga, & Pingarrón, 2013) Using horseradish peroxidase, an enzyme that acts as a fluorimetric or luminescent labeling molecule, and streptavidin, a bacterium that bonds to biotin with a high affinity, researchers were able to develop a two-sided nanostructure that could locate biotin-bound proteins via fluorescence. Methoxypolyethylene glycol thiol (PEG-SH) was also added to available sites on the gold nanoparticle surface to increase the solubility of this nanostructure. Figure 1.7 illustrates the synthesis strategy for these nanostructures. This strategy, done as a proof of concept, shows that JNPs and Janus nanostructures have the potential to be used to locate specific proteins depending on the compounds functionalized on the hemispheres.

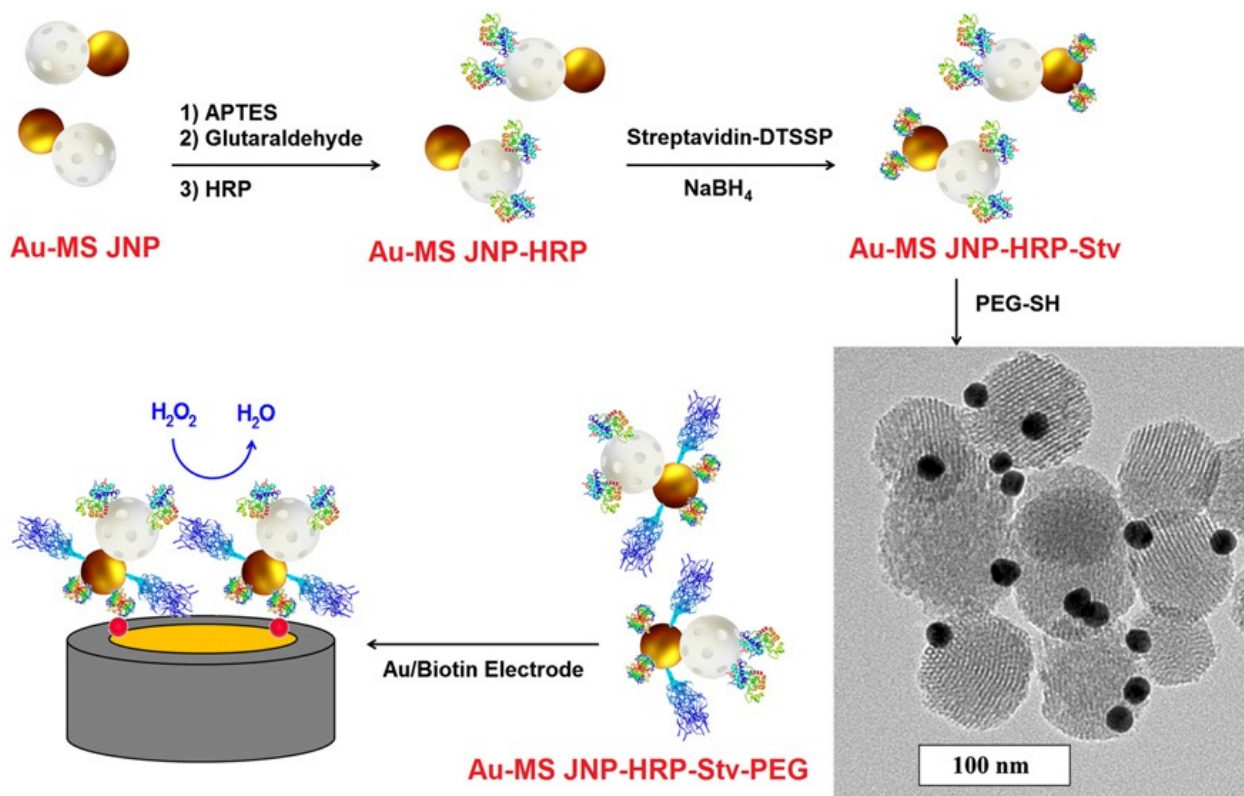


**Figure 1.7** Strategy to develop nanostructures that can act as electrochemical biorecognition-signaling systems for biotin. First, the gold and silica nanoparticles are bound together, then horseradish peroxidase is used to coat the silica face of the structure. Streptavidin is then added to the gold nanoparticle surface, followed by PEG-SH, which will bond to the remaining open sites on the gold nanoparticle surface. Reproduced from Sánchez et al. with permission Elsevier.

As mentioned previously, JNPs can also be used to produce more effective catalysts. By modifying titania, a commonly used catalyst, with gold nanoparticles, researchers at the University of Jinan in China were able to increase the photoactivity of titania and greatly improve its use as a catalyst. By creating a Janus nanostructure of gold and titania nanoparticles, the gold is able to slow down the regeneration of photogenerated charge carriers, and in that greatly increase the photocatalytic activity of titania. (Naoi, Ohkao, & Tatsuma, 2004)

### **1.3 Synthesis Methods for Janus Nanoparticles**

Developing methods for synthesis of JNPs continues to be a challenge. Strategies developed include the use of small molecules that grow into particles with differing hemispheres, or the protection of one hemisphere of a nanoparticle while modifying the other. Despite the challenges of JNP synthesis (controlling specific hemispherical functionalization's, avoiding nanoparticle crosslinking, etc.), numerous synthesis methods for JNPs have been accomplished; these methods can be separated into three categories: masking, block-copolymers, and phase separation.

#### **1.3.1 Synthesizing Janus Nanoparticles via the Masking Method**

The masking method, one of the first methods utilized to synthesize JNPs, had already been applied in the synthesis of large Janus particles, so applying it to nanoparticles was a logical step. (Walther & Muller, 2008). Simply put, this method involves protecting one hemisphere of a nanoparticle so that the other hemisphere is allowed to bond/interact with a selected modifier, such as an enzyme, surfactant, protein, or even a different nanoparticle. This method is normally accomplished by suspending nanoparticles between two different phases; solid-liquid and liquid-liquid masking methods are very common, but liquid-gas masking is also possible.

Performing a masking method by solid-liquid interface suspension involves stabilizing nanoparticles on a solid surface, such as a flat plate with available functional groups on the surface, and either flowing liquids over the plate or submerging the plate in liquid. The concept of solid-liquid interface synthesis also helped develop JNP synthesis strategies; stabilizing a nanoparticle onto another nanoparticle and then modifying them with compounds contained in the liquid phase. In 2007, a research group from the University of Utah was able to create gold JNPs utilizing this method. Using a silanized glass surface, researchers were able to stabilize gold nanoparticles on a flat plate and modify the exposed side with 11-mercapto-1-undecanol. (Sardar, Heap, & Shumaker-Parry, 2007) The nanoparticle-covered plate was then placed in a liquid suspension and sonicated in the presence of either 16-mercaptohexadecanoic or mercaptoethylamine. This step allowed the nanoparticles to release from the plate, exposing the hemisphere that was previously protected by the plate, and allowing said hemisphere to be functionalized by one of the two secondary compounds. After final washing steps, dual-functionalized gold JNPs were achieved. Figure 1.8 shows an illustration of this process.

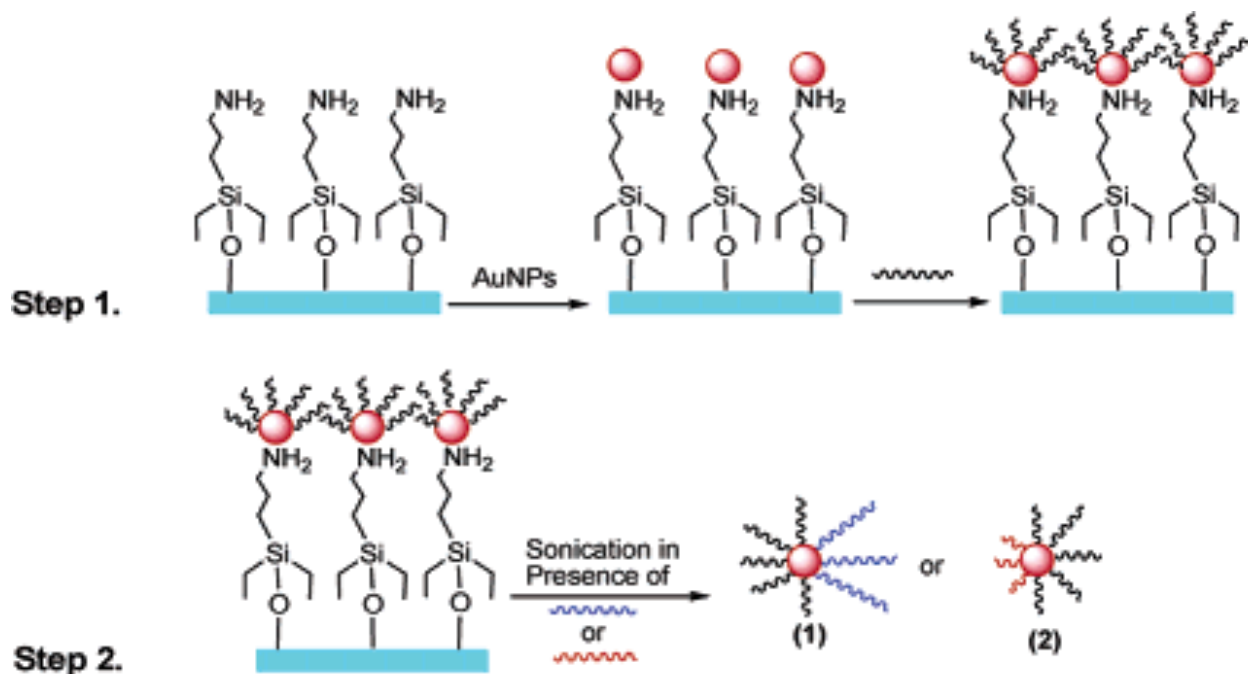


**Figure 1.8** Illustration of how Sardar et al. used solid-liquid masking to produce JNPs. Gold nanoparticles are bonded to a silanized flat plate, then modified with a polymer suspended in a liquid. The particles are then released via sonication and modified with one of two new polymers on their unmodified hemisphere. Reprinted with permission from Sardar et al. Copyright 2007, American Chemical Society.

Another example of JNPs via solid-liquid interface masking was accomplished in 2013 by a group from the University of South Carolina. By using both 500 nm and 15 nm silica nanoparticles, researchers were able to mask the smaller silica nanoparticles onto the larger ones, then modify them accordingly. (J. Li, Wang, & Benicewicz, 2013) This group chose to take advantage of the copper-mediated click reaction to attach their particles (a click reaction is defined as a simple, fast, and versatile reaction that gives high product yields). (Hein, Liu, & Wang, 2009) Once the smaller nanoparticles had formed a layer around the larger ones, azido-capped poly (methyl methacrylate) in dimethylformamide (DMF) was added to the nanoparticle suspension, forming a polymer layer on one hemisphere of the smaller nanoparticles. Upon sonication, the smaller nanoparticles (now JNPs) are released and the larger nanoparticles can be recycled to run the synthesis again. Figure 1.9 shows an illustration of this process.

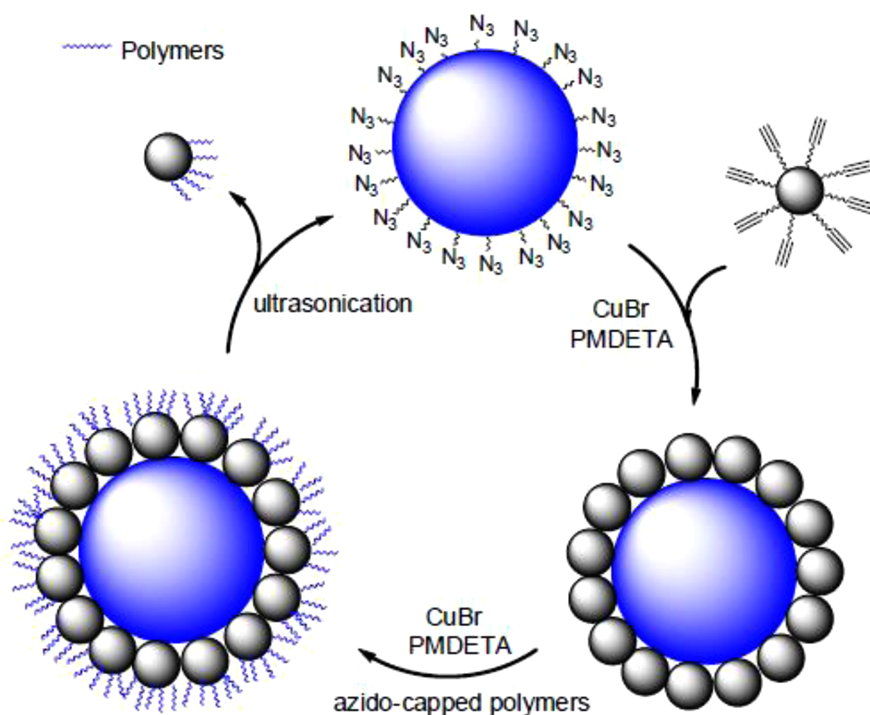


**Figure 1.9** Illustration of JNPs synthesized by a particle-on-particle solid-liquid interface masking method. Smaller nanoparticles are grafted to the surface of larger nanoparticles, modified on one hemisphere, then released as multimodal nanoparticles. Reprinted with permission from J. Li et al. Copyright 2013, American Chemical Society.

Similar to a particle-on-particle style of masking, using wax-in-water emulsions is a popular method for synthesizing JNPs. A research group from the University Bordeaux in Pessac, France was able to synthesize JNPs using a wax-in-water Pickering emulsion. (Perro, Meunier, Schmitt, & Ravaine, 2009) Initially, researchers used silica nanoparticles to stabilize a wax-in-water emulsion, and when the wax was allowed to dry, the nanoparticles had become suspended at the surface, leaving one hemisphere exposed. The nanoparticles were then exposed to a solution of aminopropyltriethoxysilane (APTES), which modified the exposed hemisphere and created JNPs. Figure 1.10 shows an illustration of this process.

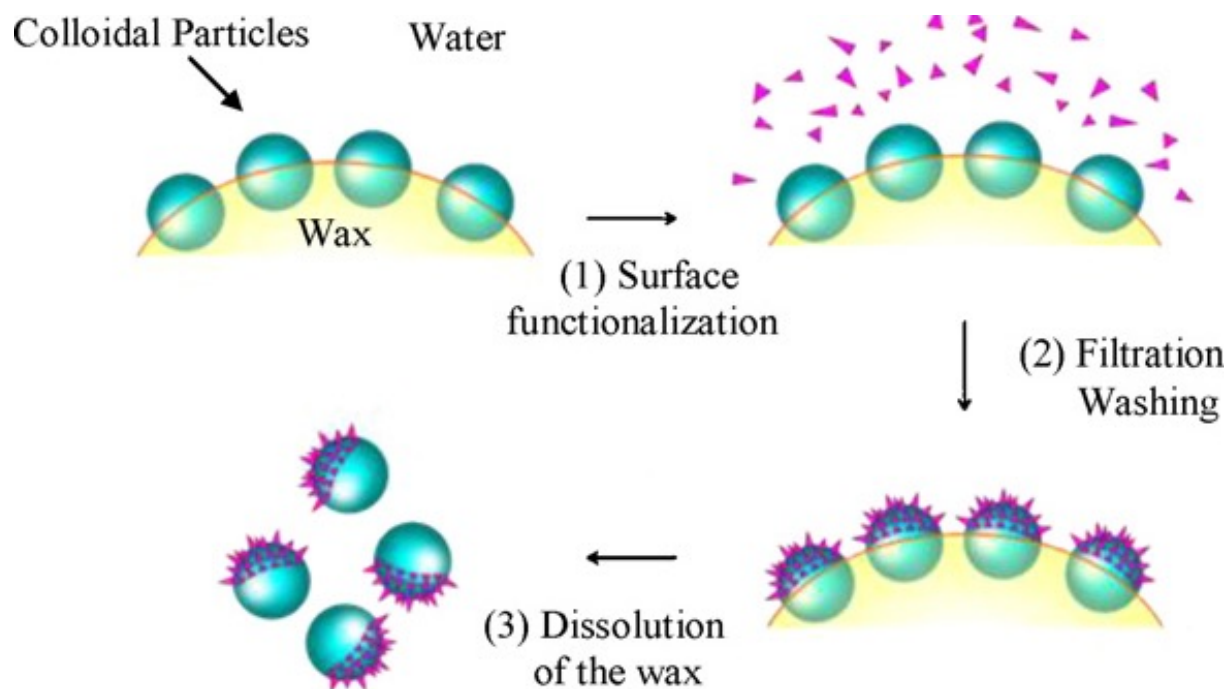


**Figure 1.10** Illustration of how JNPs can be formed using wax-in-water emulsion. While the pink polygons in this illustration represent APTES, this method will allow the use of many different modifying compounds; the compound will depend on what can bond to the nanoparticle surface. Reprinted with permission from Perro et al., 2009, with permission from Elsevier.

Synthesizing JNPs using liquid-liquid interface masking is also feasible. In 2004, as a proof-of-concept exercise, a research group from Hong Kong University developed Janus nanostructures using the interface between an organic solvent/aqueous solution emulsion. (Gu, Yang, Gao, Chang, & Xu, 2005) The team combined two nanoparticle suspensions, iron oxide nanoparticles in an organic solution and silver nanoparticles in an aqueous solution, and created an emulsification to force them to bond. The iron oxide nanoparticles acted as a stabilizing agent for the emulsion, forming a protective barrier around the microdroplets of organic solvent. This nanoparticle barrier exposed one hemisphere of the iron oxide nanoparticles to the aqueous phase of the emulsion, allowing the silver nanoparticles to bond to the available iron oxide surface via covalent bonding. Figure 1.11 shows an illustration of this process. After removing the newly formed nanostructures from the emulsification, researchers were able to selectively modify one of the two nanoparticles that makeup the nanostructure. This method has been repeated by other research groups with positive results; Glaser et al. was also able to synthesize Janus nanostructures via an organic solvent/aqueous solution interface. (Glaser, Adams, Böker, & Krausch, 2006)



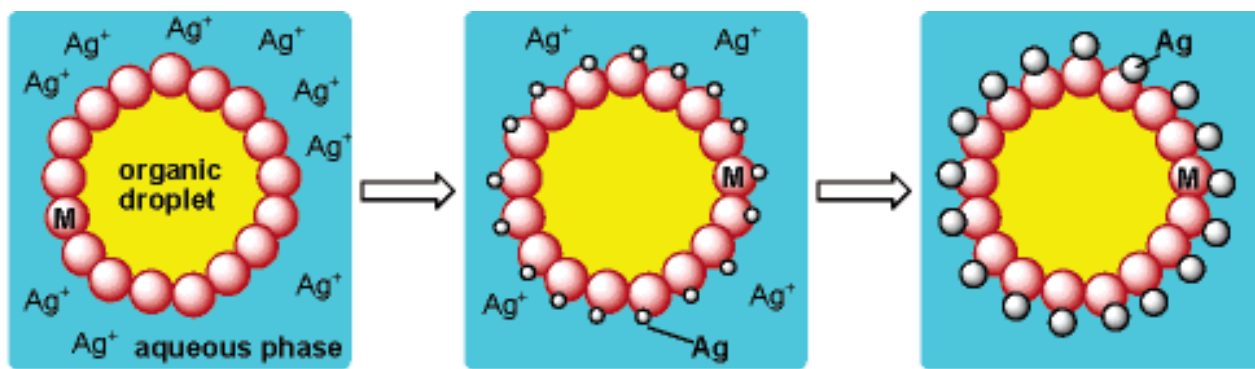


**Figure 1.11** Illustration of how Janus nanostructures can be formed using liquid-liquid interface masking. Once the organic solvent and aqueous liquid are emulsified, the iron oxide nanoparticles (shown in pink) will form a protective barrier around the microdroplets of organic solvent, and thus exposing one of their hemispheres. The silver nanoparticles in the aqueous solution are then free to bond to that hemisphere. Adapted with permission from Gu .et al. Copyright 2005, American Chemical Society

The final masking technique for JNPs synthesis takes place at the gas-liquid interface. In 2007, a research group from the University of California in Santa Cruz was able to synthesize gold JNPs by masking at the air-water interface. Using strategies adopted from the Langmuir method, which involves the forming of a thin monolayer of substrate on top of a liquid by means of compressing the liquid, researchers were able to develop a layer of hexanethiolate-capped gold nanoparticles at the air-water interface. (Pradhan, Xu, & Chen, 2007) Once the layer was formed, mercaptopropanediol was added to the water phase, causing an exchange reaction to occur with the available hexanethiolate ligands. When the monolayer was removed from the liquid, JNPs with hemispheres of hexanethiolate and mercaptopropanediol were yielded. Figure 1.12 illustrates this synthesis method.

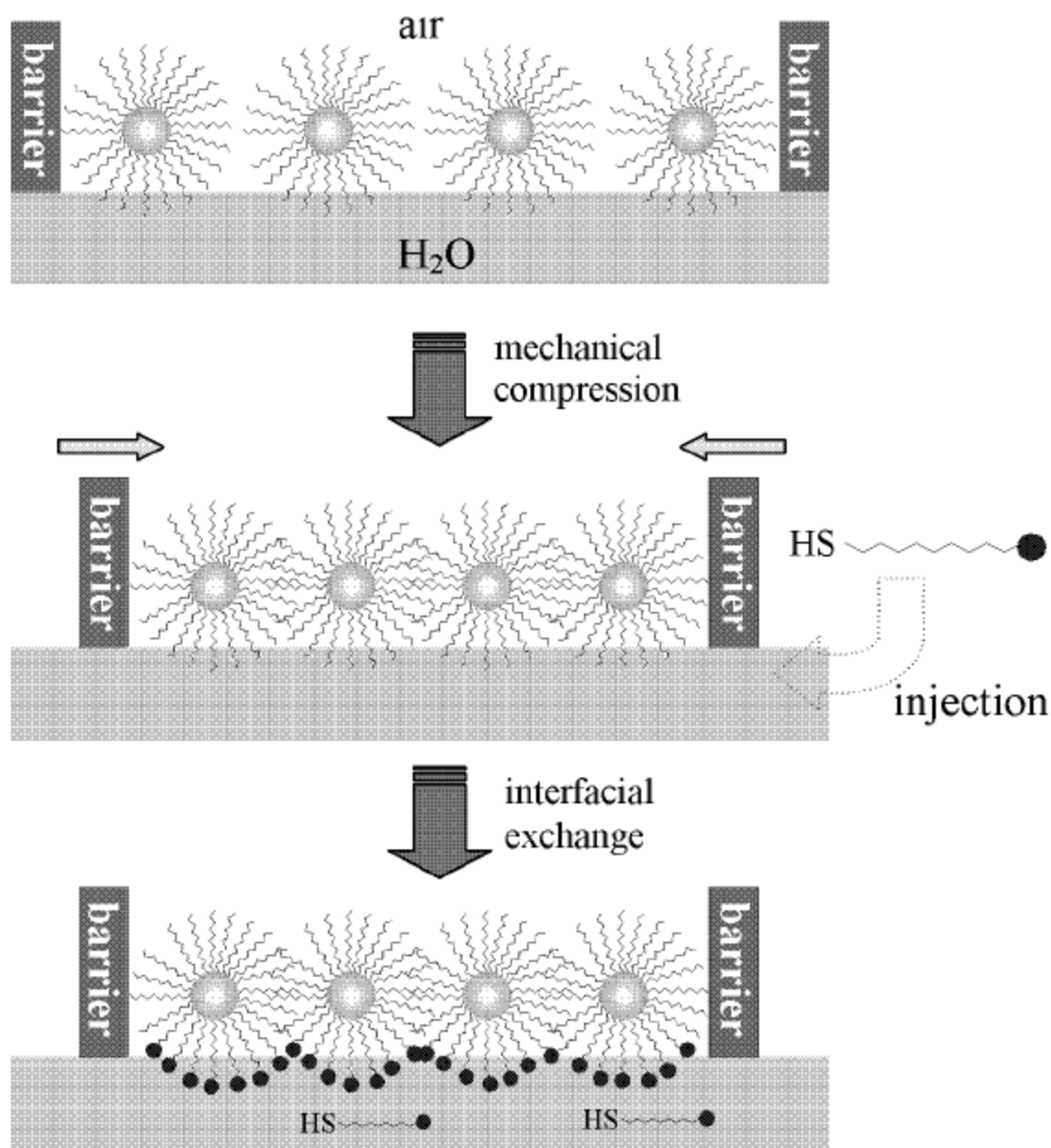


**Figure 1.12** Illustration of how JNPs can be formed at the gas-liquid interface. Once the nanoparticle layer is formed at the surface barrier, scientists are able to modify one hemisphere of the nanoparticles as long as the modifying compound is contained in the aqueous layer. Reprinted with the permission of Pradhan et al., 2007, with the permission of John Wiley and Sons, Inc.



### 1.3.2 Synthesizing Janus Nanoparticles via Block-Copolymers

Opposed to using a nanoparticle core and modifying the hemispheres, the block-copolymer method utilizes polymer chains of well-defined geometry to form a nanoparticle and different hemispheres simultaneously. (Lattuada & Hatton, 2011) Using either diblock copolymers or triblock copolymers, larger order structures can be formed that can later be crosslinked and dismantled to form JNPs. In 2000, Erhardt et al were able to synthesize JNPs with this method using the triblock copolymer polystyrene-b-polybutadiene-b-poly(methyl methacrylate). (Erhardt et al., 2001) Once polymerized, these polymer chains formed organized layers of both polystyrene and poly(methyl methacrylate); the polybutadiene in between these two polymers was therefore forced in between these layers and tightly packed on other polybutadiene chains. The polybutadiene will become the core of the JNP, while the other two polymer chains will become the opposing hemispheres. The entire structure is then cross-linked and run through selective washing steps and the newly formed JNPs are resuspended. Figure 1.13 shows an illustration of how this process occurs.

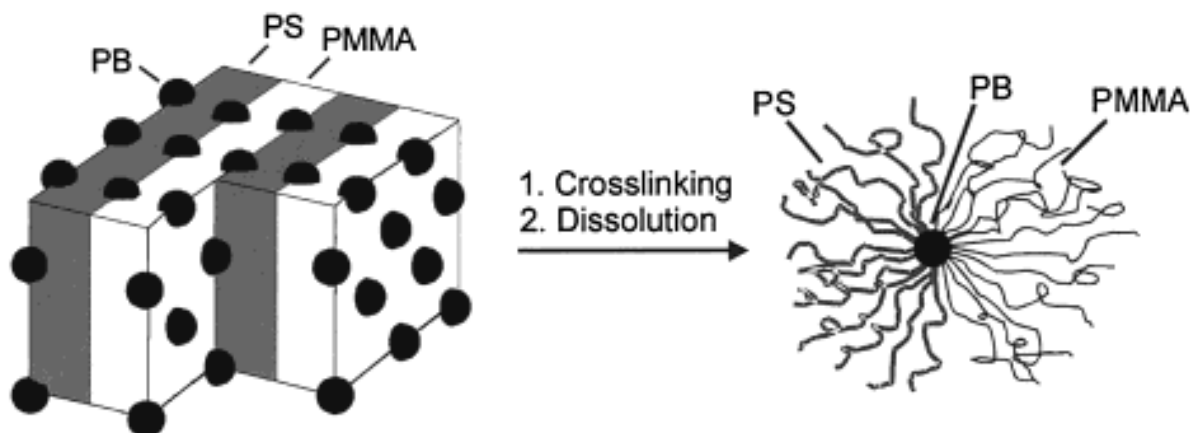


**Figure 1.13** Illustration showing the process of synthesizing JNPs using block copolymers. Reprinted with permission from Erhardt et al. Copyright 2001, American Chemical Society.

Block-copolymers have also been used to form ultra-thin films as a template for creating JNPs. In 2015, a research group in Belgium was able to prove the efficacy of this method by producing multimodal gold nanoparticles. Starting with the diblock copolymer polystyrene-b-poly (4-vinylpyridine), researchers created a thin film between 20 and 50 nm in width. (Poggi, Bourgeois, Ernould, & Gohy, 2015) Considering the nature of how block-copolymers oriented themselves, the film was saturated with core areas of poly (4-vinylpyridine), and surrounding areas of polystyrene. However,

since they formed a thin film, the poly (4-vinylpyridine), cores were not completely surrounded by polystyrene, leaving them open to functionalization. The top-left image in Figure 1.14 shows an illustration of this orientation. Available poly (4-vinylpyridine) was then exposed to gaseous 4-bromo-1-butyne so that alkyne groups could be added. Researchers concluded that 10-15% of available poly (4-vinylpyridine) chains developed an alkyne group from this process. The films are then exposed to 1,4-diiodobutane vapor to crosslink the non-functionalized poly (4-vinylpyridine). Finally, the films are exposed to PEG-N<sub>3</sub>, which bonds to the available alkyne groups to form one of the two hemispheres of the final nanoparticle. Finally, the films are dissolved and the finished Janus nanoparticles are washed and collected, now exhibiting a hemisphere of polystyrene and a PEG hemisphere. An illustration of this synthesis method is shown in Figure 1.14.

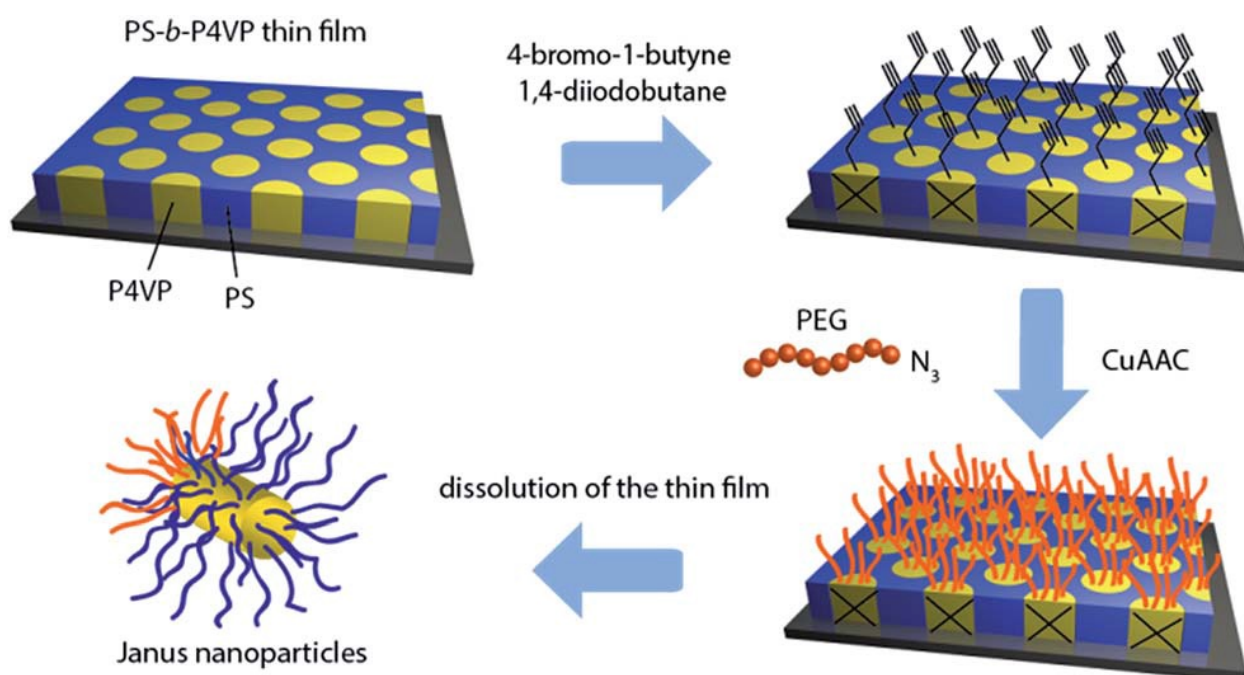


**Figure 1.14** Illustration of synthesis method for JNP using a thin film comprised of diblock copolymers and a secondary PEG compound to form a second hemisphere. Reproduced from Poggi et al. with permission from The Royal Society of Chemistry.

Block copolymers can also be used to synthesize JNPs without using a portion of their structure to create a nanoparticle core. The research group from the University of Jinan in China mentioned previously in this report, who used nanoparticle structures to increase the photoactivity of titania, used a

diblock copolymer as a stabilizing agent to synthesize their gold/titania JNPs. (Fu et al., 2011) By mixing polystyrene-b-poly (ethylene oxide) with chloroauric acid, researchers were able to create micelles with chloroauric acid situated inside of a diblock-copolymer structure. Titania sol-gel precursor was then added to the mixture, which infiltrated the micelles and contacted the chloroauric acid. Thin films of this mixture were produced via spin-coating, then allowed to dry to force the titania sol-gel precursor to react with the chloroauric acid. The films were then exposed to UV light, causing the chloroauric acid to reduce to metallic gold and remove the block copolymers from the newly formed nanoparticles. The final product is a gold/titania nanostructure, shown in image (d) of Figure 1.15.

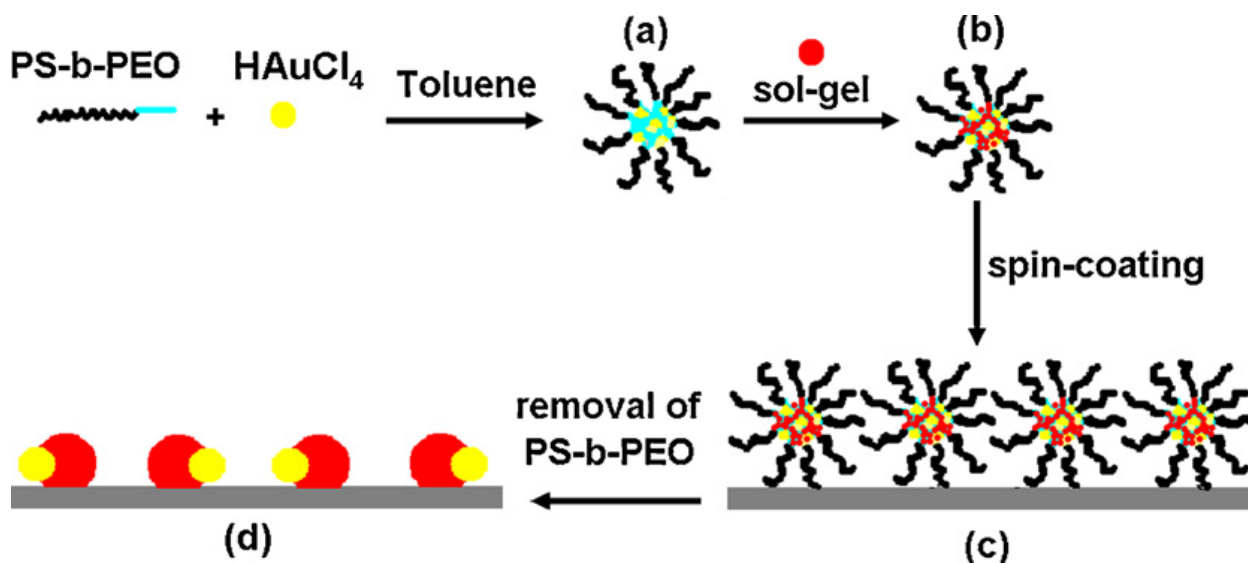


**Figure 1.15** Illustration of how gold/titania Janus nanostructures were formed using diblock copolymers as a stabilizing structure. Reprinted with permission from Fe et al., 2011, with permission from Elsevier.

### 1.3.3 Synthesizing Janus Nanoparticles via Phase Separation

The last general method for JNP synthesis is the phase separation method; this method involves combining two incompatible substances, either organic or inorganic, that will separate into distinct hemispheres and form JNPs. A specific version of this method is called co-jetting, where two incompatible fluids are combined at a fine point and allowed to form a nanoparticle, then held together by an additional force (commonly shear force from a flowing liquid or force from an electric field). (Lattuada & Hatton, 2011) Other than co-jetting, the flame synthesis methods falls within this category. In this case, incompatible compounds are combined via combustion as opposed to a fine point drip.

(Lattuada & Hatton, 2011) Examples of JNPs that have been synthesized using phase separation are to follow.

In 2009, a research group from the University of Michigan was able to use electrohydrodynamic co-jetting to create JNPs composed of polyacrylamide/poly(acrylic acid) polymer strands (PAAm-co-AA) with hemispheres that had both an affinity for human endothelial cells and no affinity toward them. (Yoshida et al., 2009) Developed by the Lahann Lab, electrohydrodynamic co-jetting involves the addition of a large electric field to a co-jetting apparatus. This electric field stretches the fluids and evaporates the solvent that the soon-to-be nanoparticle components are suspended in. Using an electric field also gives researchers more control over the final size and hemisphere coverage ratio of the JNPs. (Lahann, n.d.) Using this method, researchers were able to synthesize JNPs by combining (PAAm-co-AA) strands functionalized with biotin and (PAAm-co-AA) strands functionalized with acetylene. Once combined, the nanoparticles are totally functionalized with PEG to increase absorption in the body, and the biotin-coated hemisphere is functionalized with streptavidin, which will later bond to the biotin of a cell-specific antibody. Figure 1.16 shows an illustration of this JNP, using the PECAM antibody as an example.

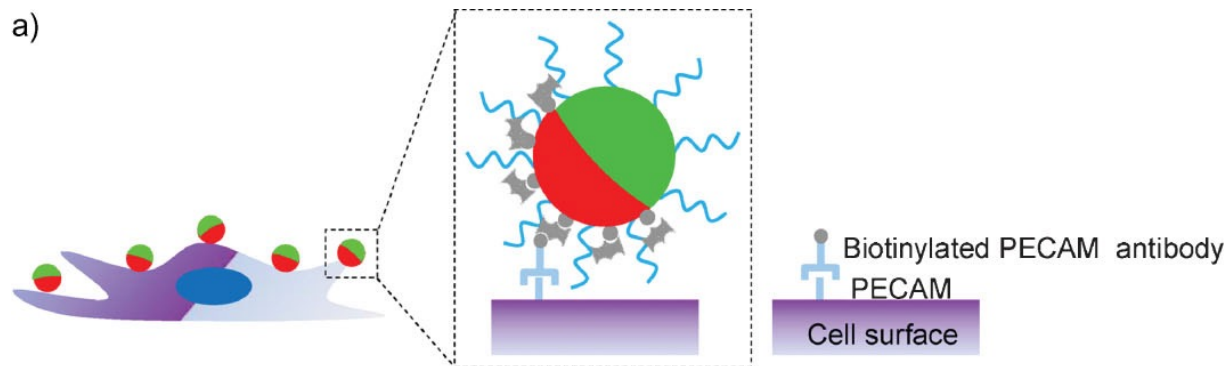


**Figure 1.16** Illustration of the JNPs synthesized via electrohydrodynamic co-jetting. The wavy blue lines represent the PEG compound that was attached to improve bioavailability; the grey circles indicated biotin both bound to the nanoparticle surface and the PECAM antibody; the grey rectangular polygons represent streptavidin that will bind to biotin. The green side of the nanoparticle represents the hemisphere coated with acetylene, while the red side represents the hemisphere coated with biotin. Adapted with the permission of Yoshida et al., 2009, with the permission of John Wiley & Sons, Inc.

In 2011, researchers at the Sanford-Burnham Medical Research Institute in LA Jolla, California were able to synthesize JNPs using co-jetting; they utilized a flowing channel in order to collect/form their nanoparticles. (Xie et al., 2012) As a proof of concept exercise, PLGA was mixed with either the dye Nile Red in dimethylformamide or one of two green dyes in acetone (Rh-6G or FITC-dextran). Below the point where the two solutions met, a channel of 1.0% PVA in water was flowing; the shear force of the fluid in the channel removed the solvents from the two co-jetted solutions and helped form the JNPs. An illustration of this method, as well as images of the resulting nanoparticles is shown in Figure 1.17 and Figure 1.18, respectively.

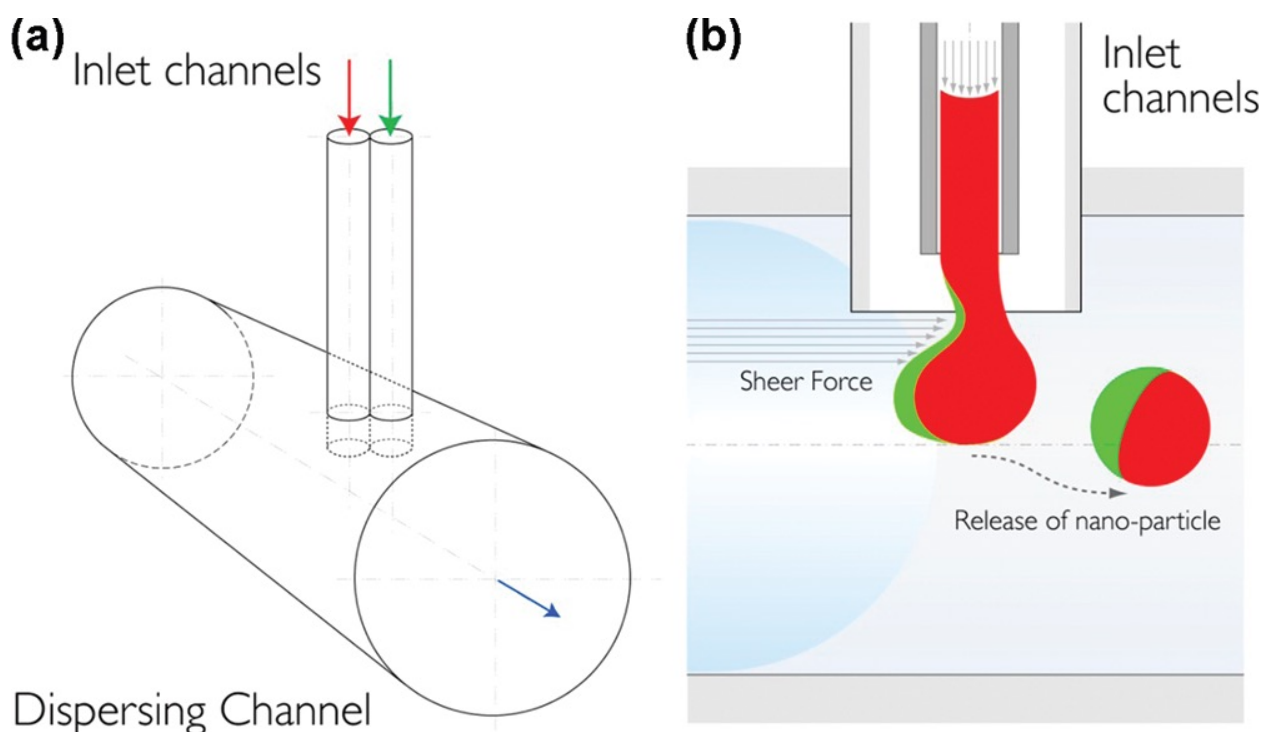


**Figure 1.17** Illustration of the co-jetting process that was used by Xie et al. to form JNPs. Reprinted with permission from Xie et al. Copyright 2012, American Chemical Society.

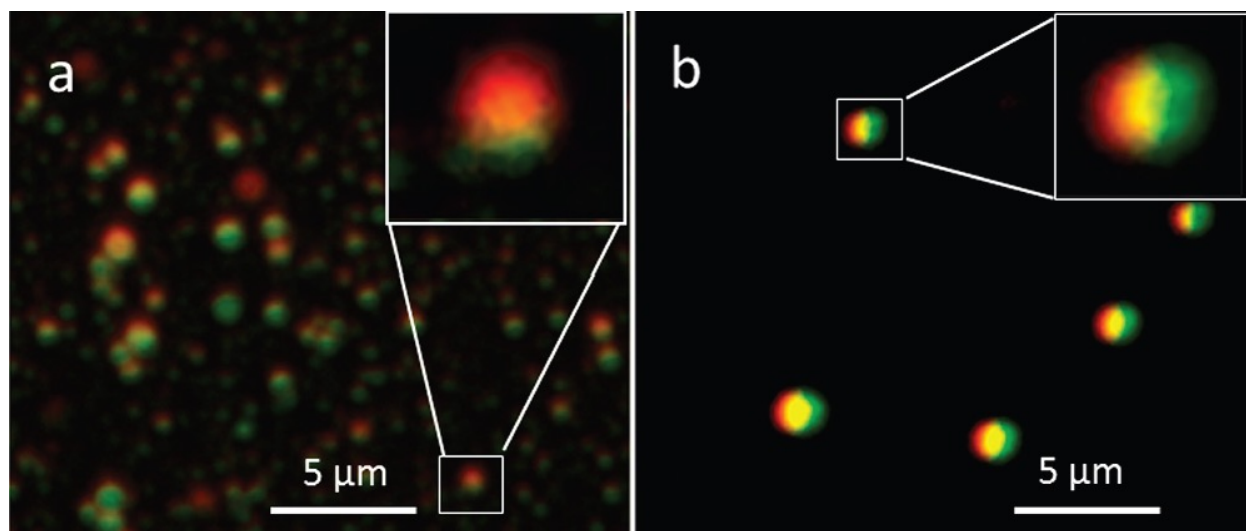


**Figure 1.18** Confocal laser scanning microscope images taken of the JNPs created via co-jetting by Xie et al. Image (a) shows the JNPs that were synthesized using the dyes Nile red and Rh-6G; image (b) shows the JNPs that were synthesized using Nile red and FITC-dextran. Reprinted with permission from Xie et al. Copyright 2012, American Chemical Society.

In 2004, researchers from the Hong Kong University of Science and Technology were able to use phase separation to synthesize Janus nanostructures composed of magnetic nanoparticles and quantum dots. (Gu, Zheng, Zhang, & Xu, 2004) Researchers began by synthesizing iron platinum (FePt) nanoparticles and coating them with sulfur. By reacting the coated particles with cadmium acetylacetonate and other non-contending compounds at a high temperature, the coating is changed from sulfur to cadmium sulfide (CdS). Finally, by raising the temperature, CdS goes through a dewetting process and changes to a crystalline state; this changes the shape of the CdS on the nanostructure from a coating to an attached nanoparticle. The final product is a heterodimer with a magnetic nanoparticle and quantum dot nanoparticle. An illustration of this synthesis method is shown in Figure 1.19.

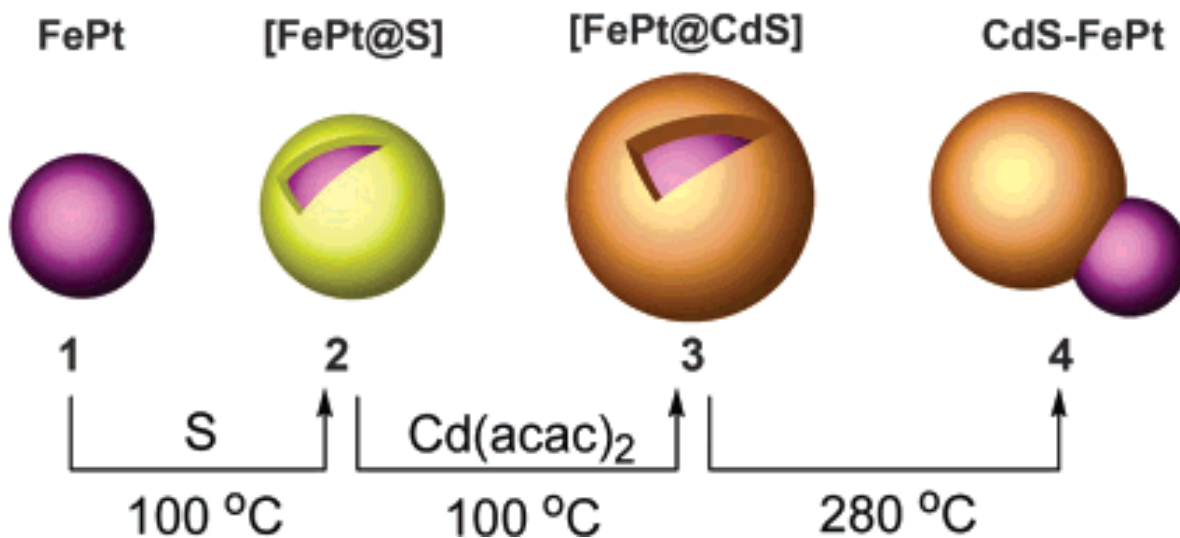


**Figure 1.19** Illustration of how Janus nanostructures can be synthesized using phase separation. By understanding how compounds will react to heat or other compounds, more complex structures can be created. Reprinted with permission from Gu et al. Copyright 2004, American Chemical Society.

As mentioned previously, flame synthesis is also a variant of the phase separation method. The nanoparticle precursors are dissolved in a solvent that also acts as a fuel; when the fuel is burned, the precursors break down and recombine to form new molecules and eventually nanoparticles. In 2009, a research group from Beijing was able to use flame synthesis to make JNPs with hemispheres of silica and iron oxide. (Zhao & Gao, 2009) Ferric triacetylacetonate was used as the iron oxide precursor and tetraethyl orthosilicate (TEOS) was used as the silica precursor. Both of these compounds were dissolved in methanol, which also acted as the fuel for the flame. An illustration of a flame synthesis apparatus is shown in Figure 1.20. Once burned, the precursors breakdown and recombined into multimodal nanoparticles and are collected on a rotating tube. The tube is constantly lubricated with water so the newly formed JNPs can be resuspended and removed from the tube into a secondary containment vessel.

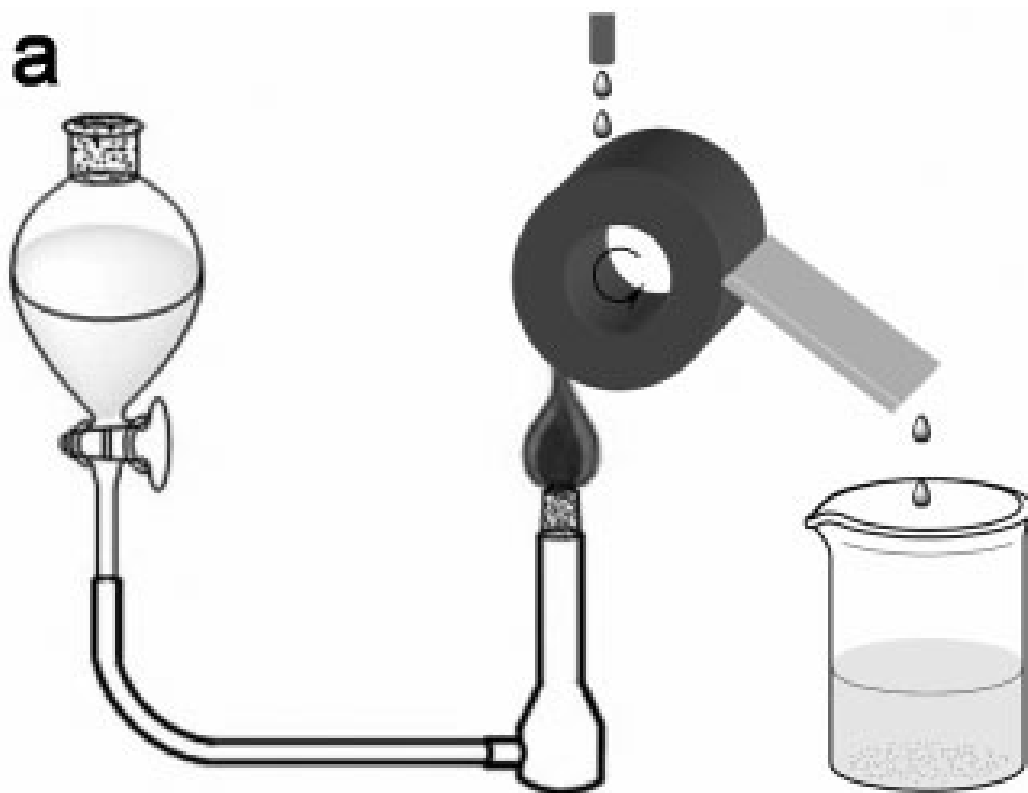


**Figure 1.20** Illustration of a flame synthesis apparatus used to create JNPs. Adapted with the permission of Zhao & Gao, 2009, with the permission of John Wiley & Sons, Inc.

#### 1.4 Challenges with Janus Nanoparticles

Developing a method to produce different JNP configurations (different core materials and difference hemisphere coverage materials) continues to be a challenge. The block copolymer method can be used to synthesize different JNP configurations, but all of them will be composed of polymer, severely limiting the applications of JNPs created via this method. The phase separation method relies on incompatible materials to form opposing hemispheres, a factor that will also limit the number of possible configurations.

Scalability of a JNP synthesis method is also a challenge. Select research groups have asserted that they have developed a method that can be scaled to an industrial level; Perro et al. have claimed that they have a modified version of a wax-in-water masking method that can be scaled to meet industrial demands. (Perro et al., 2009) Pham et al. have stated that by using a version of the block-copolymer method, the amount of Janus nanostructures they can synthesize is limited only by the size of their



reactor. (Pham, Such, & Hawsett, 2015) Verification of these assertions through scaled-up synthesis runs need to be done. Until then research still continues to develop scalable synthesis methods for JNPs.

## Chapter 2

### Synthesizing Janus Nanoparticles using an Iron Oxide Core

#### 2.1 Introduction

Iron oxide nanoparticles have applications in the fields of nano-medicine and drug delivery due to their magnetic properties and biocompatibility. Their superparamagnetic properties give them uses in biomedical imaging, partnered with limited biocompatibility (non-toxic to humans at low concentrations) which gives them application in drug delivery. (Rogers, 2014) These nanoparticles were an optimal choice for our first Janus configuration, due to their attractive properties and the extensive synthesis experience that Dr. Allan David and other group members had with iron oxide. Specifically, we used citric acid coated iron oxide magnetic nanoparticles (CA-MNP) in this first synthesis; oleic acid coated iron oxide magnetic nanoparticles (O-MNP) are synthesized first, then the coating of the nanoparticles is modified via ligand exchange. We used the fatty amine oleylamine and amine-functionalized polyethylene glycol (mPEG-NH<sub>2</sub>) to make up the hemispheres of the final JNP. This JNP should have a hydrophobic hemisphere (fatty acid) and a hydrophilic hemisphere (PEG); we predicted that when placed in a water/hexane mixture that the particle would self-assemble at the liquid interface.

Our synthesis method is based off of the masking method, specifically solid-liquid interface masking. As opposed to using a flat plate as the solid surface, we have utilized functionalized micron-sized silica particles to produce a packed layer in a column. By using micro-sized particles in the pack as opposed to nanoparticles, we can increase the surface area where synthesis can occur. Increased surface area in this version of masking leads to the potential for scalability.

The column pack is composed of spherical silica particles functionalized with the long-chain compound octadecane (C<sub>18</sub>H<sub>38</sub>). The functionalization is the foundation for this synthesis; nanoparticles will eventually be grafted onto a fatty amine coating that is applied to the silica particle pack. That coating is possible because of the attractive intermolecular between octadecane and the hydrophobic tail groups of oleylamine. This method is not limited to this specific packing materials; theoretically, as long

as there is an attractive force between the pack material and one of the two compounds that will eventually make up the hemispheres of the JNPs, the method can be accomplished (different packing material has not been tested). This aspect gives this synthesis method a great deal of flexibility regarding synthesis of different JNP configurations.

## 2.2 Experimental

### 2.2.1 Materials

For the O-MNP synthesis, iron(III) acetylacetonate (iron (III) acac) ( $\text{Fe}(\text{C}_5\text{H}_7\text{O}_2)_3$ ) was obtained from Alfa Aesar. Tetradecanediol ( $\text{CH}_3(\text{CH}_2)_{11}\text{CH}(\text{OH})\text{CH}_2\text{OH}_2$ ) was obtained from Tokyo Chemical Industry (TCI). Oleylamine ( $\text{C}_{18}\text{H}_{35}\text{NH}_2$ ) was obtained from Alfa Aesar. Oleic Acid ( $\text{C}_{18}\text{H}_{34}\text{O}_2$ , 90%) was obtained from TCI. Ethyl Ether ( $(\text{C}_2\text{H}_5)_2\text{O}$ ) was obtained from The British Drug Houses Chemicals (BDH). For the CA-MNP synthesis, citric acid monohydrate ( $\text{C}_6\text{H}_8\text{O}_7$ ) was obtained from Amresco. Dimethylformamide (DMF) ( $\text{C}_3\text{H}_7\text{NO}$ ) was obtained from Amresco. 1,2-Dichlorobenzene (DCB) ( $\text{C}_6\text{H}_4\text{Cl}_2$ , 99%) was obtained from Acros. 1.0 M sodium hydroxide (NaOH) was made from sodium chloride (NaCl) from Amresco and deionized water. For the JNP synthesis,  $\text{C}_{18}$  Spherical Silica Gel was obtained from Sorbtech. 1-ethyl-3-(dimethylaminopropyl)carbodiimide (EDC) ( $\text{C}_8\text{H}_{17}\text{N}_3$ ) was obtained from Alfa Aesar. N-hydroxysuccinimide (NHS) ( $\text{C}_4\text{H}_5\text{NO}_3$ , 98%) was obtained from TCI. mPEG-NH<sub>2</sub> (MW 5000) was obtained from NANOCS. For solvents and washing solutions for all syntheses, chloroform ( $\text{CHCl}_3$ ), hexane ( $\text{C}_6\text{H}_{14}$ ), acetone ( $\text{C}_3\text{H}_6\text{O}$ ), and methanol ( $\text{CH}_4\text{O}$ ) were obtained from BDH. Ethyl Acetate ( $\text{C}_4\text{H}_8\text{O}_2$ , 99%) was obtained from Alfa Aesar. Ethanol ( $\text{C}_2\text{H}_6\text{O}$ ) (200 proof) was obtained from EMD. Deionized water was obtained using an ELGA PURELAB Flex water purification system.

### 2.2.2 Synthesizing Oleic Acid Coated Iron Oxide Magnetic Nanoparticles

O-MNPs were synthesized via thermal decomposition following the method development by Sun et al. Iron (III) acac, tetradecanediol, oleic acid, oleylamine, and benzyl ether were combined in a 100 mL 3 neck round bottom flask. The flask was equipped with a condenser, a temperature probe, and a nitrogen line to provide a blanket over the reaction. The entire apparatus was placed in a heating mantel and allowed to heat at the temperature cycle shown in Table 2.1. Figure 2.1 shows a photograph of the equipment set-up for this synthesis.

**Table 2.1 Heating Cycle for Synthesizing O-MNPs**

| Step | Starting Temp (°C) | Final Temp (°C) | Hold Time (hours) |
|------|--------------------|-----------------|-------------------|
| 1    | 0                  | 100             | 1                 |
| 2    | 100                | 200             | 2                 |
| 3    | 200                | 250             | 1                 |
| 4    | 250                | 25              | Cool down         |



**Figure 2.1** Setup of reaction vessel for synthesizing O-MNPs

Once the heating cycle has completed and the vessel is allowed to cool down to near-room temperature, the reaction apparatus is dismantled and the remaining solution is removed and mixed with methanol and allowed to magnetically separate. Once the nanoparticles have had ample time to separate, the solvent is removed and the nanoparticles are washed three additional times in a 4:1 methanol/hexane mixture, again using magnetic separation to remove the particles between washing steps. The finished nanoparticles are stored in hexane. (Sun et al., 2004)

### 2.2.3 Synthesizing Citric Acid Coated Iron Oxide Magnetic Nanoparticles

The previously synthesized O-MNPs will have their oleic acid coating removed and replaced with citric acid via ligand exchange following the work of Hatakeyama et al. In a 100 mL round bottom flask, dry O-MNPs are combined with citric acid in a 6:5 citric acid to O-MNPs ratio by weight. DCB and DMF are added; the mixture is then put through the following heating cycle described in Table 2.2.

**Table 2.2 Heating Cycle for Synthesizing CA-MNPs**

| Step | Starting Temp (°C) | Final Temp (°C) | Hold Time (hrs) |
|------|--------------------|-----------------|-----------------|
| 1    | 25                 | 120             | 4               |
| 2    | 120                | 80              | 1               |
| 3    | 80                 | 25              | Cool down       |

After the first step of the heating cycle is completed, 2 mL of 1.0 M NaOH is added to the mixture, and the heating cycle is allowed to conclude. Once the mixture cools to room temperature, the nanoparticles are removed from the solvent via magnetic separation. They are then washed multiple times in acetone, ethyl acetate, and methanol, again using magnetic separation to isolate the nanoparticles from the solvent. Upon completion of all washing steps, the nanoparticles are stored in DI water. (Hatakeyama et al., 2011)

### 2.2.4 Synthesizing JNPs with a CA-MNP Core

The packing material for the column is made up of 40-75 micron C<sub>18</sub> Silica particles from Sorbtech. The C<sub>18</sub> coating on the surface of the particles gives us a surface to begin assembling our JNPs. A photograph of our packing material in the column where the JNP synthesis will occur is shown in Figure 2.2.

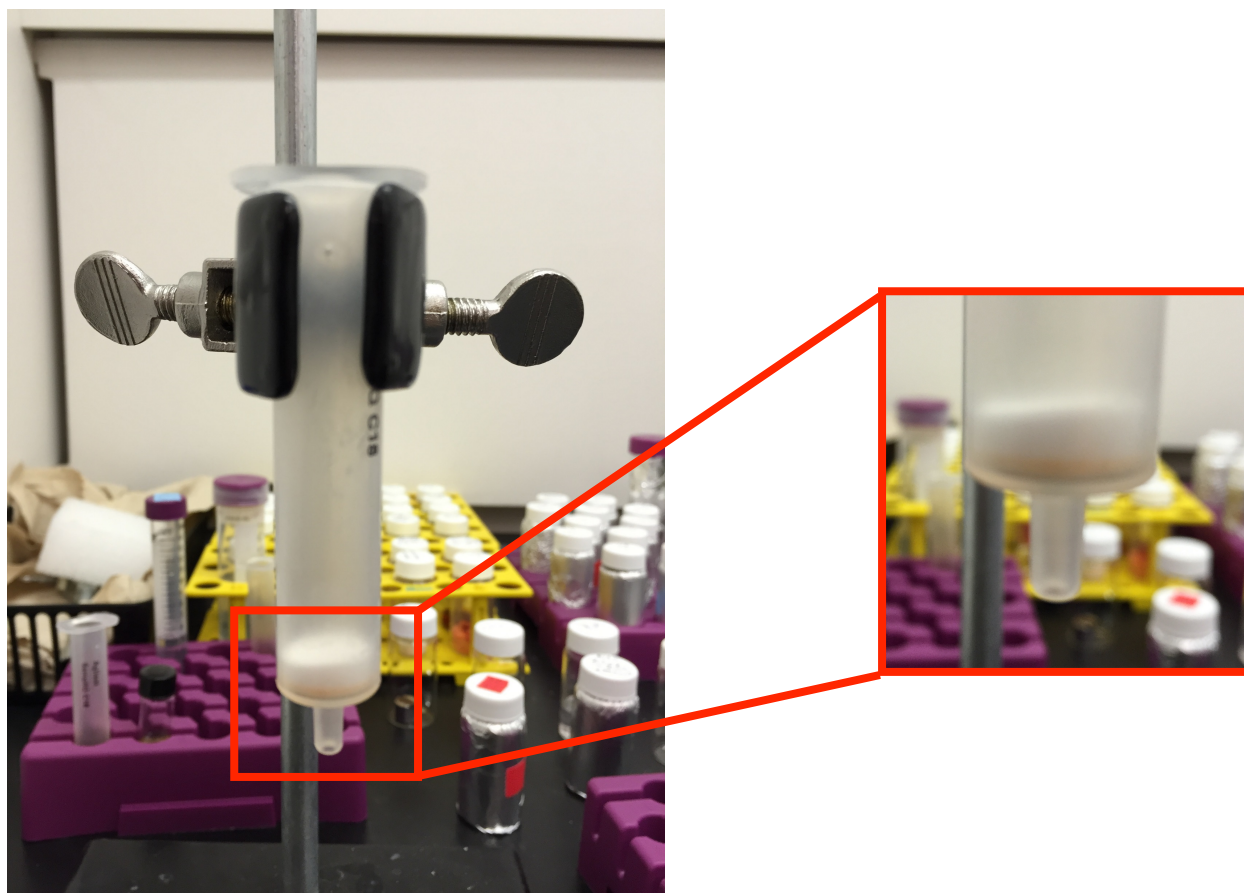


**Figure 2.2** Column with Silica particle pack where formation of JNPs will occur. Pack is supported by a small filter at the end of the column

A solution of oleylamine and ethanol is added to the column first. Once the liquid has passed the filter, the column is sealed to prevent the fluid from escaping and left idle for ten minutes. This time allows the oleylamine to completely coat the silica particles by aligning with the octadecane chains on the surface. After 10 minutes, the fluid is allowed to drain, then the column is washed with a 10% methanol/DI water solution as well as with pure DI water. A mildly diluted sample of CA-MNPs in water is mixed with NHS and EDC to activate the carboxylic acid on the surface and prepare it to bond with available amine groups (Thermo Fisher Scientific, 2016). This mixture is added to the column, which is again sealed and allowed to react for one hour. The column is then drained and washed with DI water. mPEG-NH<sub>2</sub> is dissolved in DI water and added to the column and allowed to react for one hour. The fluid is drained and the column is washed with DI water. Chloroform is passed through the column to remove the newly formed JNPs from the silica pack particles. The solvent is removed via evaporation and the particles are resuspended in a small amount of methanol and allowed to magnetically separate. The final JNPs are

collected and stored in chloroform. Figure 2.3 shows an illustration of the structure of this JNP configuration.

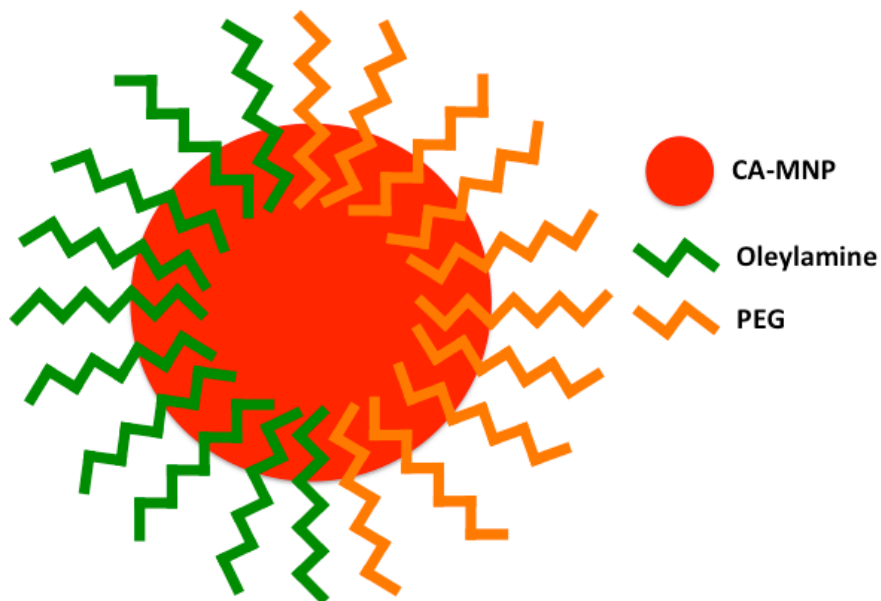


**Figure 2.3** Illustration of the strategy used to assemble a JNP with a CA-MNP core. Oleylamine molecules will bond with the activated carboxylic acid groups, anchoring the CA-MNP to the silica pack particle. mPEH-NH<sub>2</sub> will form the second hemisphere of the JNP

### 2.2.5 Complete Coating of Either Oleylamine or mPEG-NH<sub>2</sub> on CA-MNPs

CA-MNPs completely coated with either oleylamine or mPEG-NH<sub>2</sub> were also synthesized; these nanoparticles were used as control groups to make comparisons to the JNPs. For both cases, CA-MNPs are activated with NHS and EDC, and then allowed to react with either oleylamine or mPEG-NH<sub>2</sub> for 1 hour. After the hour had expired, the oleylamine coated CA-MNPs were washed with ethanol and recovered using magnetic separation, then stored in hexane. The PEG coated CA-MNPs were washed using DI water and recovered using magnetic separation, then stored in DI water.

## 2.3 Results and Discussion

### 2.3.1 Analyzing Nanoparticles using Dynamic Light Scattering

Dynamic light scattering (DLS) is used to verify the size of the O-MNPs, CA-MNPs, and JNPs. DLS takes advantage of the Brownian motion that small particles exhibit when in suspension. When a

monochromatic light source (lasers are commonly used) is fired through the sample, the Brownian motion of the nanoparticles causes it to scatter, causing fluctuations in the intensity of the light that change with time. These fluctuations can be measured by a photon counter, and directly correlate to the rate of diffusion of the particles through the solvent, which in turn correlates to the hydrodynamic radii of the nanoparticles. Results from DLS analysis on these nanoparticle samples are shown in Figure 2.4.

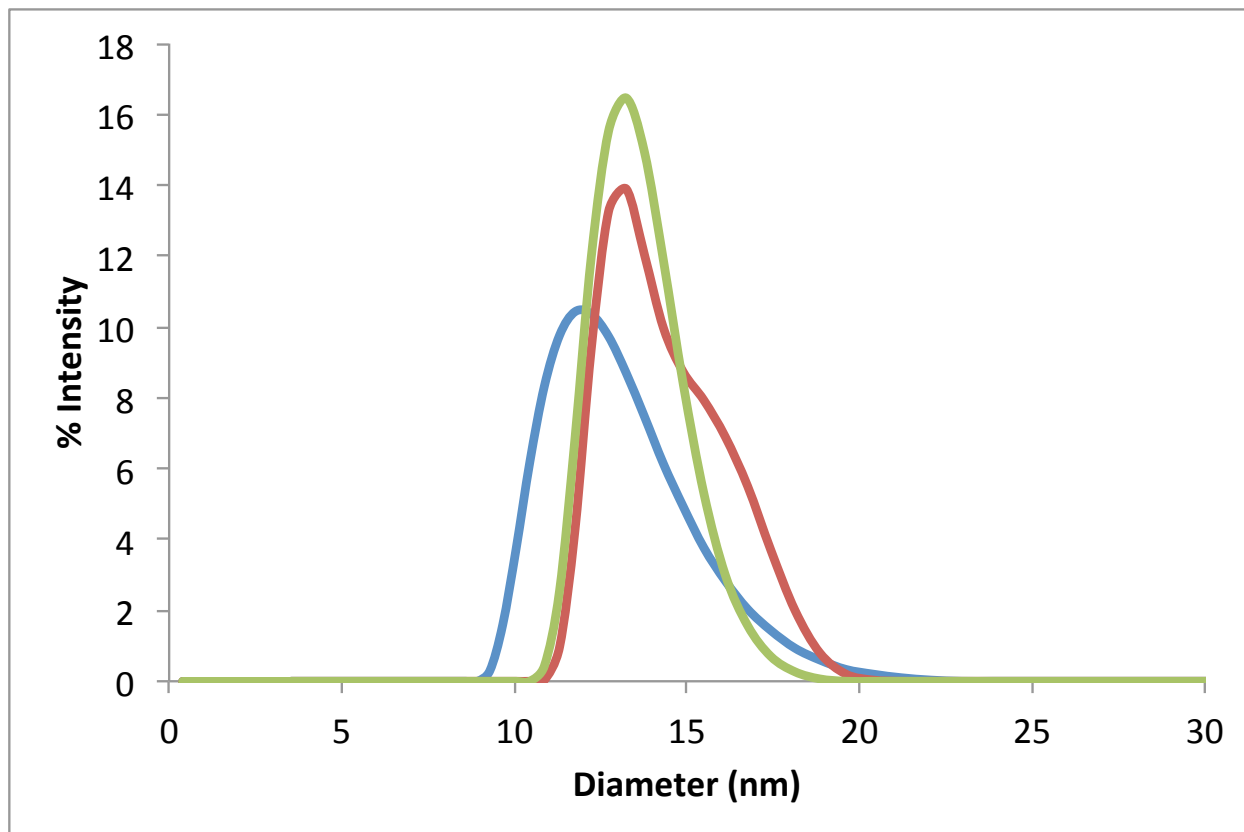


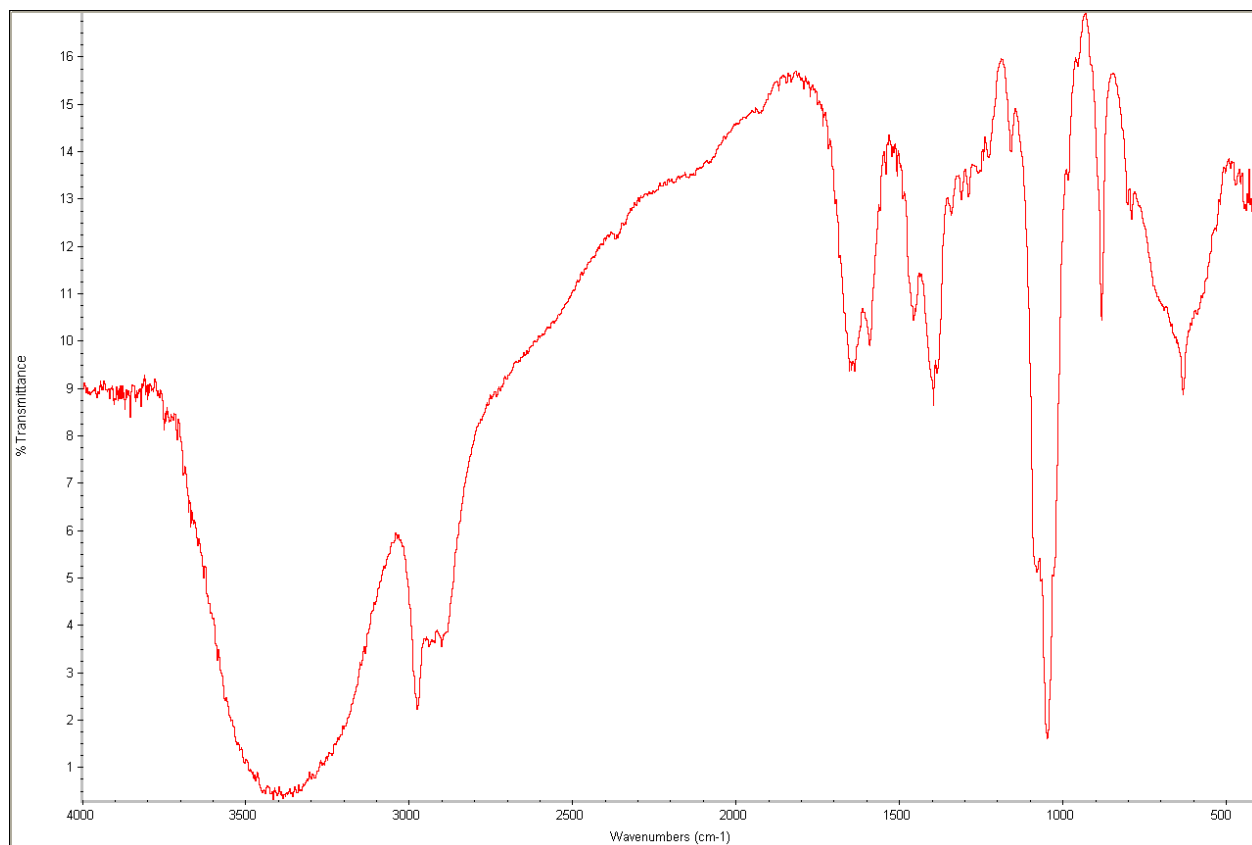
**Figure 2.4** Graph showing the average hydrodynamic diameter of the O-MNPs in hexane (blue line), CA-MNPs in water (red line), and JNPs in chloroform (green line). O-MNP samples show an average hydrodynamic diameter range from 9-20 nm with a 12 nm diameter occurring most frequently. CA-MNP samples show an average diameter range from 11-20 nm with a 14 nm diameter occurring most frequently. JNP samples show an average diameter range from 11-19 nm with a 14 nm diameter occurring most frequently



From the data seen in Figure 2.4, the size of our iron oxide nanoparticles remains constant after the surface has been modified multiple times. This indicates that the ligand exchange reaction and the Janus reaction are not causing any nanoparticle aggregation or unwanted self-assembly in these samples.

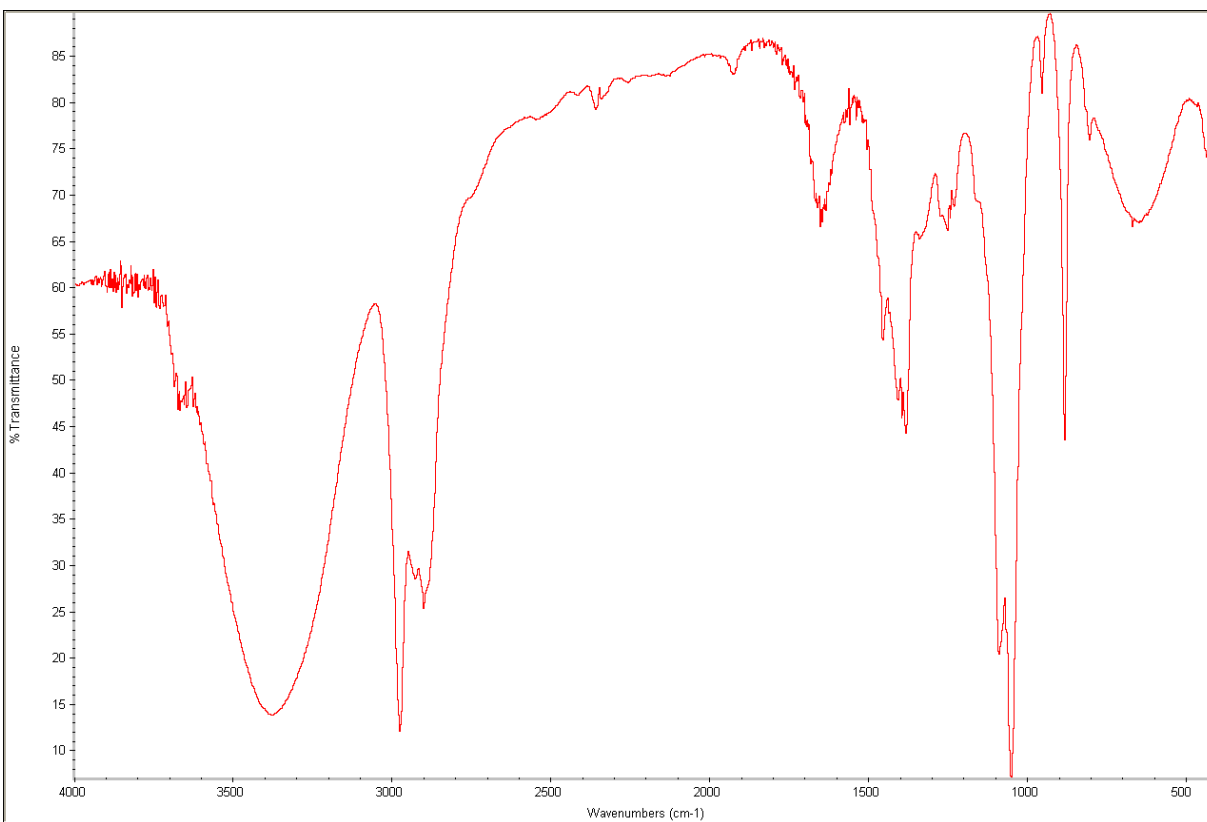
### **2.3.2 Analyzing Nanoparticles using Fourier-Transform Infrared Spectroscopy**

Fourier-transform Infrared Spectroscopy (FTIR) was utilized to determine if oleylamine and the PEG are bonding to the nanoparticles surface. FTIR uses infrared radiation and a mathematical function (Fourier Transform) to identify chemical bonds in a sample. Specifically, the sample is exposed to infrared radiation and some of this radiation is absorbed by the sample, specifically the chemical bonds within the sample; this absorbed radiation causes the bonds to stretch and/or vibrate. The beam of infrared light enters an interferometer and is split by a beam splitter; one beam moves to a stationary mirror and is reflected back. The second beam hits a moving mirror, which makes small changes to the beam path distance. These two beams are recombined at the beam splitter and sent through the sample to a detector. The Fourier Transform function is applied to the data gathered from each mirror position (interferogram), which forms the single beam spectrum that we see as the finished product. In this single beam spectrum, peaks will represent wavelengths of infrared light that were absorbed by the sample and did not reach the detector. (Smith, 1998) Research has been done to determine the infrared wavelengths that certain bonds absorb in an effort to catalog this data; some of these finding will be cited later in this thesis. We were able to identify key bonds in the samples of CA-MNPs, oleylamine coated CA-MNPs, PEG coated CA-MNPs, and JNPs. Figures 2.5, 2.6, 2.7, and 2.8 show the results of our FTIR analysis.



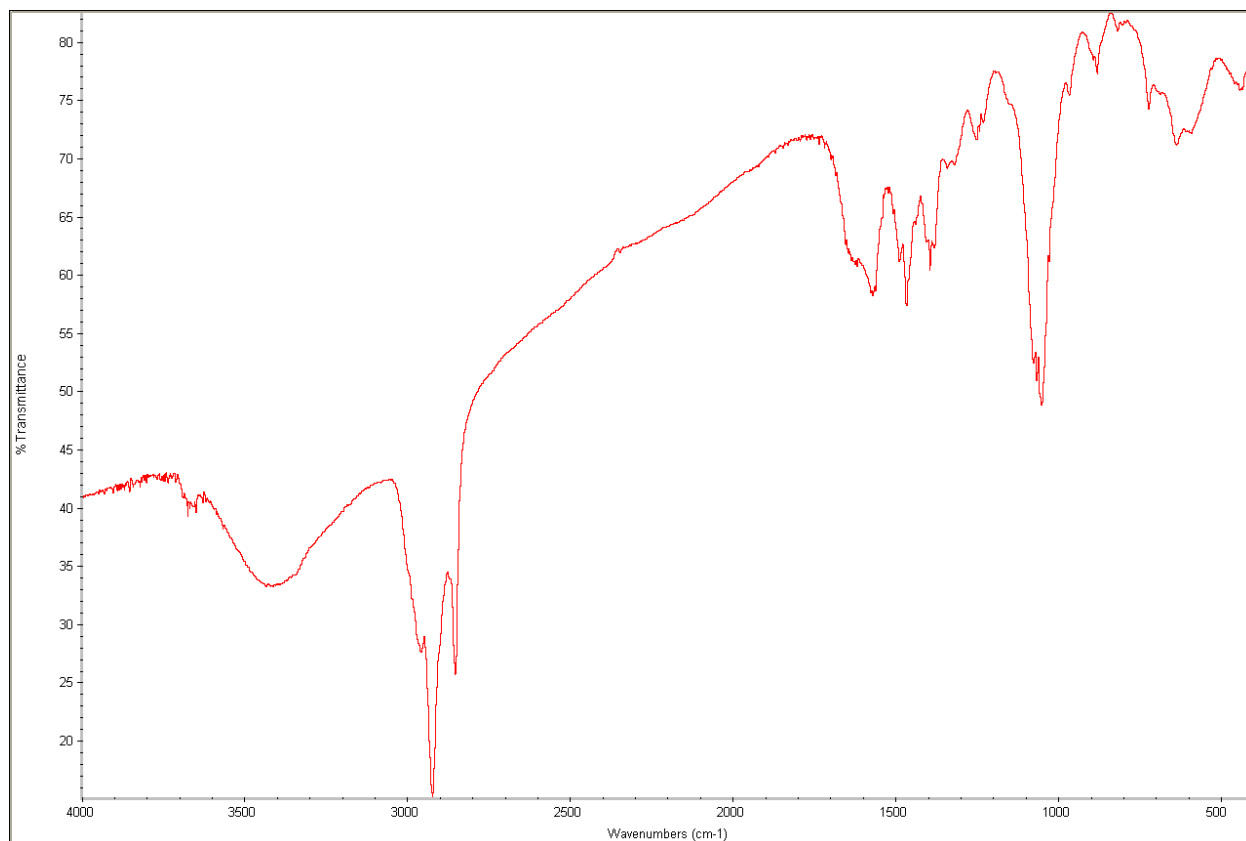
**Figure 2.5** FTIR graph of CA-MNPs.

Figure 2.5 shows the FTIR graph generated when CA-MNPs are analyzed. The large peak at  $3400\text{ cm}^{-1}$  is representative of non-dissociated OH groups, essentially meaning the presence of water, which is the solvent that these particles are stored in. The peak between  $2900\text{ cm}^{-1}$  and  $3000\text{ cm}^{-1}$  is indicative of methylene ( $\text{CH}_2$ ) bond stretching from the citric acid. (Smith, 1998) The peak seen between  $1600\text{ cm}^{-1}$  and  $1650\text{ cm}^{-1}$  can represent a carbon-oxygen double bond in citric acid, but could also indicate the presence of  $\text{CO}_2$  in the sample chamber. (Nakanishi, 1963) The peak seen at  $1400\text{ cm}^{-1}$  represents the asymmetric stretching of a carbon-oxygen single bond. (Cheraghipour et al., 2012) The peak seen between  $1000\text{ cm}^{-1}$  and  $1100\text{ cm}^{-1}$  represents the symmetric stretching of a carbon-oxygen single bond. (Nakanishi, 1963) Both carbon-oxygen peaks can be indicative of citric acid. Finally, the peak seen between  $500\text{ cm}^{-1}$  and  $600\text{ cm}^{-1}$  is indicative of iron oxide (iron bonded to oxygen). (Cheraghipour et al., 2012)



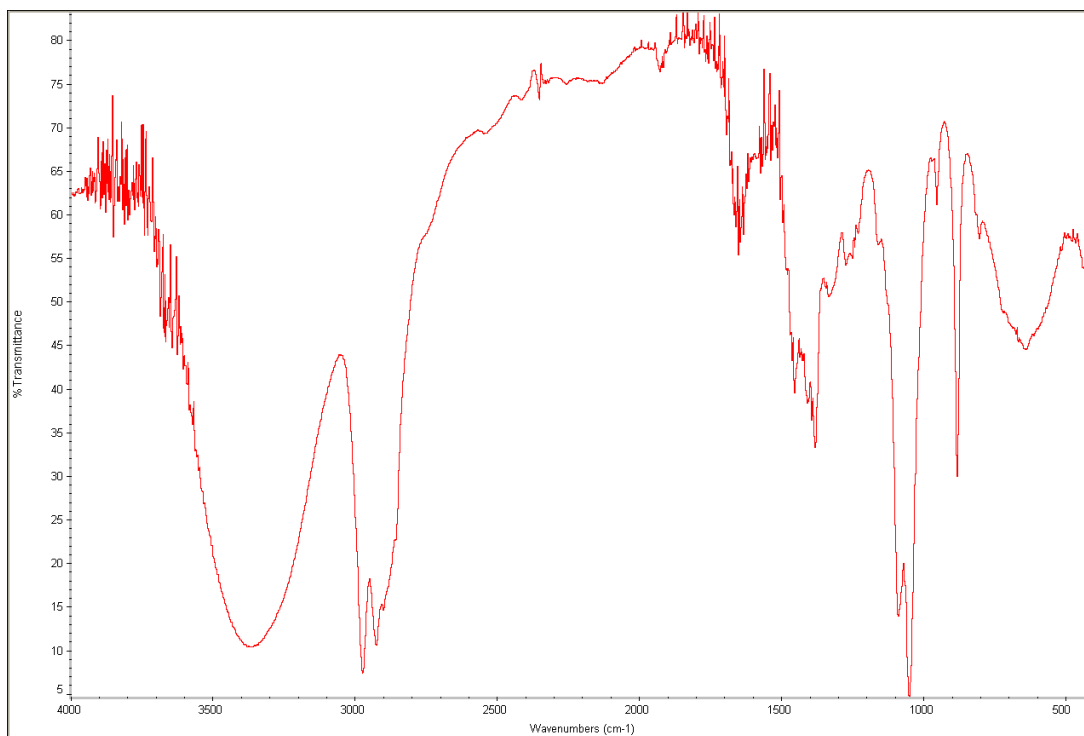
**Figure 2.6** FTIR graph for CA-MNP coated with PEG

Figure 2.6 shows the FTIR graph generated when PEG coated CA-MNPs are analyzed. The peaks we see in this figure are similar to the ones in Figure 2.5; we again see a peak at  $3400\text{ cm}^{-1}$  indicating non-dissociated OH groups, as well as a peak between  $500\text{ cm}^{-1}$  and  $600\text{ cm}^{-1}$  indicating iron oxide. We see peaks at  $1400\text{ cm}^{-1}$  and  $1100\text{ cm}^{-1}$  indicative of carbon-oxygen bond stretching; citric acid loses its carbon-oxygen single bonds when reacted with an amine, so these peaks are now caused by the presence of PEG. (Cheraghipour, Javadpour, & Mehdizadeh, 2012) We see a peak  $2900\text{ cm}^{-1}$ , indicative of methyl ( $\text{CH}_3$ ) and methylene bond stretching from the PEG molecules. (Smith, 1998) The peak between  $3250\text{ cm}^{-1}$  and  $3400\text{ cm}^{-1}$  is likely indicative of non-dissociated OH groups as in Figure 2.5, but can also indicate a nitrogen-hydrogen bond stretch, which occurs when carboxylic acid is bonded to a primary amine. (Richardson, 2011).



**Figure 2.7** FTIR graph for CA-MNP coated with Oleylamine

Figure 2.7 shows the FTIR graph generated when oleylamine coated CA-MNPs are analyzed. We see a strong at  $2900\text{ cm}^{-1}$ , referring to a larger number of methyl groups and methylene groups in this sample; this result is expected considering the molecular structure of oleylamine. (Smith, 1998) A peak between  $1000\text{ cm}^{-1}$  and  $1100\text{ cm}^{-1}$  is seen here, most likely indicative of citric acid molecules that were not reacted with an oleylamine molecule.



**Figure 2.8** FTIR graph of JNPs

Figure 2.8 shows the FTIR graph generated when the JNP sample was analyzed. We continue to see a peak at  $2900\text{ cm}^{-1}$  indicating a presence methyl and methylene groups and concurrently of oleylamine and PEG, as well peaks at  $1100\text{ cm}^{-1}$  and  $1400\text{ cm}^{-1}$  also indicating a presence of PEG. (Smith, 1988) FTIR analysis shows that all the proper compounds exist in these nanoparticle samples, but it does not give us evidence of dual hemispheres. Further analysis will be needed to verify this concept.

### 2.3.3 Analysis of Nanoparticles at Hexane/Water Interface

Each sample of nanoparticles was placed in a 1:1 mixture of hexane and DI water to examine their behavior. It was assumed that our JNPs would form a self-assembled layer at the interface between the two liquids. Results from this experiment are shown in Figure 2.9.

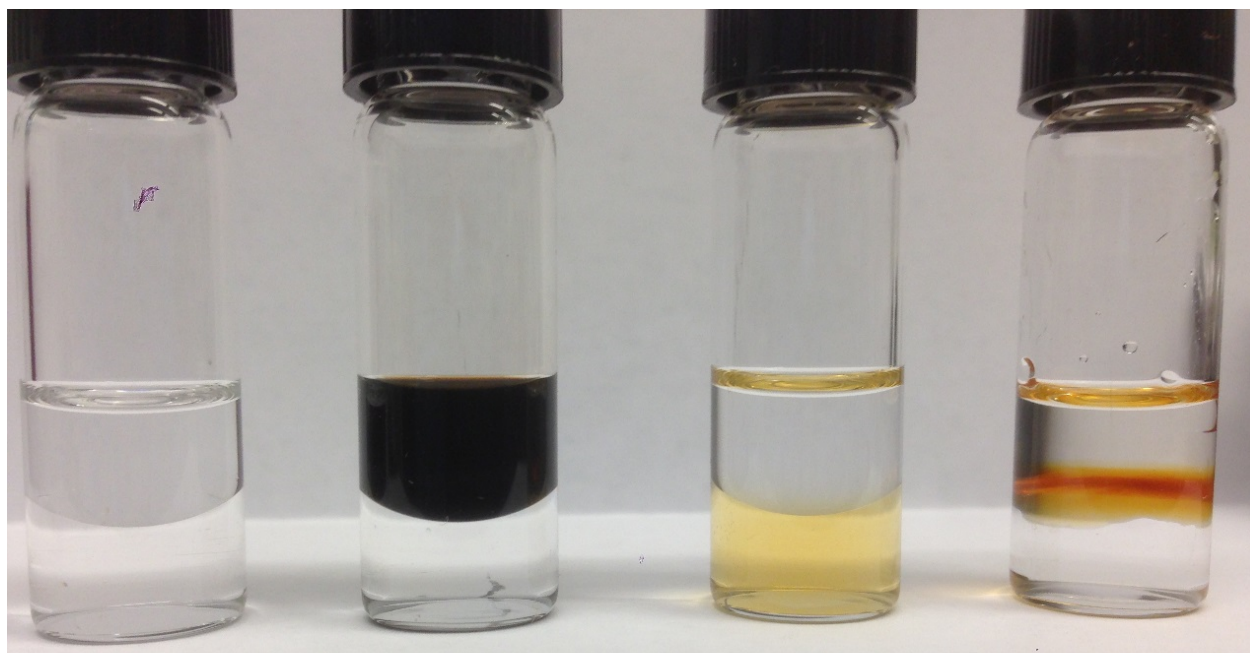


**Figure 2.9** Sample of nanoparticles suspended in a 1:1 hexane water mixture. The first vial (far left) has no nanoparticles. The second vial has 10 $\mu$ L of O-MNPs in hexane added to the mixture. The third vial has 10 $\mu$ L of CA-MNPs in DI water added to the mixture. The fourth vial (far right) has 10 $\mu$ L of JNPs in chloroform added to the mixture

In vial 2, the O-MNPs stabilize in the hexane layer, and in vial 3, the CA-MNPs stabilize in the water layer. Since the JNPs were added in chloroform, it is assumed that they would stay in that solvent and settle at the interface due to density differences between the solvents. However, the fact that the particles didn't leave the chloroform and suspend in either the water or the hexane was a behavior that could indicate multi-modal nanoparticles. An interesting phenomenon that we noticed was the change in the meniscus in the fourth vial. Adhesive forces (attractive forces between the liquid and the solid container) are responsible for determining the shape of a meniscus. Strong cohesive forces (attractive forces between molecules) cause both the water molecules and the hexane molecules to bunch together at either a liquid-liquid or air-liquid interface; more specifically, the molecules are trying to reduce their exposure to the opposing gas/liquid. This molecular behavior is what causes both the phenomenon of surface tension as well as the development of a meniscus. If the adhesive forces between the molecules are stronger than the cohesive forces, the liquid will attract to the container surface and climb the walls, forming a concave meniscus. Conversely, if the cohesive forces are stronger than the adhesive forces, a convex meniscus is formed. (Moore & Stanitski, 2005) In vials 1-3, we see a concave meniscus between the hexane and water, indicating that the nanoparticles added to vials 2 and 3 are not having an effect on the hexane or

water molecules. In vial 4, we see the development of a nearly flat/possibly convex meniscus. This behavior could be a result of the JNPs interacting with the water and hexane molecules. Specifically, the hydrophilic side of the JNPs could aligning with the water layer, allowing the water molecules to suspend more evenly at the interface and alter the shape of the meniscus. We would also expect this behavior between the hydrophobic side of the JNPs and the hexane layer.

Due to the result from the first hexane/water experiment, small samples of JNPs were allowed to dry and then attempts were made to suspend them in hexane and water, respectively. The JNPs would not suspend in pure DI water, despite vigorous agitation and sonication. However, suspension in hexane was quick and proved to be stable. This behavior could be due to uneven layers of oleylamine and PEG (not a 50/50 coating). We added dried JNPs to a hexane/water interface expecting to see similar behavior that we did in vial 4 from Figure 2.. We also agitated the forth vial from Figure 2.11 to examine the result.

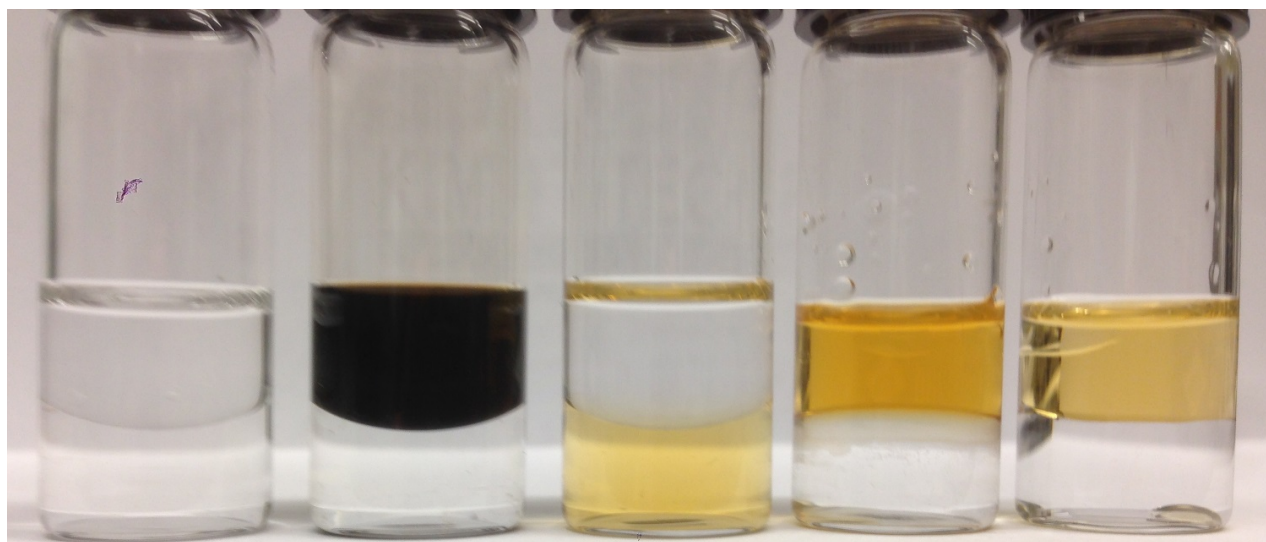


**Figure 2.10** Vials from the second hexane/water interface experiment. Vials 1-4 (starting on the left) are the same vials from Figure 2.11, but vial 4 has been agitated. The chloroform is allowed to mix with the hexane, dispersing the JNPs into the upper layer. Vial 5 is the same hexane/water mixture with 10 $\mu$ L of JNPs in chloroform, but the solvent was evaporated before addition to the hexane/water mixture

From Figure 2.10, we again see the convex meniscus formed in vial 4 and a near flat meniscus form in vial 5. The results show a possibility of the JNPs interacting with the water and hexane layers of the solution and distorting the meniscus.

### 2.3.4 Analysis of JNPs in Different Solvents

The final method we used to characterize this JNP configuration involved examining the nanoparticles in different solvents. We have already investigated their behavior in chloroform; we also wanted to examine JNPs when suspended in hexane and in water. These JNPs should not freely suspend in either hexane or water due to the insolubility of oleylamine in water the insolubility of PEG in hexane. Rather, they should self-assemble in a way to reduce the repulsive contact between the compound on one of the hemispheres and the incompatible solvent. We hypothesized that we could detect these larger structures using DLS; Figure 2.11 shows the result of this experiment.

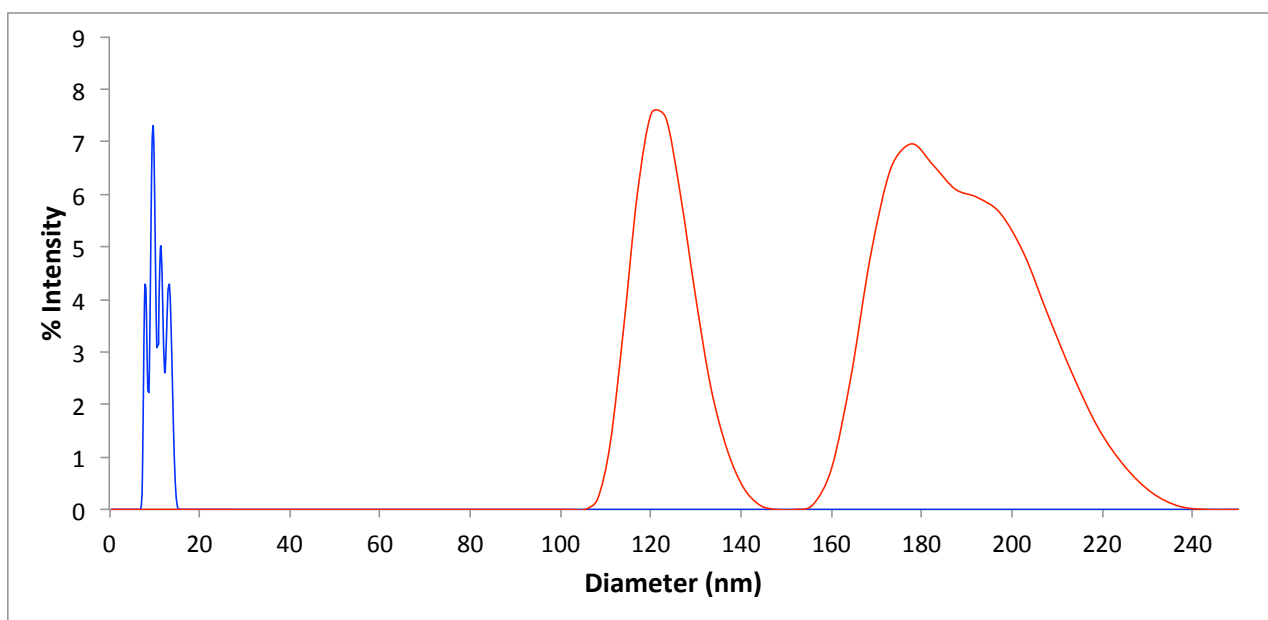


**Figure 2.11** Graph showing the average size of the JNPs suspended in chloroform (blue line) and the average hydrodynamic diameter of JNPs suspended in hexane (red line) JNPs suspended in chloroform show an average diameter range from 8-15 nms; JNPs suspended in hexane show an average diameter range from 100-240 nm

From Figure 2.11 when suspended in chloroform the nanoparticles show the same diameter as they did before modification. This indicates that the JNPs are well suspended in this solvent. In the hexane, we see a much larger size range, indicating that the JNPs must be interacting with one another; possibly forming into a micelle-like structure to protect the PEG modified side from the solvent.



Suspending the JNPs in water was more difficult than in the other solvents. Dried samples of JNPs will suspend in organic solvents like chloroform or hexane easily; dried samples of JNPs would not suspend in water despite vigorous vortexing and sonication. A small amount of oleylamine had to be added to the mixture to elicit suspension; we hypothesized that the JNPs were forming liposome structures in both hexane and water; the addition of fatty amine would fill the gaps between the nanoparticles and help elicit suspension in water. With the addition of fatty acid, the JNPs did finally suspend and could be analyzed in the particle sizer. Unfortunately, the DLS was not able to give an accurate reading on this sample. In order to verify that we have structures developing when suspended in water, we checked samples from this mixture using our optical microscope. For this experiment, we utilized an EVOS AMG Optical Microscope equipped with a 100x objective lens. Figure 2.12 shows the image developed from this experiment.

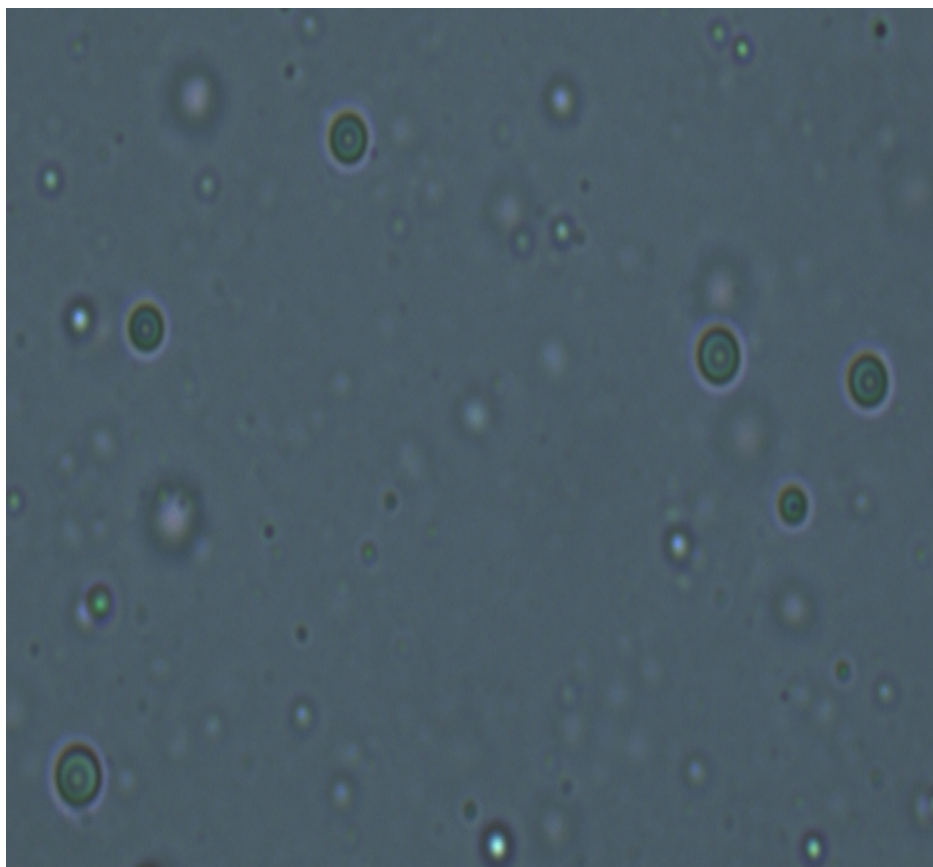


**Figure 2.12** Optical Microscope Images of JNPs suspended in water with free oleylamine

From Figure 2.12, we see circular structures developing when JNPs are suspended in water. Considering their appearance as well as their size (size of structures ranged from less than 500 nm to 2 microns), it is possible that these are groups of JNPs assembling into liposomes.

## **2.4 Conclusions**

While the experiments conducted on this set of JNPs did show signs of multi-modal nanoparticles, none of the experiments can conclusively prove the existence of dual-hemispheres. FTIR can only confirm the compounds that exist on the nanoparticle surface, and our hexane/water interface experiments as well as our microscope images can only act as circumstantial evidence, not concrete proof. It is necessary to use characterization methods that will let us visualize the hemispheres of our JNPs if we want more concrete evidence. If we want to take advantage of electron microscope systems, such as Transmission Electron Microscopes (TEMs) or Scanning Electron Microscopes (SEMs), we would need to use larger nanoparticles so we can more closely examine their surfaces. Due to this point, we decided to reattempt this synthesis using a larger core nanoparticle; this way we can take advantage of imaging with the electron microscopes and possibly obtain visual evidence of dual-hemispheres.

## Chapter 3

### Synthesizing Janus Nanoparticle using a Silica Core with an CA-MNP Hemisphere

#### 3.1 Introduction

The second JNP configuration synthesized using our method incorporates a silica nanoparticle as the core, as well as oleylamine on one hemisphere and a combination of CA-MNPs and PEG to make up the opposing hemisphere. By using a larger nanoparticle for the core (300 nm aminated silica nanoparticles) and smaller nanoparticles to make up a hemisphere (10-20 nm CA-MNPs), we theorized that we could use TEM imaging to examine the nanoparticles and visualize the difference between the hemispheres. A layer of mPEG-NH<sub>2</sub> was also added to the unexposed side of the CA-MNPs once they had been bonded to the silica nanoparticle; coating the exposed side of the CA-MNPs was necessary to prevent unnecessary bonding during washings steps. The method is unchanged excluding the addition of new compounds and additional washing steps.

#### 3.2 Experimental

##### 3.2.1 Materials

For the JNP synthesis, C<sub>18</sub> Spherical Silica Gel was obtained from Sorbtech. 1-ethyl-3-(dimethylaminopropyl)carbodiimide (EDC) (C<sub>8</sub>H<sub>17</sub>N<sub>3</sub>) was obtained from Alfa Aesar. N-hydroxysuccinimide (NHS) (C<sub>4</sub>H<sub>5</sub>NO<sub>3</sub>, 98%) was obtained from TCI. Oleylamine (C<sub>18</sub>H<sub>35</sub>NH<sub>2</sub>) was obtained from Alfa Aesar. Glutaraldehyde (CH<sub>2</sub>(CH<sub>2</sub>CHO)<sub>2</sub>) was obtained Amresco. from mPEG-NH<sub>2</sub> (MW 5000) was obtained from NANOCS. Glutaraldehyde (CH<sub>2</sub>(CH<sub>2</sub>CHO)<sub>2</sub>, 50%) was obtained from Amresco. For solvents and washing solutions for all syntheses, chloroform (CHCl<sub>3</sub>), hexane (C<sub>6</sub>H<sub>14</sub>), and methanol (CH<sub>4</sub>O) were obtained from BDH. Ethanol (C<sub>2</sub>H<sub>6</sub>O) (200 proof) was obtained from EMD. Deionized water was obtained using an ELGA PURELAB Flex water purification system.

### 3.2.2 Synthesizing JNPs with a Silica Core and a CA-MNP Functionalized Hemisphere

The same column set-up used in the previous JNP synthesis is used for this one as well. Additionally, the first step of the synthesis is also the same; oleylamine in ethanol is added to the column, allowed to attract to the octadecane molecules. The column is then drained and washed. Next, a solution of glutaraldehyde and DI water is added to the column; the column is sealed and the compounds are allowed to react for one hour. The contents are then drained and the column is washed with DI water. Glutaraldehyde acts as a cross-linker between the amine group of oleylamine and the aminated silica nanoparticle surface. 300 nm aminated silica nanoparticles suspended in water are then added to the column and allowed to react with the glutaraldehyde for one hour. The column is then drained and washed with DI water. CA-MNPs suspended in water are mixed with NHS and EDC to activate the carboxylic acid groups and added to the column. After one hour of reaction time, the liquid is drained and the column is washed with DI water. Finally, mPEG-NH<sub>2</sub> dissolved in DI water is added to the column and allowed to react for one hour; upon completion, the column is drained and washed with DI water. Chloroform is then passed through the column to remove the newly formed JNPs from the silica pack particles. The solvent is removed via evaporation and the JNPs are resuspended in a 4:1 chloroform/methanol mixture and placed on a magnetic separator for 48 hours. After the JNPs have separated, the solvent is removed and the JNPs are resuspended in chloroform. They are then further purified using 0.1 μm centrifugal filter tubes acquired from Merck. The JNPs are spun through these filters at 10,000 g for 20 minutes. After centrifugation, the particles are resuspended in chloroform and stored. Figure 3.1 shows an illustration of the configuration of these JNPs.

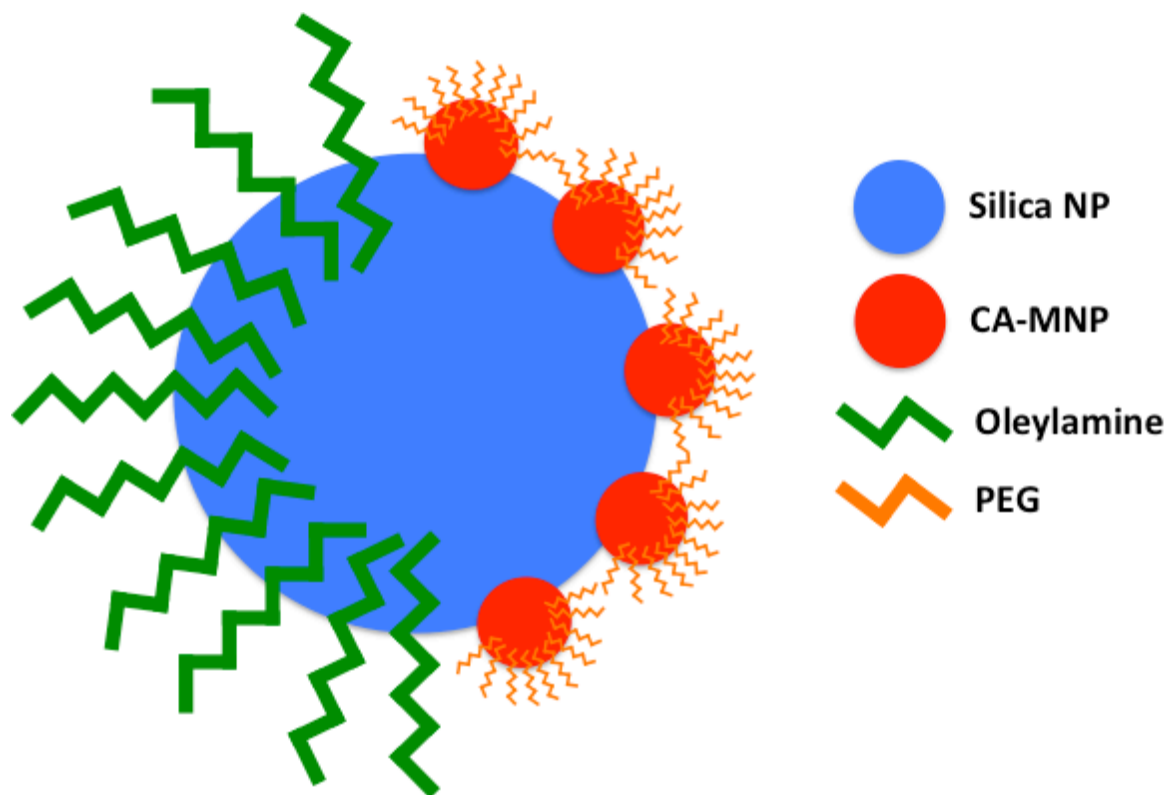


**Figure 3.1** Illustration of the strategy used to assemble a JNP with a silica core. Hydrophobic tail groups of the oleylamine molecules will attract to the  $C_{18}$  groups, then bond with one aldehyde group of the glutaraldehyde molecules. The other side of glutaraldehyde will be free to bond with the silica nanoparticle. Activated CA-MNPs will then be added to bond with the remaining amine groups on the silica nanoparticles. Finally, the exposed side of the CA-MNPs will be coated of mPEG-NH<sub>2</sub>

### 3.2.3 Synthesizing Silica Nanoparticles Completely Coated with Oleylamine

Samples of “control” nanoparticles were synthesized to compare to the JNPs. Silica nanoparticles totally coated with oleylamine were synthesized; silica nanoparticles suspended in DI water were slowly combined with a mixture of glutaraldehyde and DI water and allowed to react for one hour. An excess amount of glutaraldehyde was used in this experiment to try and prevent unwanted crosslinking between the silica nanoparticles. The mixture was centrifuged three times, discarding the liquid layer and resuspending the solute in DI water between each run. On the final step, the nanoparticles were resuspended in ethanol to prepare them for their reaction with oleylamine. A solution of oleylamine in ethanol was then added to the mixture and allowed to react for one hour. The mixture was centrifuged

three times in the same manner as before, although for this cycle ethanol was used for the suspensions. The final nanoparticles were then stored in ethanol.

### **3.2.4 Synthesizing Silica Nanoparticles Completely Coated with PEG**

Silica nanoparticles suspended in DI water were slowly combined with a mixture of glutaraldehyde and DI water and allowed to react for one hour. An excess amount of glutaraldehyde was used in this experiment to try and prevent unwanted crosslinking between the silica nanoparticles. The mixture was centrifuged three times, discarding the liquid layer and resuspending the solute in DI water after each run. A solution of mPEG-NH<sub>2</sub> in DI water was then added to the mixture and allowed to react for one hour. The mixture was centrifuged three times in the same manner as before; the final nanoparticles were then stored in DI water.

### **3.2.5 Synthesizing Silica Nanoparticles Completely Coated with CA-MNPs and mPEG-NH<sub>2</sub>**

Silica nanoparticles suspended in DI water were combined with a CA-MNP solution, also suspended in DI water. CA-MNPs were activated with NHS and EDC before the mixing occurred, and were also added in excess to the silica to help prevent unwanted crosslinking between the silica nanoparticles. After one hour of reaction time, the mixture was centrifuged three times, removing the liquid layer and resuspending the solute in DI water after each run. EDC and NHS were again added to the mixture to reactivate the remaining carboxylic acid groups on the CA-MNP surfaces, then mPEG-NH<sub>2</sub> was added to the mixture and allowed to react for one hour. Upon completion, the mixture was centrifuged three times in the same manner as before, and the final nanoparticles were stored in DI water.

### **3.2.6 Synthesizing Silica Nanoparticles Freely Mixed with both mPEG-NH<sub>2</sub> and Oleylamine**

This nanoparticle configuration was created to see if the silica nanoparticles had any reaction towards one reaction with the compounds we are utilizing. Silica nanoparticles suspended in DI water were mixed with a diluted sample of CA-MNPs suspended in DI water and a glutaraldehyde/DI water solution and allowed to react for one hour. Upon completion of the hour, the mixture was centrifuged and the liquid layer was removed. The solute was resuspended in chloroform, and the process of centrifuging was repeated two more times. The nanoparticle mixture was then exposed to mPEG-NH<sub>2</sub> and oleylamine and allowed to react for one hour. Upon completion, the same centrifuge washing steps were repeated in triplicate, resuspending in chloroform each time. The final nanoparticle solution was stored in chloroform.

### 3.3 Results and Discussion

#### 3.3.1 Analysis of JNPs and Control Nanoparticles

All nanoparticles were examined using FTIR analysis to verify both their existence and bonding of the compounds to the nanoparticle surface. The results of this experiment for all of the control nanoparticles and the JNPs are shown in Figure 3.2.

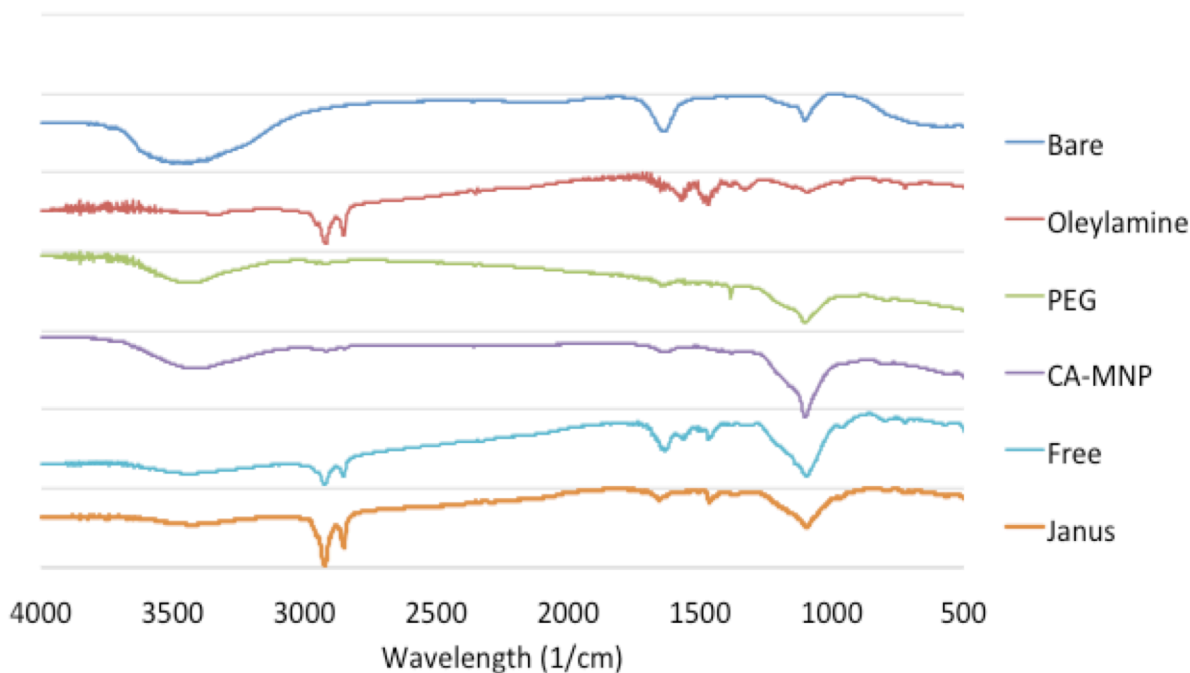


**Figure 3.2** FTIR data (wavelength vs. % transmittance) collected from all of the control groups formed using 300 nm silica nanoparticles (top to bottom): unmodified aminated silica nanoparticles, oleylamine coated silica nanoparticles, PEG coated silica nanoparticles, CA-MNP/PEG coated silica nanoparticles, and silica nanoparticles that were freely mixed with both PEG and oleylamine.

From Figure 3.2, we see peaks between  $1000\text{ cm}^{-1}$  and  $1200\text{ cm}^{-1}$  in every sample; this peak has indicated a carbon-oxygen bond stretch in previous data, but can also refer to a silicon-oxygen bond stretch from the silica nanoparticles. (Smith, 1998) Stronger peaks at this wavelength are seen in the PEG coated control group, the CA-MNP/PEG control group, the freely mixed control group, and the JNPs. Methyl

and methylene peaks ( $2900\text{ cm}^{-1}$ ) are seen in the oleylamine coated control group, the freely mixed control group, and the JNPs.

All control samples were also investigated using a transmission electron microscope (TEM). With the TEM, we were able to visualize the surface of the silica nanoparticles, which provided critical comparison data to the final JNP samples. The control nanoparticles coated with PEG (Figure 3.3, image A) and the control group coated with oleylamine (Figure 3.3, image B) appeared unmodified when examined under TEM; this was expected considering the size of PEG and oleylamine molecules. The control nanoparticles coated with CA-MNPs and then PEG (Figure 3.3, image C) had a visible coating of smaller iron oxide nanoparticles on the silica nanoparticle surface. This coated appearance will be utilized to identify hemispheres when examining the JNP samples. The freely mixed control group (Figure 3.3, image D) did not show an affinity towards either chemical bond to the silica surface. Figure 3.3 shows the TEM images of these control nanoparticles.



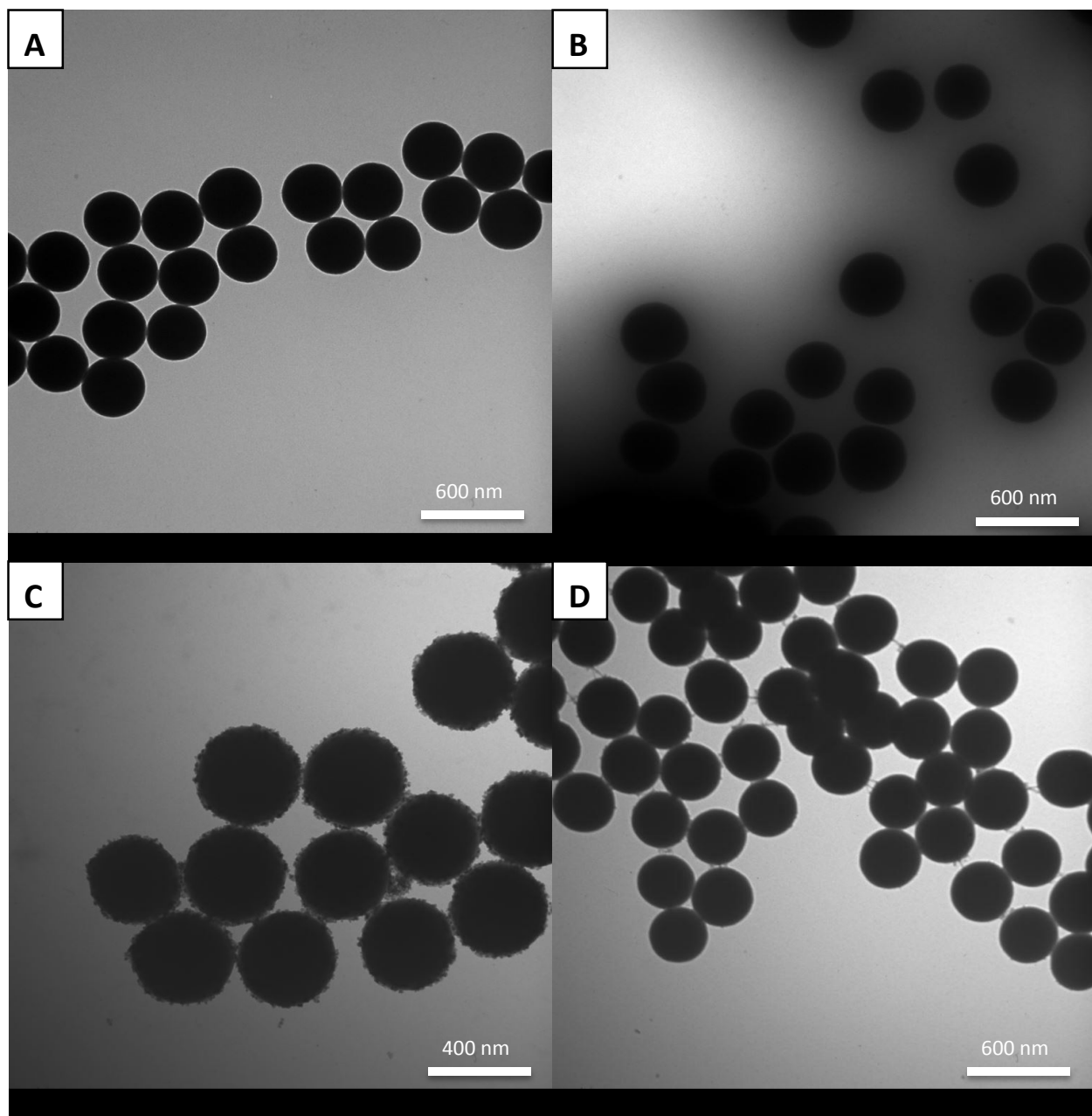


**Figure 3.3** TEM images taken of all the control group nanoparticles. A) 300 nm silica nanoparticles totally coated with PEG. B) 300 nm silica nanoparticles totally coated with oleylamine. C) 300 nm silica nanoparticles totally coated first with CA-MNPs, then totally coated with PEG. D) 300 nm silica nanoparticles freely mixed with oleylamine and PEG simultaneously.

We can now compare the TEM results from the control group nanoparticles to the JNP sample. The size difference between the coating of oleylamine molecules and the coating of CA-MNPs should be visible based on the data gathered from the control groups. Figures 3.4 and 3.5 JNPs examined using TEM .

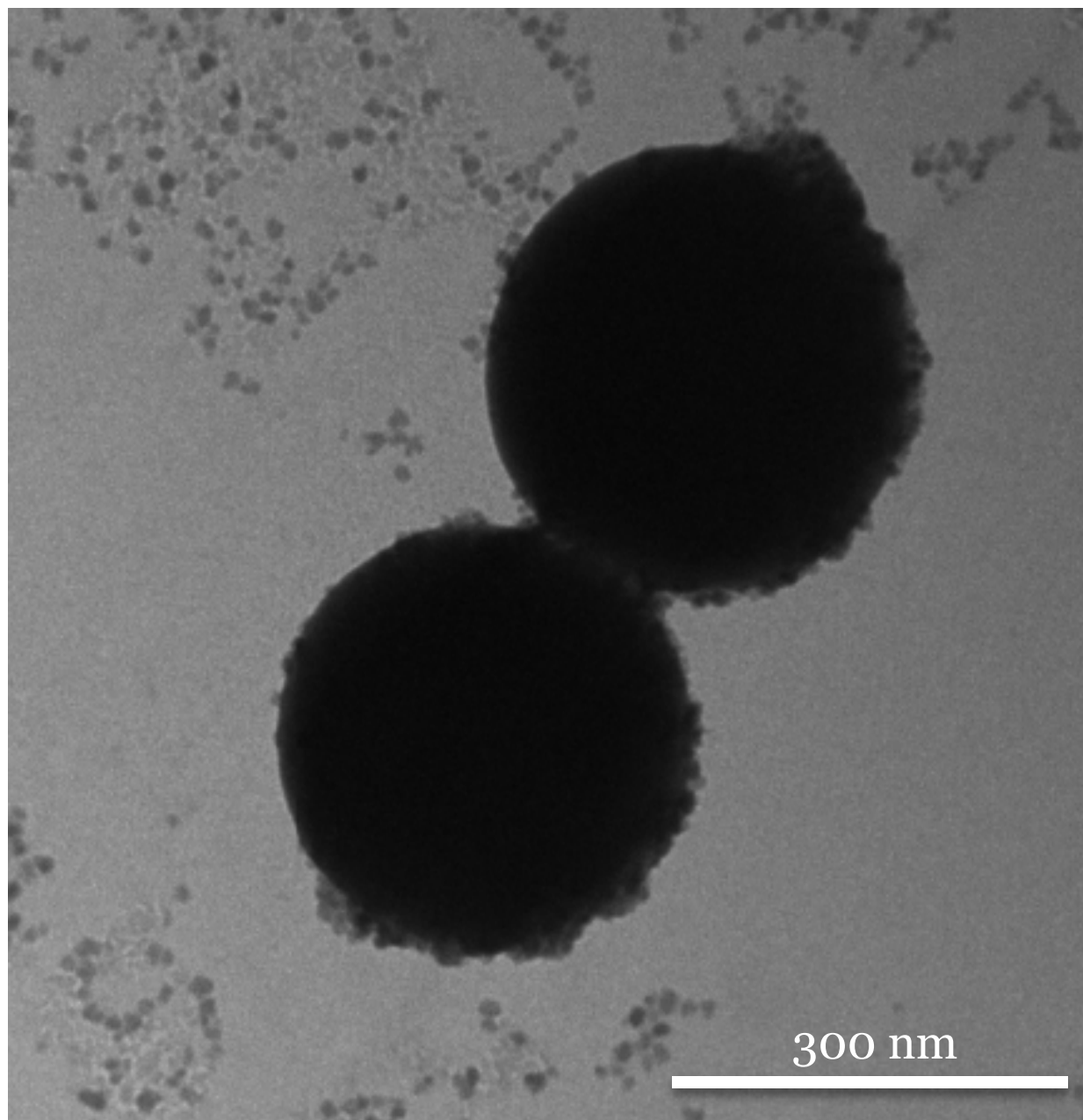


**Figure 3.4** TEM image of JNPs composed of a silica core with hemispheres of oleylamine and CA-MNPs/PEG

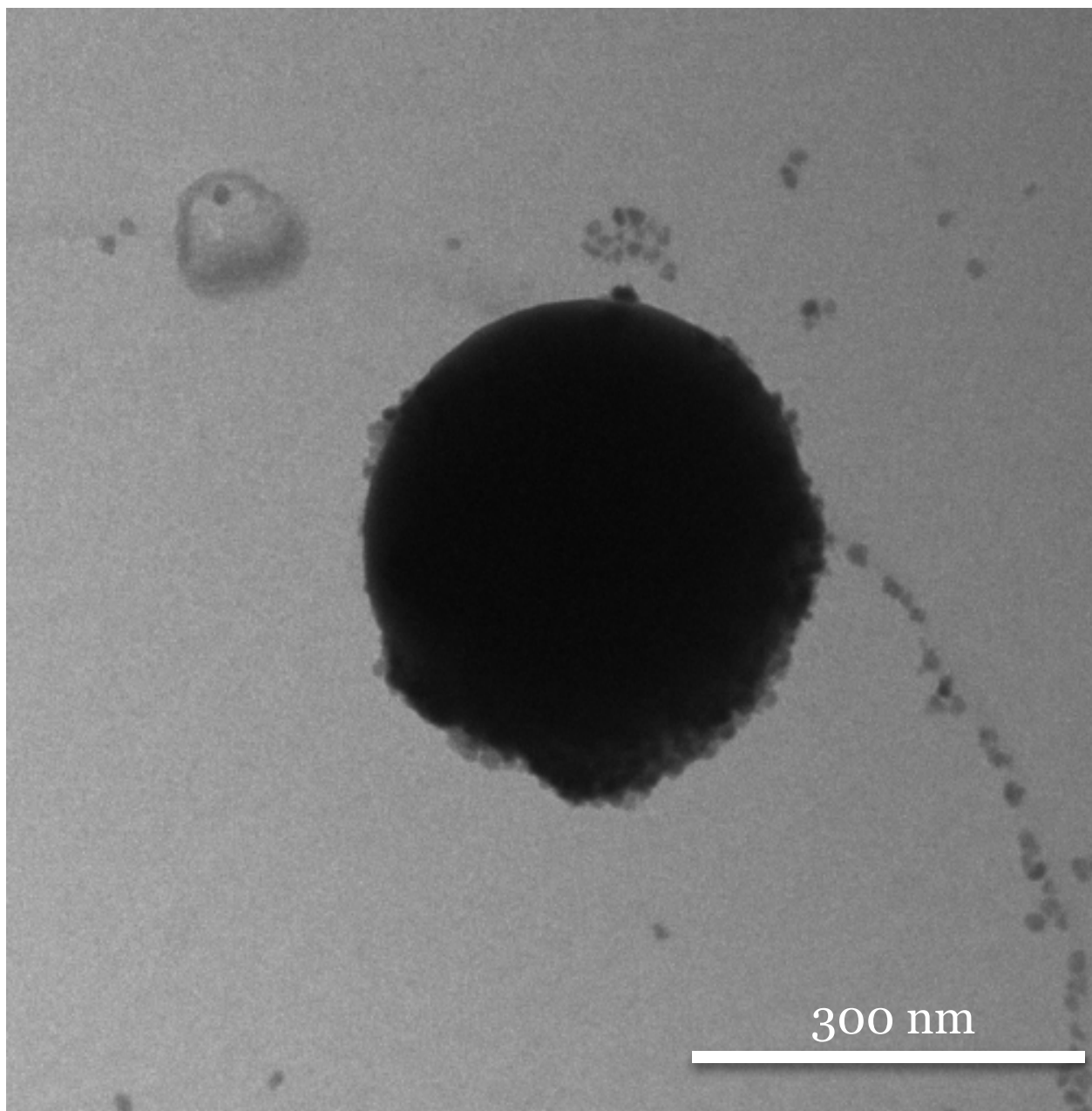


**Figure 3.5** TEM image of a JNP composed of a silica core with hemispheres of oleylamine and CA-MNPs/PEG

The same CA-MNP coating seen in the CA-MNP/PEG control group is seen on a portion of each JNP shown. Specifically, the upper nanoparticle in Figure 3.4 shows a CA-MNP coated portion from 30 degrees off top center position to 210 degrees off top center. The lower nanoparticle shows CA-MNP coverage over the same location. The nanoparticle shown in Figure 3.5 shows CA-MNP coverage from

60 degrees off top center to 240 degrees off top center. The adjacent portion of each JNP appears the same as the oleylamine coated control nanoparticles. These TEM images could possibly be identifying hemispherical coverage of oleylamine and CA-MNPs.

From the images collected from the TEM, analysis was done to see if any hemispherical ratio was favored in these samples (50/50 coverage, 60/40 coverage, etc.). By checking each image and assigning each particle a percent ratio based on an optical assessment, we were able to develop a range of ratios for these JNP samples. Figure 3.6 shows this data set.

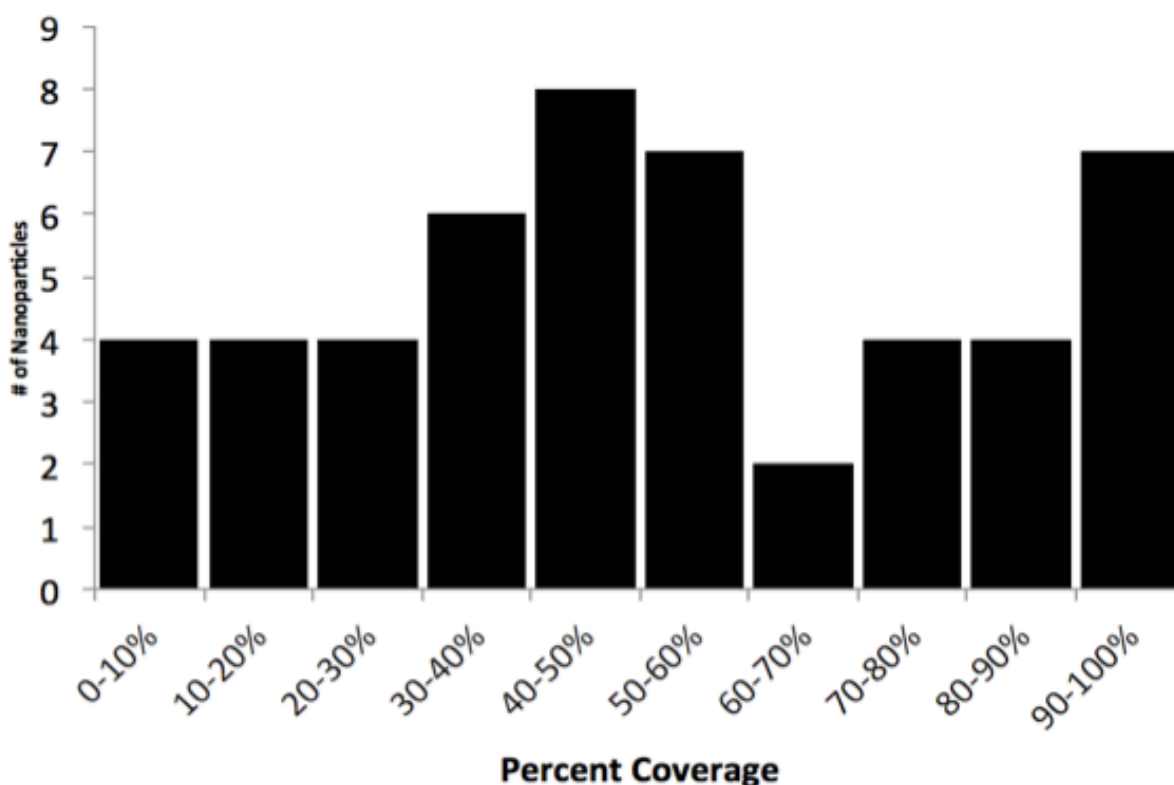


**Figure 3.6** Percent coverage of 120 nm JNPs determined from examination of TEM images. “Percentage coverage” indicates the amount of the nanoparticle that was covered with smaller iron oxide nanoparticles. The mean coverage for this data is 53.9% with a standard deviation of 23.00

While 50:50 is technically the most common, Figure 3.6 shows a broad coverage ratio range. Tuning this aspect of the JNP synthesis to control hemispherical coverage is an important step in this continued research. This concept will be discussed later in this document.

### **3.4 Conclusions**

The data presented in this chapter indicates possible hemispherical coverage on our JNPs. FTIR analysis shows peaks indicating the presence of silica nanoparticles as well as the compounds (PEG, oleylamine, and CA-MNPs) that we are attaching to the nanoparticle surface. TEM images appear to show hemispheres of CA-MNP and hemispheres modified with a small molecule, possibly oleylamine. Orientation of the nanoparticles when examined by TEM will have an affect on how the hemispheres are seen. Fixing the orientation of the JNPs before TEM imaging needs to be accomplished to validate the findings presented in this chapter. Results from this JNP configuration improved our confidence in the efficacy of this JNP synthesis method, but has still not shown concrete evidence of dual hemispheres. Additional JNP configurations need to be developed and characterized in order identify multiple hemispheres.

## Chapter 4

### Synthesizing Janus Nanoparticles using a Silica Core with a hemisphere coated with FITC

#### 4.1 Introduction

The final JNP configurations utilized a fluorescent dye on one hemisphere of the nanoparticle core; we hypothesized that we would be able to differentiate between the hemispheres using our optical microscope. The majority of the configuration is identical to the configuration described in the previous chapter; a silica nanoparticle core is coated with oleylamine and the fluorescent dye Fluorescein isothiocyanate (FITC) on respective hemispheres. For comparison to this new configuration, a similar JNP was designed that replaces the FITC dye with mPEG-NHS. FITC and PEG are soluble in similar solvents (water, ethanol, chloroform, etc.), and therefore these JNPs should behave identically except when viewed with a fluorescent camera.

#### 4.2 Experimental

##### 4.2.1 Materials

For the JNP synthesis, C<sub>18</sub> Spherical Silica Gel was obtained from Sorbtech. Oleylamine (C<sub>18</sub>H<sub>35</sub>NH<sub>2</sub>) was obtained from Alfa Aesar. Glutaraldehyde (CH<sub>2</sub>(CH<sub>2</sub>CHO)<sub>2</sub>) was obtained from Amresco. FITC-PEG-NHS was obtained from NANOCS. mPEG-NHS ester was obtained from NANOCS. 4-(2-hydroxyethyl)-1-piperazineethanesulfonic acid (HEPES) was acquired from Alfa Aesar. Fluorescein isothiocyanate (FITC) (C<sub>21</sub>H<sub>11</sub>NO<sub>5</sub>S) is obtained from Alfa Aesar. Sodium Carbonate decahydrate (Na<sub>2</sub>CO<sub>3</sub>) is obtained from Alfa Aesar. Sodium Bicarbonate (NaHCO<sub>3</sub>) is obtained from Amresco. For solvents and washing solutions for all syntheses, chloroform (CHCl<sub>3</sub>), hexane (C<sub>6</sub>H<sub>14</sub>), Dimethyl Sulfoxide (DMSO) ((CH<sub>3</sub>)<sub>2</sub>SO), and methanol (CH<sub>4</sub>O) were obtained from BDH. Ethanol (C<sub>2</sub>H<sub>6</sub>O) (200 proof) was obtained from EMD. Deionized water was obtained using an ELGA PURELAB Flex water purification system.

#### 4.2.2 Synthesizing JNPs with a Silica Core and a Hemisphere Functionalized with PEG

The column set up remains the same for this synthesis, as well as the silica nanoparticle core. Oleylamine in ethanol is added to the column and given time to align itself with the surface of the C<sub>18</sub> pack particles. The column is then washed with a solution of 10% methanol/DI water and then washed with pure DI water. A solution of glutaraldehyde in 20 mM HEPES buffer is then added to the column and given one hour to react with the fatty amine. HEPES buffer has a pH between 7.00-8.00 and is recommended for performing aldehyde-amine reactions. (Thermo Fisher, 2016) After the glutaraldehyde has reacted, the column is drained and washed with DI water. The silica nanoparticle solution (suspended in 20 mM HEPES buffer) is then added to the column and allowed to react for one hour. On completion of the reaction time, the solution is drained and the column is washed with DI water. mPEG-NHS suspended in DMSO is then added to the column and allowed to react for four hours at 4°C. DMSO is commonly used as a solvent for reacting nhs-esters with amine groups; it replaced water in this JNP synthesis. (Thermo Fisher, 2016) After the four-hour reaction time, the column is drained and washed with DI water. Chloroform is passed through the column to elute the finished JNPs; the nanoparticles are then stored in a glass vial. An illustration of this JNP configuration is shown in Figure 4.1.

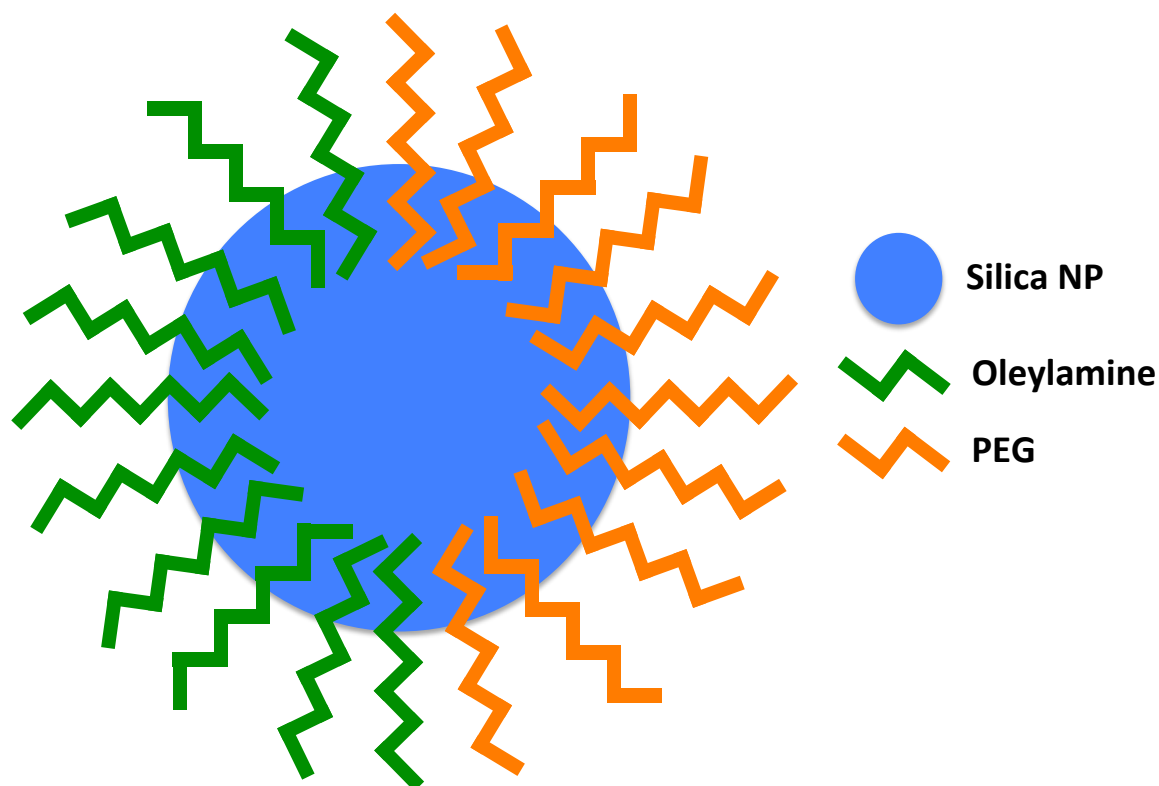


**Figure 4.1** Illustration of the strategy used to assemble a JNP with a silica core and a mPEG-NHS hemisphere. Fatty amine molecules will coat one hemisphere of the silica nanoparticle core; the other side of the silica nanoparticles will be coated with mPEG-NHS.

#### 4.2.3 Synthesizing JNPs with a Silica Core and a Hemisphere Functionalized with FITC

This synthesis is done in exactly the same manner as the synthesis described in section 4.2.2 until the second hemisphere is modified. As opposed to a PEG derivative, these nanoparticles are reacted with a solution of FITC in sodium bicarbonate buffer. Sodium bicarbonate buffer is recommended for performing FITC linkage; sodium bicarbonate is also an aqueous solution, so there is no concern for the nanoparticles detaching from the pack material during this reaction. The FITC solution is added and allowed to react with the nanoparticles for four hours at 4°C. After the reaction time is complete, the column is drained and washed with DI water. Considering FITC is only soluble in water at 0.1 mg/ml, extra washing steps are taken at this time to make sure that all free FITC is removed from the column. The nanoparticles are then eluted off of the packing material in ethanol and stored in a light protected glass vial. Figure 4.2 shows an illustration of these JNPs.



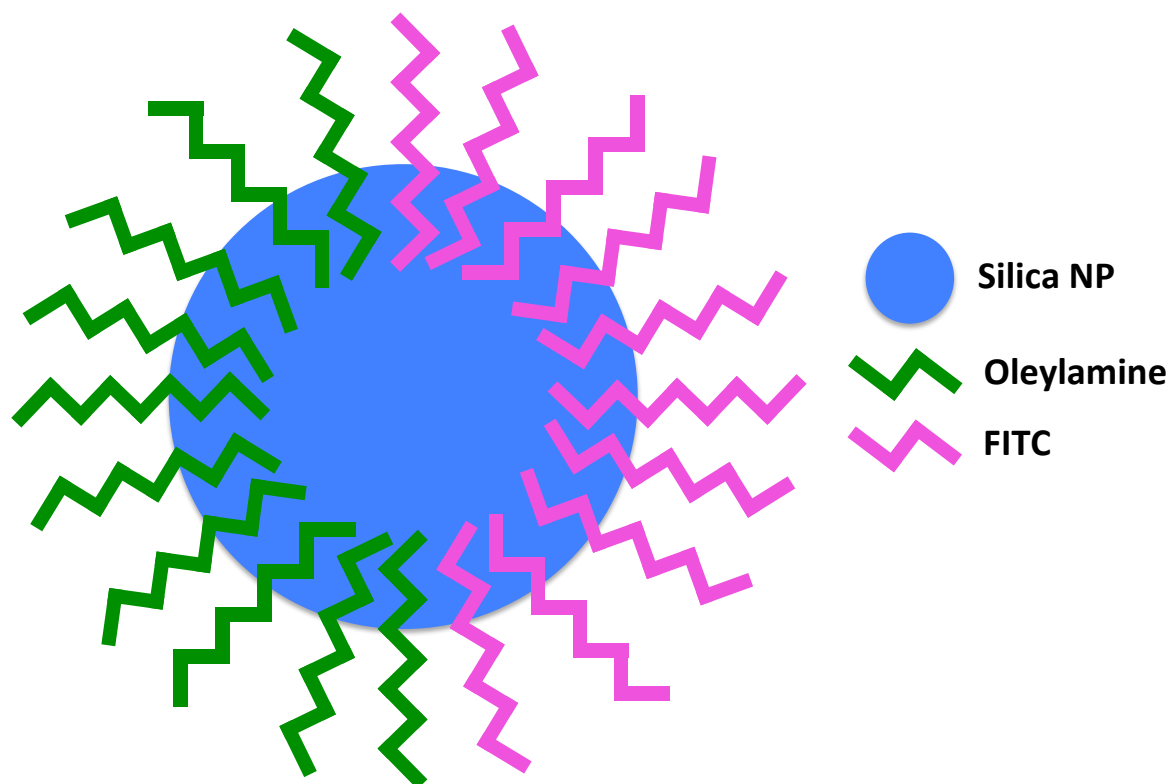


**Figure 4.2** Illustration of the strategy used to assemble a JNP with a silica core and a FITC hemisphere. Fatty amine molecules will coat one hemisphere of the silica nanoparticle core; the other side of the silica nanoparticles will be coated with FITC.

## 4.3 Results and Discussion

### 4.3.1 Analysis of JNPs Coated with FITC or PEG using an Optical Microscope

Before we began analysis of our dyed JNPs, we wanted to confirm our findings from Chapter 2 regarding the self-assembly of our JNPs when suspended in water. Samples of our JNPs coated partially with PEG were removed from chloroform and suspended in water in the presence of free oleylamine. Figure 4.3 shows optical microscope images from this experiment.

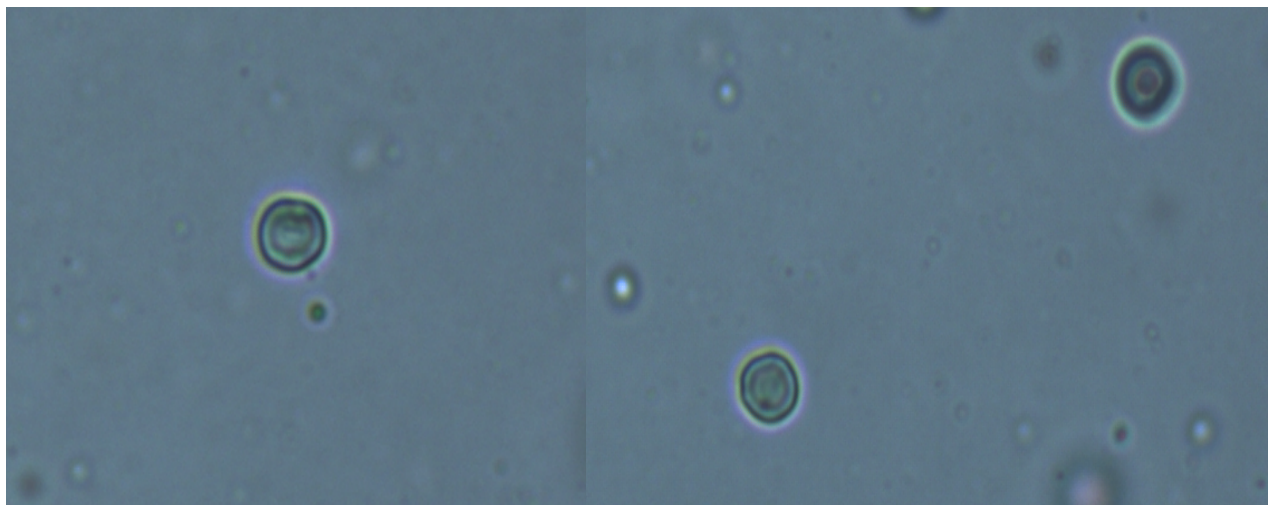


**Figure 4.3** Optical microscope images of JNPs with oleylamine and PEG hemispheres suspended in water with additional free oleylamine. The resulting structures range in size from 4-5 microns

From Figure 4.3, we see similar structures in these images to the structures seen in samples analyzed in Chapter 2. Even though these JNPs are larger and utilize a different core material, they behave in a similar manner when the solvent conditions are identical.

We utilized our optical microscope outfitted with a fluorescent filter to examine our JNPs partially coated with FITC and our JNPs partially coated with PEG for comparison. The fluorescent filter will reduce the wavelengths of light illuminating the sample to a tighter range; for this experiment we utilized a filter to limit entering light to between 470 nm and 525 nm (this range includes the peaks of the excitation and emission spectrums for FITC). (Fluorophores, 2016) Both nanoparticles sample were examined using an 100x magnification objective lens; this is the highest magnification that can be achieved using this microscope. Images were taken of the JNPs partially coated with PEG under normal light and using the fluorescent filter; images were also taken of the JNPs partially coated with FITC under normal light and using the fluorescent filter. These images are shown in Figure 4.4 and Figure 4.5, respectively.

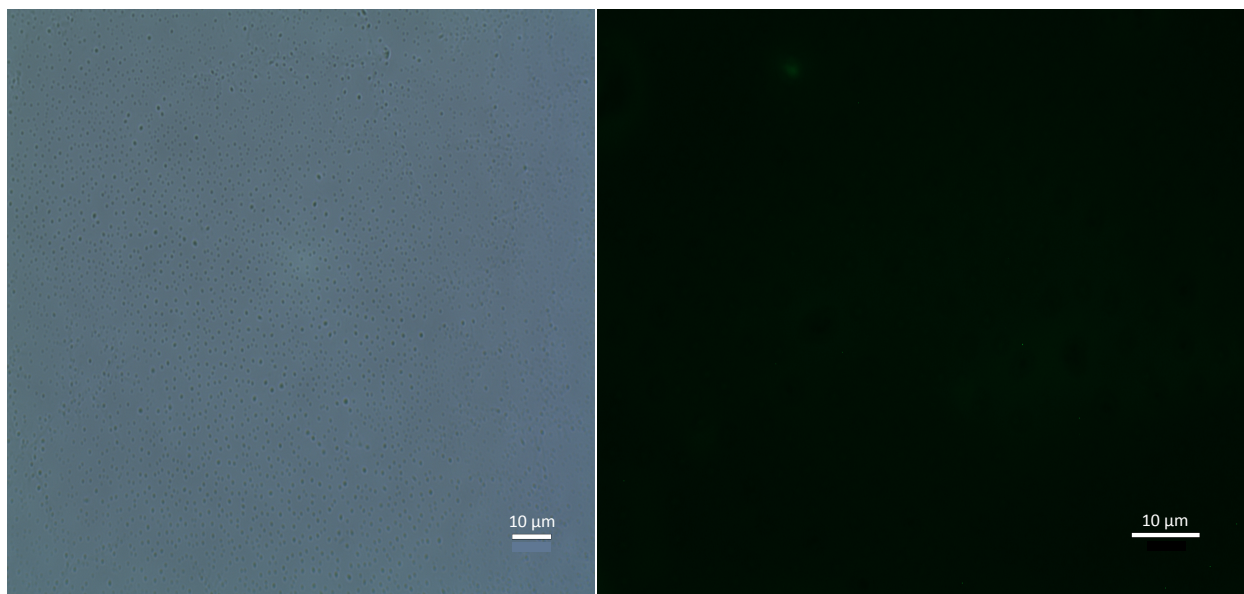


**Figure 4.4** 100X images of JNPs composed of a oleylamine hemisphere and a PEG hemisphere without a filter (left) and with a fluorescent filter (right)

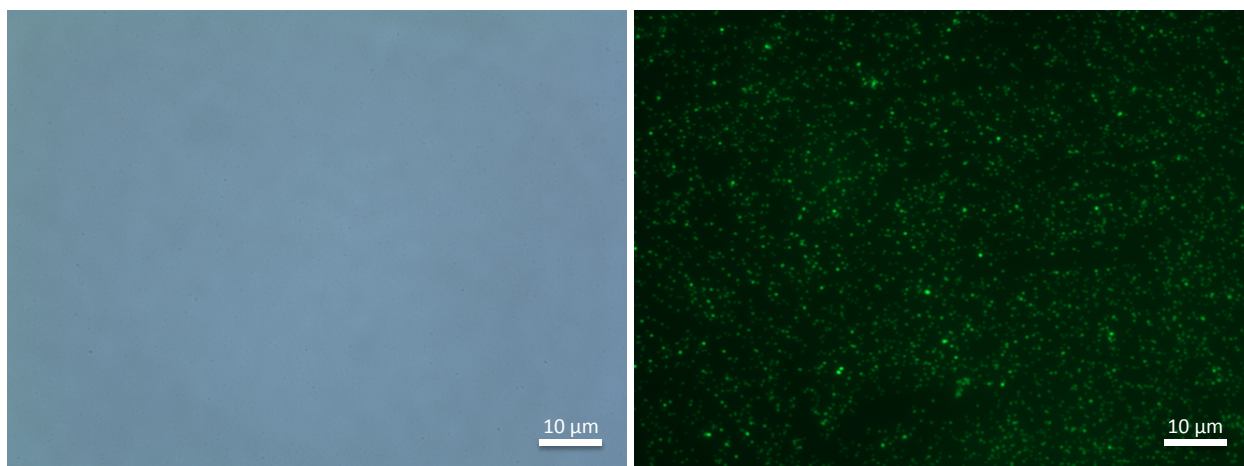


**Figure 4.5** 100X images of JNPs composed of a oleylamine hemisphere and a FITC hemisphere without a filter (left) and with a fluorescent filter (right)

From Figure 4.4, under normal light (left image) the JNPs are seen as small black dots in the image. Nothing is seen in the image when using the fluorescent filter (right image); this is expected since PEG does not fluoresce. In Figure 4.5, the JNPs partially coated with FITC also appear as small black dots without using a filter. When examined using the fluorescent filter, we see the particles clearly fluorescing

in green due to the FITC dye. These images indicate that we are getting the dye onto are particles. Due to limitation in the magnification, this microscope cannot look at these nanoparticles more closely in order to identify if FITC is bonding to one hemisphere. Due to this limitation, we looked into the use of more powerful optical microscopes.

#### **4.3.2 Analysis of JNPs Coated with FITC using an Optical Microscope Outfitted with a Dark-Field Condenser**

To attempt to visualize the surface of these JNPs, we utilized the optical microscope in the lab of Dr. Vitaly Vodyanoy (Vainrub, Pustovyy, & Vodyanoy, 2006). This microscope is unique in two ways: it can provide greater magnification than most standard optical microscopes, and it is also equipped with a dark-field condenser. In standard optical microscopes, the light source underneath the slide illuminates the sample; a portion of this light enters the objective lens and alters the appearance of the sample. A dark-field condenser is designed to keep light from entering the objective lens, making the background of the sample appear black (Omoto, n.d.). This improvement in contrast allows us to see color in nanoparticle samples; this factor combined with the use of our fluorescent dye on one hemisphere could be a way to identify hemispheres. Figure 4.6 shows images of our JNPs partially coated with PEG with and without a fluorescent filter. Figure 4.7 shows images of our JNPs partially coated with FITC with and without a fluorescent filter.



**Figure 4.6** Images from an optical microscope equipped with a dark field condenser of JNPs with a PEG functionalized hemisphere (image enlargement using digital zoom has been applied). In the left side image, no filter is being applied; on the right side image, a fluorescent filter is applied to limit the incoming light to between 470 nm and 525 nm.

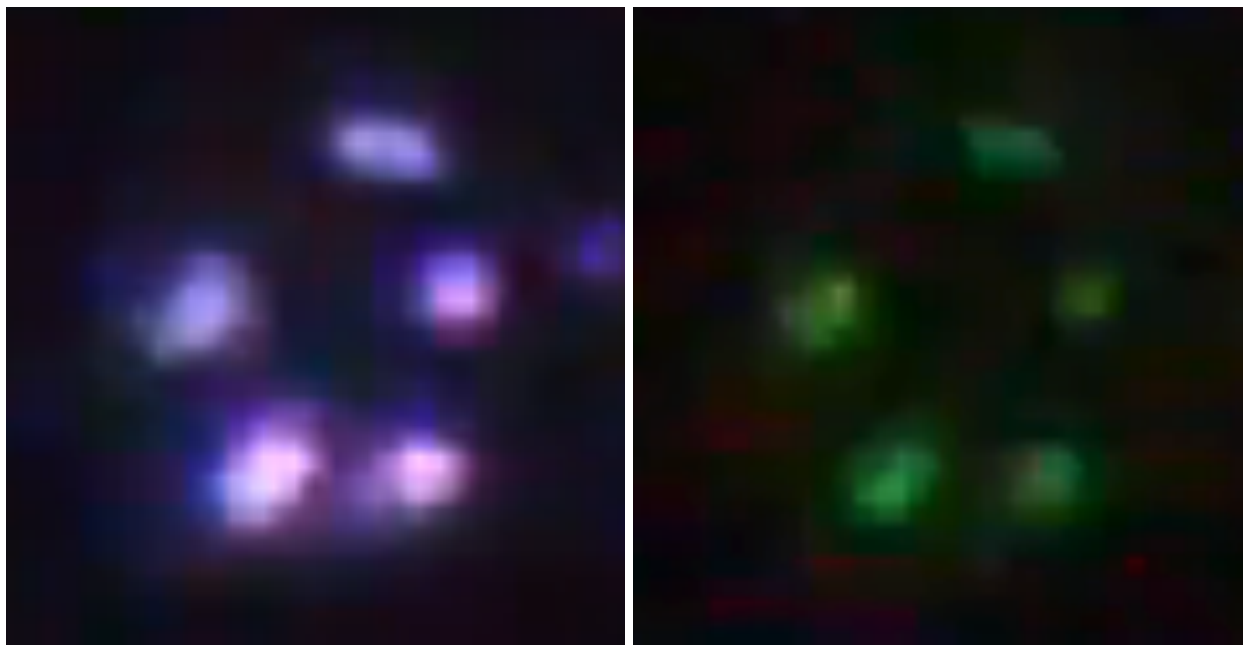


**Figure 4.7** Images from an optical microscope equipped with a dark field condenser of JNPs with a PEG functionalized hemisphere (image enlargement using digital zoom has been applied). In the left side image, no filter is being applied; on the right side image, a fluorescent filter is applied to limit the incoming light to between 470 nm and 525 nm.

From Figures 4.6 and 4.6, the same purple color is seen when examining both JNP samples without the use of a fluorescent filter. The JNPs partially coated with FITC show a green color visible under a fluorescent filter that is not seen in the partially PEG coated JNPs. An overlay of the images seen in Figure 4.7 is shown in Figure 4.8.



**Figure 4.8** Overlay of images seen in Figure 4.7 on JNP partially coated with FITC

From Figure 4.8, we seen both green and purple color emitting from the nanoparticles when the images are overlaid. This could be indicative of FITC occupying only one portion of the nanoparticle surface, but is not conclusive. More examination of these nanoparticles need to be done using this advance microscope system.

#### **4.4 Conclusions**

This JNP configuration allowed us to examine our nanoparticles using fluorescent imaging. FITC was shown to bond to our nanoparticles and could prove to be a usual compound in continued attempts to identify hemispheres. Parallels were identified between the behavior of our first JNP configuration (Chapter 2) and this configuration; similar behaviors out of JNPs with different nanoparticle cores and hemispherical coverage compounds indicates a possibility that our synthesis method could produce multiple JNP configurations without major changes to the method. We also utilized dark field microscopy in an attempt to identify hemispheres using the color of the nanoparticles and the color of

FITC. This characterization needs requires more work to unquestionably identify hemispheres, but the method should provide continued use to this project as the JNP synthesis method is improved.



## Chapter 5

### Overall Conclusions and Continued Investigation into JNP Synthesis Method

For this project, three different JNP configurations were synthesized using a new version of the masking method where masking was done around functionalized silica particle. This synthesis method was done in a way to simulate a packed column with the idea of eventually scaling up the method to supply JNPs for an industrial demand. Multiple characterization methods were applied to attempt to identify different hemispheres on the nanoparticles surface. DLS and hexane/water interface experiments gave us insights into the JNPs behavior in solvent suspension; FTIR gave us insights into the surface coverage of the compounds on the nanoparticle core. Optical microscope imaging, dark-field optical microscope imaging, and TEM imaging were used to identify differing hemispheres on the nanoparticle surface. These methods provided data that identifies the possibility of multi-modal nanoparticles, but have not definitively proven this concept. Continued work on improving our synthesis method should improve the data yielded from our existing characterization methods; we must also look into additional characterization methods to try and prove this concept. Partnered with identifying hemispheres, we must also tune our method to control hemispherical coverage ratios. Developing this control will make this synthesis method more applicable for industrial processes, an endgame goal of this research.

Testing the scalability of this method will be done once greater control of hemispherical ratio coverage is achieved. Characterization methods will also need to be investigated to compare a standard lab scale run with a scaled up run to verify efficacy. Fluorescent assays as well as Inductively coupled plasma atomic emission spectroscopy (ICP-AES) are possible method that could be use to differentiate between a standard run and a scaled up run. Scalability of this method was an primary goal at the beginning of this project and will continue to be a prioritized goal moving forward.

Finally, research into synthesizing an antimicrobial JNP configuration with the ability to form a self-assembled monolayer on a functionalized surface will be conducted once this synthesis method is verified. Investigation into materials for this JNP configuration has already begun; we will likely employing 20-30 nm silver nanoparticles to act as the antimicrobial hemisphere. We also have started

initial testing on forming JNP monolayers on a functionalized surface. Developed by the Ashurst Lab at Auburn University, a glass slide was functionalized with a hydrophobic compound in order to create a hydrophobic surface to begin investigation into forming monolayers. Figure 5.1 illustrates this concept:

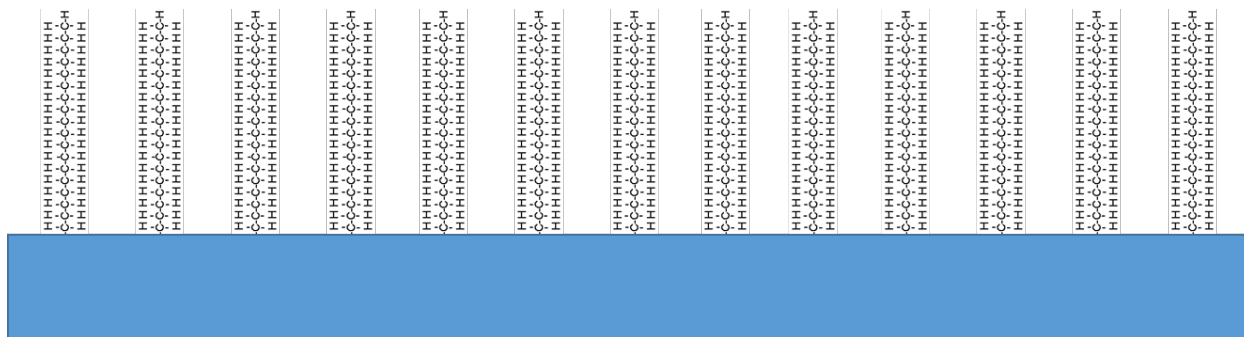


**Figure 5.1** Illustration of glass slide (represented by the blue block) functionalized with long chain hydrocarbons, creating a hydrophobic surface

We have already started examining the behavior of our nanoparticle solutions on this hydrophobic environment; so far our results have been positive. We would like to form monolayers of different JNPs as well as control particles on these slides and examine the contact angles developed by water droplets. Eventually, we would like to form monolayers of antimicrobial JNPs on this surface and expose the monolayer to e-coli cells. In theory, the expose antimicrobial hemispheres of the JNPs should kill the bacteria cells, which we intend to test with different viability and cytotoxicity assays. This antimicrobial JNP will be the first nanoparticle developed from this system with real world application. We hope that the development of this JNP as well as the improvements we plan to make to the method can help move production of Janus nanoparticles from laboratory experiments to industrial processes.

## References

- Cho, I., & Lee, K.-W. (1985). Morphology of latex particles formed by poly(methyl methacrylate)-seeded emulsion polymerization of styrene. *Journal of Applied Polymer Science*, 30(5), 1903–1926.
- Cheraghipour, E., Javadpour, S., & Mehdizadeh, A. R. (2012). Citrate capped superparamagnetic iron oxide nanoparticles used for hyperthermia therapy, 2012(December), 715–719.
- de Gennes, Pi.-G. (1992). Soft Matter (Nobel Lecture). *Angewandte Chemie International Edition in English*, 31(7), 842–845.
- Erhardt, R., Böker, A., Zettl, H., Kaya, H., Pyckhout-Hintzen, W., Krausch, G., ... Müller, A. H. E. (2001). Janus micelles. *Macromolecules*, 34(4), 1069–1075. doi:10.1021/ma000670p
- Fluorophores.org (2016). FITC. Retrieved from the Fluorophores.org website.  
<http://www.fluorophores.tugraz.at/substance/252>
- Fu, X., Liu, J., Yang, H., Sun, J., Li, X., Zhang, X., & Jia, Y. (2011). Arrays of Au-TiO<sub>2</sub> Janus-like nanoparticles fabricated by block copolymer templates and their photocatalytic activity in the degradation of methylene blue. *Materials Chemistry and Physics*, 130(1-2), 334–339.  
doi:10.1016/j.matchemphys.2011.06.054
- Gao, Y., & Yu, Y. (2013). How half-coated janus particles enter cells. *Journal of the American Chemical Society*, 135, 19091–19094. doi:10.1021/ja410687z
- Glaser, N., Adams, D. J., Böker, A., & Krausch, G. (2006). Janus particles at liquid-liquid interfaces. *Langmuir*, 22(12), 5227–5229. doi:10.1021/la060693i
- Gu, H., Yang, Z., Gao, J., Chang, C. K., & Xu, B. (2005). Heterodimers of nanoparticles: Formation at a liquid-liquid interface and particle-specific surface modification by functional molecules. *Journal of the American Chemical Society*, 127(1), 34–35. doi:10.1021/ja045220h

- Gu, H., Zheng, R., Zhang, X., & Xu, B. (2004). Facile One-Pot Synthesis of Bifunctional Heterodimers of Nanoparticles: A Conjugate of Quantum Dot and Magnetic Nanoparticles. *Journal of the American Chemical Society*, 126(18), 5664–5665. doi:10.1021/ja0496423
- Hatakeyama, M., Kishi, H., Kita, Y., Imai, K., Nishio, K., Karasawa, S., ... Handa, H. (2011). A two-step ligand exchange reaction generates highly water-dispersed magnetic nanoparticles for biomedical applications. *Journal of Materials Chemistry*, 21(16), 5959. doi:10.1039/c0jm04381h
- Hein, C. D., Liu, X.-M., & Wang, D. (2009). Click Chemistry, a Powerful Tool for Pharmaceutical Sciences. *NIH Public Access Author Manuscript*, 25(10), 2216–2230. doi:10.1007/s11095-008-9616-1.Click
- Kapoor, M. (1996). How to cross-link proteins. *Cellular, Molecular and Microbial Biology Division, ...*, (C1), 1–6. Retrieved from [http://www.fgsc.net/neurosporaprotocols/How to cross-link proteins.pdf](http://www.fgsc.net/neurosporaprotocols/How%20to%20cross-link%20proteins.pdf)
- Katepalli, H. (2014). Formation and Stability of Emulsions : Effect of Surfactant- Particle Interactions and Particle.
- Lahann, J. (n.d.). Electrohydrodynamic Co-Jetting of Particles and Fibers. Retrieved June 20, 2015, from [www.umich.edu/~lahannj/Lahann-particles.pdf](http://www.umich.edu/~lahannj/Lahann-particles.pdf)
- Lattuada, M., & Hatton, T. A. (2011). Synthesis, properties and applications of Janus nanoparticles. *Nano Today*, 6(3), 286–308. doi:10.1016/j.nantod.2011.04.008
- Li, C., Wang, J., Luo, X., & Ding, S. (2014). Large scale synthesis of Janus nanotubes and derivative nanosheets by selective etching. *Journal of Colloid and Interface Science*, 420, 1–8. doi:10.1016/j.jcis.2013.12.062
- Li, J., Wang, L., & Benicewicz, B. C. (2013). Synthesis of Janus nanoparticles via a combination of the reversible click reaction and “grafting to” strategies. *Langmuir : The ACS Journal of Surfaces and Colloids*, 29(37), 11547–53. doi:10.1021/la401990d
- Li, X., Zhou, L., Wei, Y., El-toni, A. M., Zhang, F., & Zhao, D. (2014). Anisotropic Growth-Induced Synthesis of Dual-Compartment Janus Mesoporous Silica Nanoparticles for Bimodal Triggered Drugs Delivery.
- Moore, J. W., & Stanitski, C. L. (2005). *Chemistry: The Molecular Science*.
- Nakanishi, K. (1963). Infrared Absorption Spectroscopy. *Journal of Pharmaceutical Sciences*, 52(7), 716.
- Naoui, K., Ohkado, Y., & Tatsuma, T. (2004). TiO<sub>2</sub> films loaded with Ag nanoparticles: control of multicolor photochromic behavior. *J. Amer. Chem. Soc.*, 126(5), 3664.

- Omoto, C. K. (n.d.). Using Darkfield Microscopy To Enhance Contrast - An Easy and Inexpensive Method. Retrieved from <http://public.wsu.edu/~omoto/papers/darkfield.html>
- Perro, A., Meunier, F., Schmitt, V., & Ravaine, S. (2009). Production of large quantities of “Janus” nanoparticles using wax-in-water emulsions. *Colloids and Surfaces A: Physicochemical and Engineering Aspects*, 332(1), 57–62. doi:10.1016/j.colsurfa.2008.08.027
- Pham, B. T. T., Such, C. H., & Hawckett, B. S. (2015). Synthesis of polymeric janus nanoparticles and their application in surfactant-free emulsion polymerizations. *Polym. Chem*, 6, 426–435. doi:10.1039/c4py01125b
- Poggi, E., Bourgeois, J.-P., Ernoult, B., & Gohy, J.-F. (2015). Polymeric Janus nanoparticles templated by block copolymer thin films. *RSC Adv.*, 5(55), 44218–44221. doi:10.1039/C5RA05290D
- Pradhan, S., Xu, L. P., & Chen, S. (2007). Janus nanoparticles by interfacial engineering. *Advanced Functional Materials*, 17(14), 2385–2392. doi:10.1002/adfm.200601034
- Richardson, J. (2011). IR Spectroscopy Tutorial: Amines. Retrieved January 1, 2015, from [orgchem.colorado.edu/Spectroscopy/irtutor/aminesir.html](http://orgchem.colorado.edu/Spectroscopy/irtutor/aminesir.html)
- Rogers, H. (2014). *Size Optimization of Magnetic Nanoparticles for Biomedical Applications via a Novel Size-Selective Fractionation Process*.
- Sánchez, A., Díez, P., Martínez-Ruiz, P., Villalonga, R., & Pingarrón, J. M. (2013). Janus Au-mesoporous silica nanoparticles as electrochemical biorecognition-signaling system. *Electrochemistry Communications*, 30, 51–54. doi:10.1016/j.elecom.2013.02.008
- Sardar, R., Heap, T. B., & Shumaker-Parry, J. S. (2007). Versatile solid phase synthesis of gold nanoparticle dimers using an asymmetric functionalization approach. *Journal of the American Chemical Society*, 129(17), 5356–5357. doi:10.1021/ja070933w
- Sigma Aldrich (2016) FluyuoroTag FITC Conjugation Kit. Retrieved from the Sigma Aldrich Website. <https://www.sigmaaldrich.com/content/dam/sigma-aldrich/docs/Sigma/Bulletin/fite1bul.pdf>
- Smith, B. C. (1998). *Infrared Spectral Interpretation: A Systematic Approach*.
- Sun, S., Zeng, H., Robinson, D. B., Raoux, S., Rice, P. M., Wang, S. X., & Li, G. (2004). Monodisperse MFe<sub>2</sub>O<sub>4</sub> (M = Fe, Co, Mn) Nanoparticles, 4(1), 126–132.

- Synytska, A., Khanum, R., Ionov, L., Cherif, C., & Bellmann, C. (2011). Water-repellent textile via decorating fibers with amphiphilic Janus Particles. *ACS Applied Materials and Interfaces*, 3(4), 1216–1220. doi:10.1021/am200033u
- Thermo Fisher Scientific (2016) Amine-reactive Crosslinker Chemistry. Retrieved from the Thermo Fisher Scientific Website. <https://www.thermofisher.com/us/en/home/life-science/protein-biology/protein-biology-learning-center/protein-biology-resource-library/pierce-protein-methods/amine-reactive-crosslinker-chemistry.html>
- Thermo Fisher Scientific (2016) Carbodiimide Crosslinker Chemistry. Retrieved from the Thermo Fisher Scientific Website. <https://www.thermofisher.com/us/en/home/life-science/protein-biology/protein-biology-learning-center/protein-biology-resource-library/pierce-protein-methods/carbodiimide-crosslinker-chemistry.html>
- Thermo Fisher Scientific (2016). FTIR Basics. Retrieved from the Thermo Fisher Scientific Website. <http://www.thermoscientific.com/en/about-us/general-landing-page/ftir-basics.html>
- Vainrub, A., Pustovyy, O., & Vodyanoy, V. (2006). Resolution of 90 nm in an Optical Transmission Microscope with an Annular Condenser. *Optics Letters*, 31(19), 2855–2857.
- Vortherms, A. R., Doyle, R. P., Gao, D., Debrah, O., & Sinko, P. J. (2009). Synthesis, characterization, and in vitro assay of folic acid conjugates of 3'-azido-3'-deoxythymidine (AZT): toward targeted AZT based anticancer therapeutics. *Nucleosides, Nucleotides & Nucleic Acids*, 27(2), 173–185. doi:10.1080/15257770701795946.SYNTHESIS
- Walther, A., & Muller, A. H. E. (2008). Janus Particles. *Soft Matter*, 4(4), 663–668.
- Wyatt Technology (2016). Understanding Dynamic Light Scattering. Retrieved from Wyatt Technology Website. <http://www.wyatt.com/library/theory/dynamic-light-scattering-theory.html>
- Xie, H., She, Z. G., Wang, S., Sharma, G., & Smith, J. W. (2012). One-step fabrication of polymeric Janus nanoparticles for drug delivery. *Langmuir*, 28(9), 4459–4463. doi:10.1021/la2042185
- Yi, F., Xu, F., Gao, Y., Li, H., & Chen, D. (2015). Macrocellular polymer foams from water in oil high internal phase emulsion stabilized solely by polymer Janus nanoparticles: preparation and their application as support for Pd catalyst. *RSC Adv.*, 5(50), 40227–40235. doi:10.1039/C5RA01859E

- Yoshida, M., Roh, K. H., Mandal, S., Bhaskar, S., Lim, D., Nandivada, H., ... Lahann, J. (2009). Structurally controlled bio-hybrid materials based on unidirectional association of anisotropic microparticles with human endothelial cells. *Advanced Materials*, 21(48), 4920–4925. doi:10.1002/adma.200901971
- Zahn, N., & Kickelbick, G. (2014). Synthesis and Aggregation Behavior of Hybrid Amphiphilic Titania Janus Nanoparticles via Surface-Functionalization in Pickering Emulsions. *Colloids and Surfaces A: Physicochemical and Engineering Aspects*, 461, 142–150. doi:10.1016/j.colsurfa.2014.07.039
- Zhang, L., Luo, Q., Zhang, F., Zhang, D.-M., Wang, Y.-S., Sun, Y.-L., ... Sun, H.-B. (2012). High-performance magnetic antimicrobial Janus nanorods decorated with Ag nanoparticles. *Journal of Materials Chemistry*, 22(45), 23741. doi:10.1039/c2jm35072f
- Zhao, N., & Gao, M. (2009). Magnetic janus particles prepared by a flame synthetic approach: Synthesis, characterizations and properties. *Advanced Materials*, 21(2), 184–187. doi:10.1002/adma.200800570